Aus dem
Institut für Pharmakologie und Toxikologie der Bundeswehr

Leiter: Prof. Dr. Franz Worek (ehem. Prof. Dr. Horst Thiermann)

Identifizierung neuartiger Proteinaddukte in Plasma und Haaren nach S-Lost-Exposition und Entwicklung massenspektrometrischer Methoden zur Verifikationsanalytik

Identification of novel protein adducts in plasma and hair after sulfur mustard exposure and development of mass spectrometric methods for verification analysis

Dissertation
zum Erwerb des Doktorgrades der Humanbiologie
an der Medizinischen Fakultät der
Ludwig-Maximilians-Universität zu München

vorgelegt von

Wolfgang Arnulf Schmeißer

aus

Traunstein

2025

Mit Genehmigung der Medizinischen Fakultät
der Universität München

Berichterstatter:	Prof. Dr. Theo Rein
Mitberichterstatter:	Prof. Dr. Oliver Peschel
	Prof. Dr. Ines Golly
	Prof. Dr. Kai Kehe
Mitbetreuung durch den promovierten Mitarbeiter:	Prof. Dr. Harald John
Dekan:	Prof. Dr. med. Thomas Gudermann
Tag der mündlichen Prüfung:	14.04.2025

„Verstehen kann man das Leben nur rückwärts. Leben muß man es vorwärts.“

Søren Kierkegaard

Affidavit

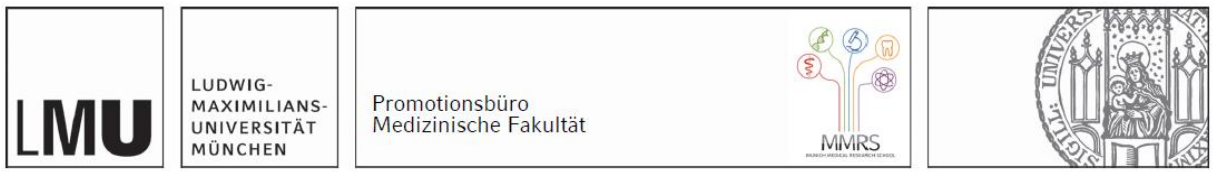

Eidesstattliche Versicherung

Schmeißer, Wolfgang

_____

Name, Vorname

Ich erkläre hiermit an Eides statt, dass ich die vorliegende Dissertation mit dem Titel:

Identifizierung neuartiger Proteinaddukte in Plasma und Haaren nach S-Lost-Exposition und Entwicklung massenspektrometrischer Methoden zur Verifikationsanalytik

selbständig verfasst, mich außer der angegebenen keiner weiteren Hilfsmittel bedient und alle Erkenntnisse, die aus dem Schrifttum ganz oder annähernd übernommen sind, als solche kenntlich gemacht und nach ihrer Herkunft unter Bezeichnung der Fundstelle einzeln nachgewiesen habe.

Ich erkläre des Weiteren, dass die hier vorgelegte Dissertation nicht in gleicher oder in ähnlicher Form bei einer anderen Stelle zur Erlangung eines akademischen Grades eingereicht wurde.

München, den 25.04.2025 Wolfgang Schmeißer

Inhaltsverzeichnis

Publikationsliste

Publikationen der kumulativen Dissertation

Wolfgang Schmeißer*, Robin Lüling*, Dirk Steinritz, Horst Thiermann, Theo Rein, Harald John. Transthyretin as a target of alkylation and a potential biomarker for sulfur mustard poisoning: Electrophoretic and mass spectrometric identification and characterization. *Drug Testing and Analysis* 2022, 14 (1), 80-91. DOI: 10.1002/dta.3146.

Wolfgang Schmeißer, Markus Siegert, Horst Thiermann, Theo Rein, Harald John. Highly stable peptide adducts from hard keratins as biomarkers to verify local sulfur mustard exposure of hair by high-resolution mass spectrometry. *Archives of Toxicology* 2022, 96 (8), 2287-2298. DOI: 10.1007/s00204-022-03307-0.

Weitere Publikationen

Robin Lüling*, **Wolfgang Schmeißer***, Markus Siegert, Harald Mückter, Alexander Dietrich, Horst Thiermann, Thomas Gudermann, Harald John, Dirk Steinritz. Identification of creatine kinase and alpha-1 antitrypsin as protein targets of alkylation by sulfur mustard. *Drug Testing and Analysis* 2021, 13 (2), 268-282. DOI: 10.1002/dta.2916.

Harald John, Tamara Lindl, Henrik Reuter, **Wolfgang Schmeißer**, Michael Schrader, Horst Thiermann. Phosphonylated tyrosine and lysine residues as biomarkers of local exposure of human hair to the organophosphorus nerve agents sarin and VX. *Drug Testing and Analysis* 2023, 15 (7), 730-744. DOI: 10.1002/dta.3459.

Catherine Schaefers, **Wolfgang Schmeißer**, Harald John, Franz Worek, Theo Rein, Simone Rothmiller, Annette Schmidt. Effects of the nerve agent VX on hiPSC-derived motor neurons. *Archives of Toxicology* 2024, 98 (6), 1859-1875, DOI: 10.1007/s00204-024-03708-3.

*: geteilte Erstautorenschaft

Posterpräsentationen

Wolfgang Schmeißer, Florian Langguth, Sebastian Rappenglück, Sonja Sichler, Franz Worek, Horst Thiermann, Karin Veronika Niessen. Funktionelle Messungen des nikotinischen Acethylcholinrezeptors mittels SSM basiertem Hochdurchsatzverfahren. 49. Jahreskongress der Deutschen Gesellschaft für Wehrmedizin und Wehrpharmazie e. V. (DGWMP), Würzburg, D, 2018.

Karin Veronika Niessen, Thomas Seeger, Catherine Schäfers, **Wolfgang Schmeißer**, Horst Thiermann, Franz Worek. Functional measurements of nicotinic acethylcholine receptors: High-throughput screening of potential antidotes for the treatment of nerve agent poisoning. 17th Medical Chemical Defense Conference (MCDC), München, D, 2018.

Andreas Kranawetvogl, **Wolfgang Schmeißer**, Markus Siegert, Florian Eyer, Horst Thiermann, Harald John. Simultaneous detection of phosphorylated tyrosines and cysteine-proline disulfide-adducts of human serum albumin as biomarkers of omethoate/dimethoate pesticide-poisoning. 18th Medical Chemical Defense Conference (MCDC), München, D, 2019.

Andreas Kranawetvogl, **Wolfgang Schmeißer**, Markus Siegert, Florian Eyer, Horst Thiermann, Harald John. Nachweis einer Omethoat/Dimethoat Pestizidvergiftung mittels simultaner Detektion phosphorylierter Tyrosin und Cystein-Prolin Disulfid-Addukte aus humanem Plasma. 50. Jahreskongress der Deutschen Gesellschaft für Wehrmedizin und Wehrpharmazie e. V. (DGWMP), Leipzig, D, 2019.

Harald John, **Wolfgang Schmeißer**, Tamara Lindl, Henrik Reuter, Michael Schrader, Horst Thiermann. Neue Methoden der Forensik: bioanalytischer Nachweis von Kampfstoff-Expositionen über modifizierte Haarproteine. 54. Kongress der Deutschen Gesellschaft für Wehrmedizin und Wehrpharmazie e.V. (DGWMP), Ulm, D, 2023

Erklärung über den Eigenanteil

Transthyretin as a target of alkylation and a potential biomarker for sulfur mustard poisoning: Electrophoretic and mass spectrometric identification and characterization

Wolfgang Schmeißer*, Robin Lüling*, Dirk Steinritz, Horst Thiermann, Theo Rein, Harald John, *Drug Testing and Analysis* 2022, 14 (1), 80-91. DOI: 10.1002/dta.3146

*: geteilte Erstautorenschaften

Diese Arbeit beschreibt die Identifizierung von bisher unbekannten Plasmaproteinen als Zielstrukturen des Alkylanzes Bis(2-chlorethyl)sulfid (S-Lost) und darauf aufbauend die Entwicklung einer massenspektrometrischen Methode zur Verifikation einer S-Lost-Exposition durch Detektion von Biomarkerpeptiden.
Initial wendete ich die zweidimensionale Thiol-Differenz-Gelelektrophorese (2D-thiol-DIGE)-Methode an. Dies beinhaltete die Depletion von humanem Serumalbumin und Immunglobulin G aus Plasma, Expositionsexperimente, die Derivatisierung von Plasmaproteinen mit Maleimid-Farbstoffen, sowie die 2D-Gelelektrophorese. Das so identifizierte Protein Transthyretin (TTR) unterzog ich einer umfangreichen Literaturrecherche. Für die Isolierung von TTR aus Plasma optimierte ich eine Immunomagnetische Seperation (IMS) hinsichtlich des verwendeten Antikörpers, dessen eingesetzter Menge und der Inkubationszeit in Plasma.
Für die detaillierte Untersuchung der durch S-Lost-verursachten Adduktierung an TTR nutzte ich im Anschluss an die IMS Trypsin zur Proteolyse und Flüssigchromatographie in Kopplung mit hochauflösender Flugzeitmassenspektrometrie (LC-TOF-MS/HR-MS) zur Detektion von potentiellen Biomarkerpeptiden. Alle experimentellen und instrumentellen Teilaspekte (Proteolysedauer, interindividuelle Variationen, Adduktstabilität, Selektivität, technische Messparameter) wurden von mir charakterisiert und optimiert.
Zur Analyse der erhobenen Daten setzte ich spezielle Auswertesoftware ein. Die generierten Ergebnisse wertete ich graphisch mittels GraphPad Prism Software aus und erstellte ein Manuskript, das in der Fachzeitschrift *Drug Testing and Analysis* erschienen ist.

Begründung zur geteilten Erstautorenschaft

Das gesamte Projekt der Entwicklung der 2D-thiol-DIGE-Methode bis zur Validierung eines Biomarkerpeptids zur massenspektrometrischen Verifikation einer S-Lost-Intoxikation stellte eine institutsinterne, arbeitsgruppenübergreifende Zusammenarbeit dar. Basierend auf den ergänzenden Expertisen wurden synergistische Effekte genutzt. Herr Robin Lüling legte mit seinen Erfahrungen im Bereich Proteomanalytik die Grundlage für die 2D-thiol-DIGE-Methode. Die umfangreichen Analysen hierfür wurden gemeinsam von ihm und mir durchgeführt. Die anschließenden Untersuchungen mittels matrixunterstützter Laser-Desorption/Ionisation Flugzeitmassenspektrometrie wurden von Herrn Robin Lüling durchgeführt, während die LC-TOF-MS/HR-MS-Experimente von mir ausgeführt wurden. Die gemeinsam generierten neuen Forschungsergebnisse wurden in zwei Veröffentlichungen mit jeweils geteilter Erstautorenschaft (siehe Publikationsliste) erfolgreich vorgestellt.

Highly stable peptide adducts from hard keratins as biomarkers to verify local sulfur mustard exposure of hair by high-resolution mass spectrometry

Wolfgang Schmeißer, Markus Siegert, Horst Thiermann, Theo Rein, Harald John, *Archives of Toxicology* 2022, 96 (8), 2287 2298. DOI: 10.1007/s00204-022-03307-0

Ziel dieser Arbeit war es, Haare und deren Hauptbestandteile Hartkeratine als Zielstruktur nach S-Lost-Exposition zu untersuchen sowie eine Methode zur Generierung und massenspektrometrischen Detektion von Biomarkerpeptiden zu entwickeln.
Als Grundlage organisierte ich Haare, bereitete diese vor und führte Expositionsexperimente durch. Basierend auf einer ausführlichen Literaturrecherche testete ich verschiedene Lysepuffer und Aufarbeitungsmethoden. Darauf aufbauend optimierte ich die Lysepufferzusammensetzung und Lysedauer. Für die Proteolyse testete ich mehrere Enzyme in Abhängigkeit von der Zeit. Für die Bestätigung der Hartkeratine als Zielstrukturen von S-Lost und Ursprung der Biomarkerpeptide führte ich Natriumdodecylsulfat-Polyacrylamidgelelektrophorese und In-Gel Proteolysen durch.
Zur selektiven Detektion der Biomarkerpeptide entwickelte ich eine LC-TOF-MS/HR-MS-Methode, für die ich die Trennsäule und technischen Messparameter optimierte.
Die zentralen Aspekte der Biomarkerpeptide, wie die Adduktformierung, die Stabilität, die inter- und intraindividuellen Unterschiede und die Nachweisgrenzen, wurden von mir in Einzelexperimenten untersucht.
Für die Interpretation der erhobenen Messdaten bediente ich mich spezieller Auswertesoftware. Neben der graphischen Umsetzung (GraphPad Prism Software) erstellte ich das Manuskript zur Publikation in der Fachzeitschrift *Archives of Toxicology*.

Abkürzungsverzeichnis

AE(-HETE)IRSDL	AlaGlu(-HETE)IleArgSerAspLeu, Heptapeptid-Addukt mit kovalenter HETE-Modifikation
CBB	Coomassie-Brilliant-Blue (Coomassie-Brillant-Blau)
CEES	2-Chloroethylethylsulfid
C(-HETE)P	Cys(-HETE)Pro, Dipeptid-Addukt mit kovalenter HETE-Modifikation
C(-HETE)PF	Cys(-HETE)ProPhe, Tripeptid-Addukt mit kovalenter HETE-Modifikation
C(-HETE)PLMVK	Cys(-HETE)ProLeuMetValLys, Hexapeptid-Addukt mit kovalenter HETE-Modifikation
COPD	chronic obstructive pulmonary disease (chronisch obstruktive Lungenerkrankung)
CWÜ	Chemiewaffenübereinkommen
2D-DIGE	two-dimensional difference gel electrophoresis (zweidimensionale Differenz-Gelelektrophorese)
2D-GE	zweidimensionale Gelelektrophorese
DNA	deoxyribonucleic acid (Desoxyribonukleinsäure)
FKTIE(-HETE)EL	PheLysThrIleGlu(-HETE)GluLeu, Heptapeptid-Addukt mit kovalenter HETE-Modifikation
GC	gas chromatography (Gaschromatographie)
Hb	Hämoglobin
HETE	Hydroxyethylthioethyl
HETE-Val	Valin-Addukt mit kovalenter HETE-Modifikation
HSA	humanes Serumalbumin
IgG	Immunglobulin G
LC	liquid chromatography (Flüssigchromatographie)
LC-MS/HR-MS	liquid chromatography coupled to high-resolution mass spectrometry (Kopplung von Flüssigchromatographie und hochauflösender Massenspektrometrie)
LE(-HETE)TKLQF	LeuGlu(-HETE)ThrLysLeuGlnPhe Heptapeptid-Addukt mit kovalenter HETE-Modifikation
LOD	limit of detection (Nachweisgrenze)

MALDI-TOF-MS/MS	matrix-assisted laser desorption/ionization time-of-flight mass spectrometry (matrixunterstützte Laser-Desorption/Ionisation Flugzeitmassenspektrometrie)
MS	Massenspektrometrie
OVCW	Organisation für das Verbot Chemischer Waffen
RNA	ribonucleic acid (Ribonukleinsäure)
RSDL	Reactive Skin Decontamination Lotion (Lotion zur Hautdekontamination)
SDS-PAGE	sodium dodecyl sulfate - polyacrylamide gel electrophoresis (Natriumdodecylsulfat-Polyacrylamidgelelektrophorese)
S-Lost	Bis(2-chlorethyl)sulfid
TDG	Thiodiglykol
TDGO	Thiodiglykol-Sulfoxid
TOF-MS/HR-MS	high-resolution time-of-flight mass spectrometry (hochauflösende Flugzeitmassenspektrometrie)
TTR	Transthyretin

1 Einführung

Der Einsatz des chemischen Kampfstoffes Bis(2-chlorethyl)sulfid ist international geächtet und kann schwerwiegende politische Konsequenzen nach sich ziehen (*1, 2*). Dafür ist ein eindeutiger bioanalytischer Nachweis spezifischer Biomarker von elementarer Bedeutung (*3, 4*). Dieser geschieht in designierten Laboratorien unter Einhaltung strenger Vorgaben der Organisation für das Verbot Chemischer Waffen (OVCW) (*5*). Diesbezüglich besteht ein großes Interesse an der Erweiterung des bestehenden Repertoires an Biomarkern zur Verifikationsanalytik von Bis(2-chlorethyl)sulfid.

1.1 S-Lost

1.1.1 Klassifizierung

Chemische Kampfstoffe sind synthetisch hergestellte Substanzen oder Gemische von Substanzen, deren kriegerischer Einsatz eine Schädigung, Kampfunfähigkeit oder Tötung gegnerischer Kräfte bewirken soll (*6*). Sie werden nach den primär betroffenen Organen oder Geweben unterteilt. Neben den Nervenkampfstoffen sind die hautschädigenden Kampfstoffe aufgrund ihrer Toxizität von größter Bedeutung (*6*). Die Gruppe der blasenbildenden Hautkampfstoffe wird von Strukturanaloga der Schwefelloste, Stickstoffloste und chlorhaltigen organischen Arsenverbindungen gebildet (*6*).

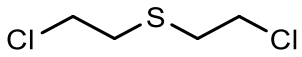

Abbildung 1: Chemische Struktur von Bis(2-chlorethyl)sulfid (*7*).

Bei den Schwefellosten handelt es sich um eine Stoffgruppe endständig chlorierter Thioether, von der das Bis(2-chlorethyl)sulfid (CAS Nummer 505-60-2, $C_4H_8Cl_2S$) (Abbildung 1) der militärisch relevanteste Vertreter und unter einer Vielzahl von Synonymen bekannt ist (*8*):

- 2,2'-Dichlordiethylsulfid
- Schwefellost
- S-Lost
- Yperit
- Senfgas
- Gelbkreuz
- H. HS. HD

In dieser Arbeit wird das Synonym S-Lost verwendet. In den anschließenden Kapiteln werden die Hintergründe und Grundlagen der aktuellen S-Lost-Forschung, insbesondere im Hinblick auf die Verifikationsanalytik, dargestellt.

1.1.2 Historie und gegenwärtige Relevanz

Nach der Reaktion von Ethylen mit Schwefeldichlorid beschrieb César-Mansuète Despretz 1822 erstmals die übelriechende Substanz, welche später als S-Lost bekannt wurde (*9*). Die erste Erwähnung der blasenbildenden Eigenschaften von S-Lost erfolgte zeitgleich im Jahr 1860 durch Frederick Guthrie und Albert Niemann, jedoch unabhängig voneinander (*10, 11*). 1886 gelang es Viktor Meyer durch ein neues Syntheseverfahren, das final die Chlorierung von Thiodiglykol (TDG) nutzt, hochreines S-Lost herzustellen (*12, 13*). Auf die beiden Wissenschaftler Wilhelm Lommel und Wilhelm Steinkopf, die 1916 am Kaiser-Wilhelm-Institut für Physikalische Chemie und Elektrochemie in Berlin ein Syntheseverfahren im großtechnischen Maßstab entwickelten, geht das Akronym Lost (**Lo**mmel/**St**einkopf) zurück. Der erste militärische Einsatz erfolgte durch die deutschen Truppen während des Ersten Weltkrieges 1917 nahe Ypern (Belgien), wovon sich das Synonym Yperit ableitet (*6*). Die Angaben zu S-Lost-bedingten Opferzahlen im Ersten Weltkrieg divergieren, aber es wird von bis zu 1.200.000 Exponierten und mehr als 90.000 Toten ausgegangen (*14–17*). In den folgenden Jahrzehnten kam es in diversen Konflikten weltweit zum Einsatz von S-Lost (Japan 1936, Ägypten 1963–1967) (*15*). Insbesondere der vielfache Einsatz von S-Lost während des Ersten Golfkrieges (Iran gegen den Irak, 1980-1988) forderte Tausende Todesopfer (*18*). Mehrere Zehntausend Iraner leiden bis heute an den gesundheitlichen Spätfolgen einer S-Lost-Exposition (*16, 19–21*). Unter anderem führten diese Ereignisse zum 1997 in Kraft getretenen Chemiewaffenübereinkommen (CWÜ), welches die Entwicklung, Herstellung, Lagerung und den Einsatz chemischer Waffen verbietet und deren Vernichtung reguliert. Die Überwachung der Einhaltung des CWÜ obliegt der OVCW, die bei Verstößen die Generalversammlung und den Sicherheitsrat der Vereinten Nationen einschalten kann. Letzterer ist befugt zur Verhängung von Sanktionen (*2*). Für ihren „umfassenden Einsatz für die Vernichtung von Chemiewaffen“ erhielt die OVCW 2013 den Friedensnobelpreis (*22*). Trotz der internationalen Ächtung kam es 2015 und 2016 zum Einsatz von S-Lost in Syrien und im Irak (*4, 23, 24*). Dies zeigt die bis heute von S-Lost ausgehende Gefahr für das Militär und die Zivilbevölkerung.

1.1.3 Physikochemische Eigenschaften

S-Lost ist bei Raumtemperatur eine farb- und geruchlose ölige Flüssigkeit, die nur durch technische Verunreinigungen eine leicht gelbliche Farbe sowie einen leicht senf- oder knoblauchartigen Geruch entwickelt (*6*). Dies ist für die teilweise verwendete Bezeichnung „Senfgas“ verantwortlich (*6*). In einen gasförmigen Aggregatszustand geht S-Lost aber erst ab 217,5 °C über (*6, 8*). Es ist überaus lipophil. Die Hydrolyse im wässrigen Milieu findet mit einer Halbwertszeit von ca. 6 min bei 25 °C statt und dessen Ausmaß verringert sich bei erhöhtem Salzgehalt der Umgebung (*25*). Die wichtigsten physikochemischen Eigenschaften sind in Tabelle 1 aufgeführt.

Tabelle 1: Physikochemische Eigenschaften von S-Lost (*7, 26–28*).

Molekulargewicht	159,08 g/mol
Farbe	farblos, leicht gelblich bei Verunreinigung
Aggregatzustand (25 °C)	ölige Flüssigkeit
Dichte	1,27-1,34 g/cm^3
Schmelzpunkt	14,45 °C
Siedepunkt	217,5 °C
Löslichkeit	schlecht in Wasser (920 mg/L bei 22 °C) gut in organischen Lösungsmitteln
Dampfdruck	0,11 mmHg bei 25 °C
Dampfdichte	5,5 g/cm³
Verteilungskoeffizient log K_{OW}	1,37

1.1.4 Toxizität und Symptomatik

Das Auftreten von Symptomen nach einer S-Lost-Exposition, zumeist in dampfförmigem oder flüssigem Zustand ausgebracht, ist abhängig von der aufgenommenen Dosis. Nach einer zunächst beschwerdefreien Latenzzeit sind insbesondere die Haut, der Respirationstrakt und die Augen betroffen (*19, 21*). Die maximale Ausprägung der Symptome kann auch erst nach mehreren Tagen erreicht werden (*21, 29*). Die ineinandergreifenden multifaktoriellen Schädigungsmechanismen führen unter anderem zum Zelltod durch Apoptose und Nekrose, zu Inflammation und gestörter Wundheilung (*30–32*). Die am schwerwiegendsten betroffenen Organe und Gewebe werden im Folgenden genauer betrachtet.

Haut

Bei Kontakt mit 100-300 mg min/m^3 S-Lost-Dampf bzw. 10-20 µg/cm^2 Flüssigkeit kommt es beim Menschen zu Hautrötungen und Juckreiz. Erst ab 1000–2000 mg min/m^3 Dampf und 40-100 µg/cm^2 Flüssigkeit kommt es zur Ausbildung von mit gelblichem Exsudat gefüllten Blasen (*19*). Diese können, auch ohne erneuten Kontakt zu S-Lost, noch mehrere Wochen nach Exposition entstehen (*19*). Bei schweren Verläufen bilden sich Ulzerationen, die aufgrund von auftretenden Wundheilungsstörungen nur unzureichend ausheilen (*32, 33*). Die Empfindlichkeit gegenüber S-Lost wächst dabei mit steigender Temperatur und Feuchtigkeit der Umgebung sowie bei vorherigen Läsionen der Haut (*34*).

Respirationstrakt

Das Ausmaß der Schädigung ist stark dosisabhängig und betrifft den gesamten Respirationstrakt von der Nasenschleimhaut bis zu den Bronchiolen (*35*). Bei niedrigen Aerosol-Konzentrationen ab 100 mg min/m^3 treten erste Symptome wie Husten und der Verlust von Geruchs- und Geschmackssinn auf (*19, 35*). Bei hohen Konzentrationen folgen schwere Verläufe mit Lungenembolien bis hin zum akuten Lungenversagen (*35*). Die akuten Symptome gehen oft in chronische Krankheitsverläufe über, die sich in ähnlicher Symptomatik wie bei

einer chronisch obstruktiven Lungenerkrankung (englisch „chronic obstructive pulmonary disease“, COPD) äußern und unter dem Begriff „Mustard Lung“ bekannt sind (*36*).

Augen

Die Augen sind am empfindlichsten gegenüber S-Lost. Bei Konzentrationen von 50-100 mg min/m^3 kommt es zu ersten Symptomen wie Konjunktivitis und einem Fremdkörpergefühl (*18, 21*). Mit steigenden Konzentrationen treten Lidödeme und starke Schmerzen bis hin zu Ulzerationen auf (*18, 21, 35*).

1.1.5 Toxikokinetik

Neben dem Verständnis für die schädigende Wirkung eines Giftstoffes, sind Kenntnisse über die Prozesse, denen dieser Stoff im Körper unterliegt, auch für die Verifikationsanalytik von entscheidender Bedeutung. Deshalb wird im Folgenden die Absorption, Distribution, Metabolisierung und Elimination von S-Lost genauer betrachtet (*37*).

Absorption

Die bedeutendste systemische Absorption von S-Lost erfolgt über direkten Hautkontakt und den Respirationstrakt, wohingegen die ebenso stattfindende Aufnahme über die Augen oder den Gastrointestinaltrakt eine untergeordnete Rolle spielt (*35*). Für die Penetrationsrate von *ex vivo* 71-294 µg/cm^2h^1 über die Haut sind deren Dicke, Temperatur und Feuchtigkeit, vorhandene Läsionen sowie ein möglicher Okklusionseffekt entscheidende Faktoren (*34, 38*). Letzterer kann durch Salben, die zur Behandlung von S-Lost-Wunden verwendet werden, entstehen und eine verstärkte Reservoir-Bildung und letztlich Aufnahme von S-Lost bewirken. Ohne Okklusion evaporieren ca. 80% unmittelbar, ca. 20% penetrieren durch die Haut. Von diesen 20% gehen wiederum 80% in die Zirkulation und ca. 20% reagieren mit Biomakromolekülen in der Haut (*19, 38*). Die Aufnahme von S-Lost über den Respirationstrakt erfolgt über Aerosole und findet sowohl in den oberen als auch in den unteren Atemwegen statt (*35*).

Distribution

In Tierstudien mit Ratten wurde zur Beschreibung der Verteilung von S-Lost ein 2-Kompartimentmodell ermittelt. Dabei kommt es zunächst zu einer schnellen Verteilung (initiale Halbwertszeit, $t_{1/2\,\alpha}$ = 5,56 min; Verteilungsvolumen in steady state, V_{dss} = 74,4 l/kg), gefolgt von einer langsamen Eliminationsphase (terminale Halbwertszeit, $t_{1/2\,\beta}$ = 3,59 h) (*39*). Eine Anreicherung konnte insbesondere in lipophilen Geweben und Organen, wie z. B. dem subkutanen Fettgewebe der Haut und dem Gehirn, nachgewiesen werden (*40*).

Metabolisierung

Das bifunktionelle S-Lost geht unter physiologischen Bedingungen über ein hochreaktives intermediär gebildetes Episulfonium Ion verschiedene Reaktionswege ein, deren Produkte oftmals für die Verifikationsanalytik verwendet werden (*4, 41, 42*).

- Durch Oxidation entsteht Bis-ß-chlorethyl Sulfoxid. Das nach Hydrolyse gebildete TDG kann weiter zu Thiodiglycol-Sulfoxid (TDGO) und Thiodiglycol-Sulfon oxidieren (*43–46*).

- Nach der Reaktion mit Glutathion, anschließender Oxidation und der darauf folgenden β-Lyase-katalysierten Spaltung werden die Produkte 1,1´-Sulfonylbis-[2-S-(N-acetylcysteinyl) ethan], 1,1´-Sulfonylbis-[2-(methylthio) ethan], 1-Methylsulfinyl-2-[2-(methylthio) ethylsulfonyl] ethan und 1,1´-Sulfonylbis-[2-(methylsulfinyl) ethan] gebildet (*47, 48*).

- Bei der Reaktion mit nukleophilen Atomen endogener Moleküle, wie N-Acetylcystein, Hormonen, Desoxyribonukleinsäure (DNA)-/Ribonukleinsäure (RNA)-Basen und Proteinen kann es zu intra- oder intermolekularen Quervernetzungen über einen Ethylthioethyl-Linker kommen oder es bildet sich nach anschließender Hydrolyse eine charakteristische kovalent gebundene Hydroxyethylthioethyl (HETE)-Einheit aus (Abbildung 2) (*4, 41, 42, 49–52*).

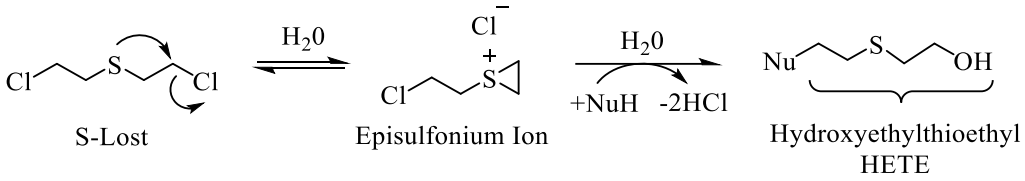

Abbildung 2: Reaktionsmechanismus von S-Lost im wässrigen Milieu. S-Lost bildet über einen intramolekularen Ringschluss das hochreaktive elektrophile Episulfonium Ion. Nach Reaktion mit nukleophilen Gruppen endogener Moleküle (NuH) und anschließender Hydrolyse kommt es zur Ausbildung einer Hydroxyethylthioethyl (HETE)-Einheit (*7, 41*).

Für die Toxizität von S-Lost wird überwiegend die Adduktierung der DNA- und RNA-Basen Adenin an der N^3-Position (N^3-[2-[(2-Hydroxyethyl) thio] ethyl] -adenin), Guanin an den Positionen N^7 und O^6 (N^7-[2-[(2-hydroxyethyl) thio] ethyl] -guanin, O^6-[2-[(2-Hydroxyethyl) thio] ethyl] -guanin), sowie zwischen zwei Guaninen (Bis[2-(guanin-7-yl) ethyl] sulfid) verantwortlich gemacht (*51, 53, 54*).
Aufgrund der Abundanz und Langlebigkeit sind die S-Lost-Addukte am humanen Serumalbumin (HSA) und dem Hämoglobin (Hb) von großer Bedeutung für den analytischen Nachweis einer S-Lost-Exposition (siehe 1.1.8 Massenspektrometrische Verifikationsanalytik) (*4, 41*).

Elimination

Mit einer Gesamtkörper-Clearance von ca. 21 L/kg/h werden ca. 80% des S-Lostes über die Niere, respektive den Urin ausgeschieden (*39*). Dabei wurden in tiermedizinischen Studien mit radioaktiv markiertem S-Lost, hauptsächlich an Glutathion konjugiertes S-Lost sowie

Metabolisierungsprodukte im Urin gefunden (*55*). Nur 3% des inkorporierten S-Lostes werden über den Fäzes eliminiert (*39*).

1.1.6 Schutzmaßnahmen und Therapie

Im Falle einer S-Lost-Exposition müssen betroffene Personen möglichst schnell dekontaminiert werden, um damit die Menge aufgenommenen Kampfstoffes zu minimieren. Das Entfernen der Kleidung bewirkt schon eine Dekontamination von ca. 80% (*56*). Augen werden mit isotonischer Kochsalzlösung (0,9% w/v) gespült, der restliche Körper wird idealer Weise mit speziellen Hautdekontaminationsmitteln, z. B. Reactive Skin Decontamination Lotion (RSDL), von verbliebenem S-Lost befreit (*56*). Stehen diese nicht zur Verfügung ist schon das Abwaschen mit Seife und Wasser hilfreich (*56*). Eine vollständige Entfernung des anhaftenden S-Lostes ist aber auch mit RSDL nicht möglich. Insbesondere Haare halten dampfförmiges S-Lost zurück und verhindern dessen schnelle Verdunstung (*56*). Bei Untersuchungen mit 2-Chloroethylethylsulfid (CEES), welches als Strukturanaloga von S-Lost eingesetzt wird, war auch mit RSDL nur ein maximaler Dekontaminations-Erfolg der Haare von ca. 80% erreichbar (*57*). Im Fall des Entfernens der Haare müssen deren bestehende Kontaminationsgefahr und das Vermeiden von Läsionen der Kopfhaut, welche eine dermale Penetration verstärken könnten, besonders berücksichtigt werden (*57*). Trotz intensiver Forschung gibt es bis heute kein Antidot und keine kausale Therapie gegen eine S-Lost-Vergiftung (*58*). Eine Therapie kann immer nur individuell, symptomatisch und abgestimmt auf die betroffenen Körperregionen erfolgen (*58*).

1.1.7 2D-thiol-DIGE

Die multifaktorielle Komplexität einer S-Lost-Intoxikation bedingt das Fehlen einer kausalen Therapie sowie das unvollständige Verständnis der zugrundeliegenden Pathomechanismen. Um diesbezüglich neue Einblicke zu erhalten, sind ganzheitliche Untersuchung zu Auswirkungen auf das Proteom nach S-Lost-Einwirkung umso bedeutender (*59–61*). Ein eigens entwickeltes Verfahren basierend auf der zweidimensionalen Differenz-Gelelektrophorese (englisch „two-dimensional difference gel electrophoresis“, 2D-DIGE) (*62–65*), dient der Identifizierung von an Cysteinen alkylierten Proteinen (Abbildung 3) (*66*). Mit dieser 2D-thiol-DIGE-Technik können zwei Proteinproben, eine mit und eine ohne Exposition mit Alkylanzien, simultan auf einem Gel miteinander verglichen werden. Dabei wird das bekannte S-Lost-Analogon CEES als monofunktionales Alkylanz eingesetzt, das im Gegensatz zu S-Lost keine Quervernetzungen und damit eine weniger komplexe Proteinmischung erzeugt (*67, 68*). Dies und die Depletion von HSA und Immunglobulinen G aus Plasma ohne CEES (Blank) und mit CEES (Probe) vereinfacht und ermöglicht eine fokussierte elektrophoretische Trennung (Abbildung 3 a) (*69*). Die Proteine in Blank und Probe werden mit unterschiedlichen Thiolgruppen-reaktiven Infrarot-Maleimid-Fluoreszenzfarbstoffen (DY-680, DY-800), die sich in ihrer Extensions- und Emissionswellenlänge unterscheiden, versetzt (Abbildung 3 b). Dabei kommt es zur Ausbildung einer kovalenten Bindung an freie Thiolgruppen (*68, 69*). Dieses „Markieren“ hat keinen Einfluss auf die relative Migration der Proteine bei der anschließenden zweidimensionalen Gelelektrophorese (2D-GE) einer aus Blank und Probe kombinierten Mischung (Abbildung 3 c) (*69, 68*). Gleiche Proteine liegen bei den entstehenden Spots übereinander und zeigen ein bestimmtes relatives Fluoreszenz-Signal-Verhältnis.

Äquivalente Mengen werden als Mischfarbe der eingesetzten Farbstoffe detektiert (Abbildung 3 d). Abweichungen des Fluoreszenz-Signal-Verhältnisses weisen auf eine unterschiedliche Menge an zum Labeln zur Verfügung stehenden Cysteinseitenketten als Folge einer zuvor erfolgten Alkylierung hin. Die 2D-thiol-DIGE-Methode ist dabei hochsensitiv und reproduzierbar. Eine Identifizierung der visualisierten Proteine erfolgt anschließend aus einem äquivalent hergestellten und mit Coomassie-Brillant-Blau (englisch: „Coomassie-Brilliant-Blue“, CBB) gefärbten 2D-Gel mittels matrixunterstützter Laser-Desorption/Ionisation Flugzeitmassenspektrometrie (englisch „matrix-assisted laser desorption/ionization time-of-flight mass spectrometry“, MALDI-TOF-MS/MS) (Abbildung 3 e, f) (*64, 70*).

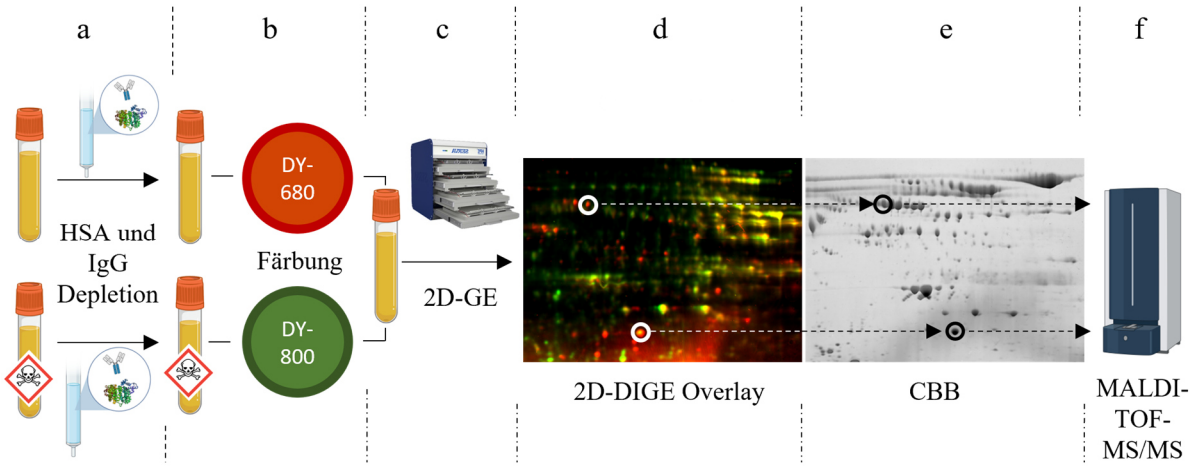

Abbildung 3: Schema des Arbeitsablaufes der 2D-thiol-DIGE-Methode zur Identifizierung von durch Alkylanzien modifizierten Plasmaproteinen. (a, b) Plasma ohne 2-Chloroethylethylsulfid (CEES) Zugabe und mit CEES-inkubiertes Plasma werden nach Depletion von humanem Serumalbumin (HSA) und Immunglobulinen G (IgG) mit unterschiedlichen Thiolgruppen-reaktiven Maleimid-Farbstoffen (DY-680, DY-800) versetzt. (c, d) Nach Vereinigung gleicher Proteinmengen und zweidimensionaler Gelelektrophorese (2D-GE) weisen intensivere rote Spots in der überlagerten Darstellung der aufgenommenen Floreszenz (2D-DIGE Overlay) auf an Cysteinen alkylierte Proteine hin. (e, f) Die Identifizierung der Proteine erfolgt aus äquivalent angefertigten und mit Coomassie-Brilliant-Blau (CBB) gefärbten Gelen mittels matrixunterstützter Laser-Desorption/Ionisation Flugzeitmassenspektrometrie (MALDI-TOF-MS/MS) (*66*).

1.1.8 Massenspektrometrische Verifikationsanalytik

Für die Umsetzung des CWÜ ist eine eindeutige Verifikation von Reaktions- und Abbauprodukten des S-Lost Grundvoraussetzung. Dafür arbeitet die OVCW mit Laboratorien zusammen, die durch alljährliche Biomedical Proficiency Tests designiert sind und die über hochselektive und sensitive bioanalytische Verfahren zur Detektion verfügen (*58, 71, 72*). Gaschromatographische (englisch „gas chromatography“, GC) und flüssigchromatographische (englisch „liquid chromatography“, LC) Trennverfahren in Kopplung mit

Massenspektrometrie (MS) dienen heutzutage standardmäßig der Detektion von Biomarkern, die aus unterschiedlichen Matrices (Blut, Plasma, Serum, Urin, Gewebe) gewonnen werden (*4, 40, 41*). Die nach Hydrolyse, Oxidation oder auch durch β-Lyase gebildeten Biotransformationsprodukte sind dabei nur wenige Tage nachweisbar (*41*). TDG und TDGO sind zudem mit Konzentrationen von bis zu 16 ng/ml bzw. 36 ng/ml endogen im Körper vorhanden, was deren Eignung als Biomarker zusätzlich einschränkt (*45, 46*). Nur eine deutlich erhöhte Konzentration kann zum Nachweis einer exogenen Zufuhr und damit einer S-Lost-Intoxikation herangezogen werden. Aufgrund ihrer in geringsten Konzentrationen langen *in vivo* Nachweisbarkeit von Wochen bis zu Monaten nach Exposition sind Proteinaddukte von herausragender Bedeutung für die Verifikationsanalytik (*4, 41, 58*). Etablierte Methoden umfassen unter anderem die Addukte von S-Lost mit dem höchst abundanten Plasmaprotein HSA. Die Alkylierung findet überwiegend an der Thiolgruppe der Seitenkette des Cysteins in Position 34 (Cys^{34}) statt, wobei eine Vielzahl von weiteren Aminosäuren im HSA konzentrationsabhängig mit S-Lost reagiert (*4, 71, 73, 74, 3, 75–77*). Das nach Proteolyse generierte Dipeptid Cys^{34}(-HETE)Pro (C^{34}(-HETE)P), sowie das Tripeptid Cys^{34}(-HETE)ProPhe (C^{34}(-HETE)PF) stellen die derzeit sensitivsten Biomarker einer S-Lost-Exposition dar (*4, 52, 71, 73, 77, 74*). Beim Hb entstehen HETE-Addukte insbesondere am N-terminalen Valin (Val) sowie weiteren Valinen und Histidinen. (*44, 52, 78*). Über das nach enzymatischer Spaltung generierte HETE-Val lässt sich S-Lost bis zu drei Monate nach Exposition nachweisen (*41, 52*). Damit stellt das adduktierte N-terminale Valin den aktuell am längsten zu detektierenden Biomarker in der Zirkulation dar.

1.1.9 Probengewinnung und Transport

Der Einsatz von S-Lost findet zumeist in infrastrukturschwachen Krisengebieten statt (*4*). Dies birgt große Herausforderungen für die Probennahme und den anschließenden Transport in ein für die Verifikationsanalytik verantwortliches, designiertes Labor. Die dafür verwendeten typischen Probenmatrices, wie flüssiges Blut, Plasma oder Serum, müssen mittels invasiver Verfahren gewonnen werden, die geschultes Personal und Schutzausrüstung erfordern. Zudem stellen diese Matrices potentiell infektiöses Material dar (*79*). Für den Transport zu den designierten Laboratorien gelten deshalb, je nach Transportart, strenge Regularien bezüglich Verpackung und Deklaration. Beim Transport im Flugzeug müssen die international gültigen Vorschriften der Internationalen Luftverkehrs-Vereinigung (International Air Transport Association) und deren Gefahrgutvorschriften „Dangerous Goods Regulations“ beachtet werden (*80*). Entsprechende Regelungen gibt es auch für die Beförderung auf der Straße (Agreement concerning the International Carriage of Dangerous Goods by Road) und zur See (International Maritime Dangerous Goods Code) (*81, 82*). Getrocknetes Blut oder Plasma, das mittels Microsampling Devices (Mitra Microsampling Devices und Noviplex Duo Cards) generiert wurde, gilt nicht als potentiell infektiöses Material und kann deshalb unkomplizierter versandt werden (*83*). Der Nachweis einer S-Lost-Exposition mittels LC-MS aus den Microsampling Devices wurde am Institut für Pharmakologie und Toxikologie der Bundeswehr etabliert (*83*). Dennoch ist die Notwendigkeit einer invasive Probennahme am Menschen bisher kaum zu vermeiden.

1.1.10 Haare als Probenmatrix

Haarproben sind im Gegensatz zu Blut- und Urinproben einfach, nicht invasiv zu gewinnen. Die Haare dienen in der forensischen Analytik als wichtige Probenmatrix für den Nachweis einer Vielzahl von anhaftenden oder eingelagerten Substanzen, wie beispielsweise von Rauschgiften oder Medikamenten (*84*). Die Inkorporation in die Haare erfolgt dabei über den Blutkreislauf, über Schweiß und Talg sowie über den Kontakt mit Stäuben, Aerosolen oder Flüssigkeiten (*85*).
So konnten die S-Lost-Analoga CEES und Salicylsäuremethylester, nach *in vitro* mit diesen Substanzen bedampften Haaren, nachgewiesen werden (*86*). Nicht biotransformiertes S-Lost wurde in Haarproben einer im Irak-Iran Krieg 1986 exponierten Person nach einer Methylenchlorid-Extraktion mittels GC-MS detektiert (*87*).
Hauptbestandteile von Haaren sind mit 60-95% die Proteine Hartkeratine (*85*). Aufgrund deren helikaler Struktur sowie starker intramolekularer Disulfidverbrückungen von Cysteinen, weisen Haare eine besonders hohe Rigidität auf (*88, 89*). Für Untersuchungen des Haarproteoms ist deshalb eine spezielle Lyse der Haare, bei der die Disulfidbrücken reduziert werden und die Haarproteine in Lösung gehen, eine wichtige Voraussetzung (*90, 91*). Im Gegensatz zu im Blut zirkulierenden Proteinaddukten unterliegen insbesondere die Haarschäfte keiner kontinuierlichen Biotransformation und stellen somit eine interessante Probenmatrix für den Nachweis von Stoffen über Monate hinweg dar (*92*). Ein Analyseverfahren zur Detektion einer S-Lost-Exposition über adduktierte Haarproteine war bisher nicht bekannt.

2 Zielsetzung der Arbeit

Bei neuen Biomarkern liegen die Hauptaugenmerke auf Charakteristika wie Selektivität, Regiospezifität, zeit- und konzentrationsabhängigen Nachweisgrenzen, sowie Komplexität der Probennahme und des Transportes.

2.1 Erster Teil der Arbeit: Plasmaproteine

Der erste Teil der Dissertation sollte sich mit der Identifizierung von bisher nicht als Zielstruktur von S-Lost bekannten Plasmaproteinen und der darauf basierenden Entwicklung eines neuen potentiellen Biomarkers für eine S-Lost-Intoxikation befassen. Dafür war die Verwendung der eigens etablierten 2D-thiol-DIGE-Methode vorgesehen, um durch das S-Lost-Analogon CEES an reaktiven Cysteinen modifizierte Plasmaproteine zu visualisieren (*66*). Die eindeutige Identifizierung der alkylierten Proteine sollte über 2D-GE mit CBB-Färbung, anschließender In-Gel Proteolyse und MALDI-TOF-MS/MS erfolgen (*66*). Der direkte Nachweis des entsprechenden S-Lost-Proteinadduktes, eines auf diese Weise identifizierten CEES-alkylierten Proteins aus menschlichem Plasma, war bisher nicht erfolgt und daher ein Ziel dieser Arbeit.
Für die Etablierung einer Verifikationsmethode, also für den Nachweis eines aus dem alkylierten Protein generierten potentiellen Biomarkerpeptids, war die Entwicklung und Optimierung einer Aufarbeitungsmethode von komplexen Plasmaproben notwendig. Zentrale Elemente waren dabei die Aufkonzentrierung des Zielproteins und dessen enzymatische Proteolyse. Die Detektion des damit generierten Peptids, das die durch S-Lost-gebildete HETE-Modifikation am Cystein trägt, war mittels LC gekoppelter hochauflösender Massenspektrometrie (englisch „liquid chromatography coupled to high-resolution mass spectrometry“, LC-MS/HR-MS) angedacht. Bei der Charakterisierung dieses Biomarkerpeptids sollten Aspekte, wie die Nachweisgrenze und deren Verhältnisses zu etablierten Biomarkern sowie interindividuelle Unterschiede, untersucht werden.

2.2 Zweiter Teil der Arbeit: Haarproteine

Die aufwendige Beprobung und der Versand von Blut, Plasma und Urin für die Verifikationsanalytik, die häufig in internationalen Krisengebieten mit schlechter Infrastruktur erfolgen, stellen große Herausforderungen dar (*4, 23*). Damit besteht die akute Notwendigkeit der Erweiterung des Methodenspektrums auf eine einfach zu handhabende Matrix.
In einem realen Expositionsszenario kommt es meist zu einer großflächigen Ausbreitung von flüssigem und gasförmigem S-Lost und damit auch zur äußerlichen Benetzung von Haut und Haaren (*4, 58*). Deshalb sollten im zweiten Teil der Dissertation Haarproteine als potentielle Zielstruktur von S-Lost untersucht werden. Haare müssen nicht mittels invasiver Verfahren gewonnen werden und gelten im Vergleich zu flüssigem Blut, Plasma und Urin nicht als potenziell infektiöses Material. Sie unterliegen diesbezüglich keinen strengen Transportregularien und sind damit unkompliziert zu versenden (*79–82*).
Bis jetzt gibt es nur sehr wenige Analysen zu kovalenten Proteinmodifikationen in Haaren und keine Methode, mit der potentielle Addukte von chemischen Kampfstoffen an den strukturgebenden Haarproteinen Hartkeratine untersucht werden können (*90, 93, 94*).

Weichkeratine aus der Haut und kultivierten menschlichen Keratinozyten sind bereits dafür bekannt von S-Lost modifiziert zu werden (*61, 95*).
Deshalb sollte eine Methodik entwickelt werden, die es ermöglicht, eine regionale S-Lost-Exposition von Haaren über kovalente Hartkeratinaddukte und daraus gewonnene Biomarkerpeptide zu verifizieren. Für die Aufarbeitung sollte ein Lyseverfahren entwickelt werden, das es erlaubt, Hartkeratine in Lösung zu bringen, anschließend enzymatisch zu proteolysieren und adduktierte Peptide als potentielle Biomarker mittels LC-MS/HR-MS zu identifizieren. Eine eindeutige Zuordnung der Hartkeratine als Ursprung der Biomarkerpeptide sollte über Natriumdodecylsulfat-Polyacrylamidgelelektrophorese **(**englisch „sodium dodecyl sulfate polyacrylamide gel electrophoresis“, SDS-PAGE) erfolgen. Neben der Charakterisierung und Optimierung aller Aufarbeitungsschritte war beabsichtigt, die Biomarkerpeptide hinsichtlich Selektivität, Nachweisgrenze, interindividueller Unterschiede und Regiospezifität zu validieren. Aufgrund der Rigidität der Haare sollte ein besonderes Augenmerk auf die Langlebigkeit potenzieller Addukte an Hartkeratinen und die damit verbundene Generierung von adduktierten Peptiden als Langzeitbiomarker gelegt werden.

Die erzielten Ergebnisse werden im Folgenden jeweils als Zusammenfassungen und in den Originalarbeiten dargestellt.

3 Veröffentlichungen

3.1 Erste Veröffentlichung

Transthyretin as a target of alkylation and a potential biomarker for sulfur mustard poisoning: Electrophoretic and mass spectrometric identification and characterization

W. Schmeißer, R. Lüling, D. Steinritz, H. Thiermann, T. Rein, H. John.
Drug Testing and Analysis, 14(1):80-91, 2022.
DOI: 10.1002/dta.3146

Zunächst sollten bisher unbekannte Plasmaproteine identifiziert werden, welche reaktive Cysteine enthalten und Zielstrukturen von Alkylanzien darstellen. Nach der Abtrennung von HSA und IgG wurde mit CEES (Probe) und EtOH (Blank) präinkubiertes Plasma separat mit den Cystein-selektiven Infrarot-Maleimid-Farbstoffen DY-800 (Probe) und DY-680 (Blank) versetzt. Nach der Vereinigung gleicher Proteinmengen von Probe und Blank und anschließender simultaner 2D-GE wiesen zwei getrennte Spots (Spot 1 und 2), bei ca. 15 kDa Molekulargewicht und einem Isoelektrischen Punkt von 5, eine eindeutig intensivere Färbung vom DY-680 Farbstoff ausgehend auf. Dies deutete auf eine, bedingt durch eine vorherige Alkylierung, verringerte Bindung von DY-800 an einem Cystein hin. Um zu zeigen, dass der detektierte Farbunterschied nicht auf unterschiedlichen Proteinmengen beruht, wurden jeweils von Probe und Blank 2D-Gele angefertigt und mit CBB gefärbt. Hier wiesen die gemessenen Färbungsintensitäten keinen Unterscheid auf, was bewies, dass gleiche Mengen des Proteins vorhanden sind und der zuvor detektierte Farbunterschied ein alkyliertes Protein anzeigt.

Für die Identifizierung der Proteine von Spot 1 und 2, wurden die Spots aus einem mit CBB gefärbten Gel ausgeschnitten, eine In-Gel Proteolyse mit Trypsin durchgeführt und anschließend mittels MALDI-TOF-MS/MS analysiert. Für beide Spots wurde mit einer Sequenzübereinstimmung von 98.8% für Spot 1 und 93.9% für Spot 2 Transthyretin (TTR) identifiziert. Das beide Spots TTR aufwiesen, wurde auf unterschiedliche posttranslationale Modifikationen, wie z. B. Phosphorylierungen, zurückgeführt (*96*).

Auf diesen Ergebnissen aufbauend sollte die Übertragung auf S-Lost erfolgen und die Alkylierungsstelle in TTR identifiziert werden. Das mit S-Lost inkubierte Plasma wurde mit Trypsin proteolysiert, um die generierten Peptide nach LC-Auftrennung mittels hochauflösender Flugzeitmassenspektrometrie (englisch „high-resolution time-of-flight mass spectrometry“ TOF-MS/HR-MS) in einem informationsabhängigen Messmodus (englisch „information-dependent aquisition“) gemessen. Bei der Auswertung wurden insbesondere die für ein HETE-modifiziertes Cystein charakteristischen Produktionen bei *m/z* 105,037 und *m/z* 137,009 als diagnostische Marker herangezogen (*52, 71, 73*). Über die Detektion der bei der Fragmentierung gebildeten Produktionen konnte das Hexapeptid Cys^{10}(-HETE)ProLeuMetValLys (C^{10}(-HETE)PLMVK) identifiziert werden, das an der im TTR an Position 10 befindlichen Cysteinseittenkette (Cys^{10}) alkyliert ist. Für den Vergleich der gemessenen und theoretischen Produktionen galt eine akzeptable Massenabweichung von Δ m/z < 10 ppm. Eine Betrachtung der animierten Kristallstruktur von TTR zeigte, dass das Cys^{10} gut zugänglich auf der Oberfläche des Proteins lokalisiert ist und dessen Reaktivität

aufgrund der räumlichen Nähe zu einem Histidin zusätzlich gesteigert ist. Dies untermauerte, dass das Cys^{10} in TTR von S-Lost alkyliert wird.

Daraufhin sollte die Eignung von C^{10}(-HETE)PLMVK als Biomarkerpetpid für eine Verifikationsanalytik von S-Lost untersucht werden. Für die folgenden Versuche wurden deshalb mit einer sensitiveren gezielten Messmethode (englisch „targeted analysis“) die Übergänge auf die intensivsten Produktionen gemessen.

Für die Aufreinigung und -konzentration von alkyliertem TTR wurde eine spezifische immunomagnetische Separation durchgeführt (*97*). Hierfür wurden verschiedene monoklonale Antikörper getestet. Der Antikörper, der die höchste zu detektierende Menge an C^{10}(-HETE)PLMVK erbrachte, wurde für das Standardprotokoll beibehalten.

Um die Validität der Methode zu zeigen, wurde die Stabilität des alkylierten TTR in Plasmaproben nach fünfmaligem Einfrieren und Auftauen (Frier-Tau-Zyklus), sowie bei der Lagerung über 14 Tage bei 37°C überprüft. Außerdem wurde die Stabilität des C^{10}(-HETE)PLMVK in der Messlösung im Autosampler (15°C) getestet. Unter allen gewählten Bedingungen konnte das Biomarkerpeptid gleichbleibend gemessen werden. Dies zeigte, dass die Methode auf gefrorene und nicht gekühlte Proben angewendet werden kann und die Messung eines größeren Probensatzes ohne Probleme möglich ist. Bei der Messung von 7 Blankplasmen (ohne S-Lost) konnten keine störenden Interferenzen bei der erwarteten Retentionszeit von C^{10}(-HETE)PLMVK detektiert werden, was die hohe Selektivität der Methode zeigt.

Für eine optimale Ausbeute an Biomarkerpeptid wurden, nach unterschiedlichen Zeitpunkten der Proteolyse von alkyliertem TTR mit Trypsin, Messungen durchgeführt. Die zu detektierende Menge an C^{10}(-HETE)PLMVK ging nach 2 h in ein stabiles Plateau über, weshalb für die Standardproteolysezeit 4 h festgelegt wurde, um eine maximale Ausbeute zu erreichen.

Die Ermittlung der, mit der optimierten Methode über C^{10}(-HETE)PLMVK, minimal nachweisbaren Konzentration (Nachweisgrenze, englisch „limit of detection“, LOD) an S-Lost in Plasma, ergab unter Berücksichtigung der Vorgaben der OVCW eine Konzentration von 32,25 µM. Diese ist deutlich höher als die Nachweisgrenze der aus HSA generierten Biomarkerpeptide C^{34}(-HETE)P und C^{34}(-HETE)PF. Ursächlich dafür sind wahrscheinlich die deutlich geringere Plasmakonzentration von TTR im Vergleich zu HSA im Plasma. Außerdem treten, aufgrund der hohen Reaktivität des Cys^{10} im TTR, dort in hohem Maße posttranslationale Modifikationen auf (*98–100*).

Für die Untersuchung von interindividuellen Unterschieden wurden S-Lost-inkubierte Plasmaproben von 7 verschiedenen Personen verwendet. Bei allen 7 Proben konnte C^{10}(-HETE)PLMVK eindeutig nachgewiesen werden. Die gemessene Menge zwischen den Proben variierte hingegen deutlich. Dies wurde auf individuelle TTR Konzentrationen und die posttranslationalen Modifikationen zurückgeführt (*98–100*).

Die Ergebnisse zeigen, dass TTR eine neue Zielstruktur im Plasma für eine Alkylierung durch S-Lost darstellt. Zudem erweitert das nach Proteolyse generierte Hexapeptid C^{10}(-HETE)PLMVK das Spektrum bisher bekannter Biomarker für die Verifikationsanalytik einer S-Lost-Exposition.

Received: 7 May 2021 | Revised: 6 August 2021 | Accepted: 9 August 2021

DOI: 10.1002/dta.3146

RESEARCH ARTICLE

WILEY

Transthyretin as a target of alkylation and a potential biomarker for sulfur mustard poisoning: Electrophoretic and mass spectrometric identification and characterization

Wolfgang Schmeißer[1] | **Robin Lüling**[1,2] | **Dirk Steinritz**[1,2,3] | **Horst Thiermann**[1] | **Theo Rein**[4] | **Harald John**[1]

[1]Bundeswehr Institute of Pharmacology and Toxicology, Munich, Germany

[2]Walther-Straub Institute of Pharmacology and Toxicology, Ludwig-Maximilians-Universität Munich, Munich, Germany

[3]Bundeswehr Medical Service Academy, Munich, Germany

[4]Department of Translational Research in Psychiatry, Max Planck Institute of Psychiatry, Munich, Germany

Correspondence
Harald John, Bundeswehr Institute of Pharmacology and Toxicology, Munich, Germany.
Email: haraldjohn@bundeswehr.org

Funding information
German Research Foundation, Grant/Award Number: GRK 2338

Abstract

For the verification of exposure to the banned blister agent sulfur mustard (SM) and the better understanding of its pathophysiology, protein adducts formed with endogenous proteins represent an important field of toxicological research. SM and its analogue 2-chloroethyl ethyl sulfide (CEES) are well known to alkylate nucleophilic amino acid side chains, for example, free-thiol groups of cysteine residues. The specific two-dimensional thiol difference gel electrophoresis (2D-thiol-DIGE) technique making use of maleimide dyes allows the staining of free cysteine residues in proteins. As a consequence of alkylation by, for example, SM or CEES, this staining intensity is reduced. 2D-thiol-DIGE analysis of human plasma incubated with CEES and subsequent matrix-assisted laser desorption/ionization time-of-flight (tandem) mass-spectrometry, MALDI-TOF MS(/MS), revealed transthyretin (TTR) as a target of alkylating agents. TTR was extracted from SM-treated plasma by immunomagnetic separation (IMS) and analyzed after tryptic cleavage by microbore liquid chromatography-electrospray ionization high-resolution tandem-mass spectrometry (μLC-ESI MS/HR MS). It was found that the Cys^{10}-residue of TTR present in the hexapeptide C(-HETE)PLMVK was alkylated by the hydroxyethylthioethyl (HETE)-moiety, which is characteristic for SM exposure. It was shown that alkylated TTR is stable in plasma in vitro at 37°C for at least 14 days. In addition, C(-HETE)PLMVK can be selectively detected, is stable in the autosampler over 24 h, and shows linearity in a broad concentration range from 15.63 μM to 2 mM SM in plasma in vitro. Accordingly, TTR might represent a complementary protein marker molecule for the verification of SM exposure.

KEYWORDS
2D-thiol-DIGE, high-resolution mass spectrometry, sulfur mustard, transthyretin, verification

Schmeißer and Lüling contributed equally to this work.

1 | INTRODUCTION

Sulfur mustard (SM, bis[2-chloroethyl] sulfide, CAS No. 505-60-2) is a well-known chemical warfare agent belonging to the class of vesicants.[1,2] Depending on the amount of SM and the time of contact to the skin, a symptom-free latency period of up to 24 h may appear followed by erythema, blisters and subsequent difficult-to-heal ulcerations.[3,4] After the first use for military purposes in World War I, SM was used in other armed conflicts until today.[3] The Chemical Weapons Convention (CWC) prohibits the development, production, stockpiling, and use of chemical warfare agents in general.[5] Nevertheless, the Organisation for the Prohibition of Chemical Weapons (OPCW), which is responsible for the supervision and compliance of the CWC, has evidence for the repeated use of SM in the ongoing violent conflict in the Middle East.[6,7] Therefore, analytical and especially bioanalytical methods are indispensable to prove or disprove an alleged use of any chemical warfare agent and related poisoning.

For verification of SM poisoning, protein-adducts are well-suited analytical target molecules because of their long half-lives compared to those of hydrolysis and enzymatic biotransformation products.[8,9] As a highly electrophilic compound, SM reacts with nucleophilic groups of endogenous molecules like proteins, DNA bases, hormones, or glutathione, thus forming covalent modifications by addition of a characteristic hydroxyethylthioethyl (HETE)-moiety.[2,10–14] In particular, free thiol-groups of cysteines represent highly reactive targets for alkylation by SM. Human serum albumin (HSA) contains a free cysteine residue at position 34 (Cys^{34}), which may be alkylated by SM. Following its enzymatic proteolysis, biomarker peptides containing the alkylated Cys^{34} residue are produced and detected to prove SM poisoning.[9,15–18] However, the identification of additional protein-adducts is of general interest for verification purposes.

For the investigation of proteome variations, the technique of fluorescent two-dimensional difference gel electrophoresis (2D-DIGE) presented for the first time by Ünlü et al. has been established.[19,20] 2D-DIGE allows covalent labeling of proteins in various samples (e.g., a control and a test group) with different fluorescent dyes, followed by mixing and simultaneous separation by two-dimensional gel electrophoresis (2D-GE) in a single gel.[21,22] Common dyes used are cyan fluorescent dyes, binding to the epsilon amino-group of lysine residues and infrared (IR) maleimide dyes, binding to free thiol-groups of cysteines.[23,24] For detection, the distinct fluorescence of the dyes is recorded, which intensity depends on the amount of the protein-attached dye.[25] This allows relative quantification of the respective protein amounts and post-translational modifications, which occur at the same binding sites as those of the dyes and prevent dye binding.[26] As recently published, a specific 2D-thiol-DIGE method was developed by our group for the identification of proteins modified by covalent binding of alkylating agents like SM or CEES (2-chloroethyl ethyl sulfide) to free thiol-groups of cysteines, which thus show a reduced binding capacity for IR maleimide dyes.[27]

The aim of this study was to identify proteins that are targets of alkylating substances by 2D-thiol-DIGE and matrix-assisted laser desorption/ionization time-of-flight (tandem) mass-spectrometry, MALDI-TOF MS(/MS). Subsequently, a microbore liquid chromatography-electrospray ionization high-resolution tandem-mass spectrometry (μLC-ESI MS/HR MS) method was developed and optimized for the detection of a protein-derived peptide to characterize its suitability for verification of SM exposure.

2 | MATERIALS AND METHODS

2.1 | Chemicals

Acetonitrile (ACN, LC-MS grade), ethanol (EtOH, ≥99.8%), formic acid (FA, >98%), methanol (MeOH, hypergrade for LC-MS), ProteoExtract^{R} Albumin-IgG Removal Kit MAXI, sodium azide (NaN_3, extra pure), trifluoroacetic acid (TFA, ≥99.0% for HPLC), Tween® 20, ultrafiltration (UF) devices (Amicon Ultra-0.5 centrifugal filter unit, 0.5 ml, molecular weight cut-off, MWCO, 10 kDa), and water (LC-MS grade) were obtained from Merck (Darmstadt, Germany). 2-Chloroethyl ethyl sulfide (CEES, 97%), 3-[(3-cholamidopropyl)dimethylammonio]-1-propanesulfonate (CHAPS, 98%), dimethyl pimelimidate dihydrochloride (DMP), dithiothreitol (DTT, ≥98%, HPLC), glacial acetic acid (HAc), iodoacetamide (IAA, ≥99%), L-cysteine (≥97%), *N*,*N*-dimethylformamide (DMF, 99.8%), phosphate buffered saline (PBS), NaCl (≥99%), thiourea (≥99%), triethanolamine (TEA, ≥99% [GC]), trypsin from porcine pancreas (BioReagent), trypsin profile in-gel digestion (IGD) kit, and urea (≥98%) were from Sigma-Aldrich (Steinheim, Germany). Dynabeads™ Protein G were from Thermo Fisher Scientific (Waltham, Massachusetts, USA) and recombinant monoclonal anti-prealbumin antibodies (ab185127 and ab204997) from Abcam (Cambridge, United Kingdom). Anti-prealbumin mouse monoclonal antibodies (clone: 9G6 and clone: 10E1) were from VWR International (Radnor, Pennsylvania, USA). NH_4HCO_3 (ultra-grade, ≥99.5%) was purchased from Fluka (Buchs, Switzerland), threefold deuterated atropine (d_3-Atr) from CDN Isotopes (Pointe Claire, Quebec, Canada), tris(hydroxymethyl) aminomethane (TRIS) from Roche Diagnostics (Mannheim, Germany), and trichloroacetic acid (TCA, ≥99%) from Carl Roth (Karlsruhe, Germany). 2D-Quant Kit and PhastGel Blue R were from GE Healthcare (Freiburg, Germany). 2D HPE™ Large Gel NF 12.5% Kit, immobilized pH gradient (IPG) Blue Strip pH 4–7/24 cm and HPE™ IPG strip buffer were purchased from SERVA Electrophoresis GmbH (Heidelberg, Germany). Infrared maleimide dyes (DY-680 and DY-800) were provided by Dyomics (Jena, Germany) and α-cyano-4-hydroxycinnamic acid (CHC, ultra-pure) by Bruker Daltonics (Bremen, Germany). Human EDTA plasma from different individuals was purchased from in.vent Diagnostica (Hennigsdorf, Germany). SM was provided by the German Ministry of Defense and integrity as well as purity were proved in-house by nuclear magnetic resonance spectroscopy.

2.2 | 2D-thiol-DIGE and MALDI-TOF MS(/MS) analysis

2.2.1 | Incubation of plasma with CEES and labeling with IR maleimide dyes

EDTA plasma (487.5 µl) was mixed with 12.5 µl CEES in EtOH (final concentration in plasma 5 mM). Blanks were mixed with 12.5 µl EtOH exclusively. Subsequent incubations were carried out for 1 h at 37°C under continuous shaking. Samples and blanks were frozen at −20°C until further processing. Using the ProteoExtract^{R} Albumin-IgG Removal Kit MAXI, samples and blanks were depleted of HSA and immunoglobulin G (IgG) according to the manufacturer's instructions. Depleted plasma was mixed with twice the volume ice-cold 10% (w/v) TCA for protein precipitation and centrifuged (50,000 RCF, 15 min, 5°C). The pellet was washed twice with pre-cooled EtOH (200 µl), dried and redissolved in labeling buffer (7 M urea, 2 M thiourea, 2% w/v CHAPS and 10 mM TRIS). The protein concentration was determined by the 2D-Quant Kit and the solutions were frozen at −80°C until further use.

Samples (DY-680) and blanks (DY-800) were mixed with different IR maleimide dye solutions. Stock solutions of the IR maleimide dyes were prepared in DMF (final concentration 400 nmol/ml). Stock solution (4 µl) was added to a plasma aliquot containing 200 µg protein. After a 30 min incubation at room temperature (RT), the labeling process was stopped by adding L-cysteine (final concentration 5 mM, 10 min on ice). Equal amounts of sample and blank were combined and diluted with immobilized pH gradient (IPG) strip rehydration buffer (8 M urea, 2% w/v CHAPS, 0.5% w/v DTT, 0.5% v/v IPG strip buffer) to a final volume of 450 µl.

2.2.2 | 2D-thiol-DIGE

Solutions containing labeled proteins (450 µl, Section 2.2.1) were added to an IPG BlueStrip in an Immobiline drystrip IPGbox (GE Healthcare) for overnight rehydration. The iso-electric focusing (IEF) was carried out in the Ettan IPGphor II system (GE Healthcare) at a maximum voltage of 10 kV until 50 kVh were reached. Strips were equilibrated twice for 15 min each in IPG strip equilibration buffer (6 ml, containing 360 mg/ml urea, SERVA Electrophoresis) containing DTT (10 mg/ml, first equilibration) and IAA (25 mg/ml, second equilibration). Afterwards, strips were transferred gel-side down to a 2D HPE™ large (24 cm) gel for overnight gel electrophoresis (GE) with a maximum voltage of 1 kV according to the manufacturer's protocol using the HPE™ BlueTower (SERVA Electrophoresis).

Subsequent to GE, gels were washed with water for 5 min and afterwards placed upside down in an Odyssey Scanner CLx (Li-COR, Lincoln, Nebraska, USA) to scan the emitted light at 700 and 800 nm (absorption at 690 and 777 nm) with a spatial resolution of 160 µm in the automatic intensity mode. Images were analyzed using the Progenesis SameSpots software version 5.0 (Nonlinear Dynamics, Newcastle, UK). Images acquired with the two different wavelengths were overlaid and differences in light intensity were used to identify differently labeled proteins. To calculate the average of the normalized spot volume, gels of three independent biological replicates ($n = 3$) were analyzed.

2.2.3 | 2D-GE and Coomassie brilliant blue staining

Sample and blank (1 mg protein each, not labeled with any dye) were separated by 2D-GE as described in Section 2.2.2. Subsequent to GE gels were stained with colloidal Coomassie Brilliant Blue (CBB) following common protocols. Stained gels were scanned in the Odyssey Scanner CLx for quantitative comparison of protein amounts. CBB-stained gels were prepared in four independent biological replicates ($n = 4$), and the mean of the normalized spot volume was calculated.

2.2.4 | Preparation of protein spots for MALDI-TOF MS(/MS) analysis

Protein spots detected by 2D-thiol-DIGE, that showed significant differences (at least 2.0-fold change in relative abundance, p-value ≤0.05) between the staining intensity of samples and blanks, were localized, and their corresponding spots found in CBB stained gels were cut out manually. Afterwards, in-gel proteolysis of proteins was performed with the trypsin profile IGD kit according to the manufacturer's instructions. The incubation mixture obtained was desalted, concentrated, and purified using ZipTip-C18 pipette tips (Merck, Burlington, Massachusetts, USA). Elution of peptides was done with 10 µl ACN/0.1% (v/v) TFA (4:1 v/v) solution. By using the dried-droplet technique, 1 µl eluted sample and 1 µl CHC solution (5 mg/ml in 0.1% v/v TFA/ACN [2:1 v/v]) were spotted onto a polished steel target (Bruker Daltonics).

2.2.5 | Protein identification by MALDI-TOF MS(/MS)

An Autoflex III smartbeam MALDI-TOF/TOF mass spectrometer equipped with a modified pulsed all-solid-state laser 355 nm (Bruker Daltonics) was used for the analysis of the spotted peptide mixtures. The peptide mass fingerprint (PMF) was monitored in a mass range from m/z 800 to m/z 3400 applying the following parameters: ion source I, 19 kV, ion source II 16.5 kV, lens 8.3 kV, reflector 21 kV, and reflector II 9.75 kV. MS/MS experiments were carried out in the LIFT mode with the following parameters: ion source I 6 kV, ion source II 5.3 kV, lens 3.0 kV, reflector 27 kV, reflector II 11.6 kV, LIFT I 19 kV, and LIFT II 4.2 kV.

The mass spectrometer was calibrated with the peptide standards bradykinin (1-7), angiotensin I, angiotensin II, substance P, bombesin, renin substrate, ACTH clip (1-17), ACTH clip (18-39), and somatostatin (peptide calibration standard II, Bruker Daltonics). The flex control software v.3.0, flex analysis v.3.0, and BioTools v.3.1.2.22

software were used for the instrument control, data processing, and final protein identification via the Mascot database (v.2.6.2).

2.3 | µLC-ESI MS/HR MS analysis

2.3.1 | Chromatography

For µLC separation, a microLC 200 pump (Eksigent Technologies LLC, Dublin, CA, USA) was used combined with a HTC xt DLW autosampler (CTC Analytics, Zwingen, Switzerland, kept at 15°C) equipped with a 20 µl sample loop (Sunchrom, Friedrichsdorf, Germany). Chromatographic separation was performed at 35°C on an Atlantis T3 column (50 × 1.0 mm I.D., 3 µm, 100 Å, Waters, Eschborn, Germany) protected by a precolumn (Security Guard™ Ultra Cartiges UHPLC C18 peptide 2,1 mm I.D., Phenomenex, Aschaffenburg, Germany). The µLC system and the mass spectrometer (Section 2.3.2) were operated with the Eksigent control 4.2 and the Analyst TF 1.7.1 software (ABSciex, Darmstadt, Germany).

The following gradients were used for chromatographic separation:

Gradient 1: For information-dependent acquisition (IDA) peptides were eluted with a linear gradient of solvent A (0.05% v/v FA) and solvent B (ACN/H_2O 80:20 v/v, 0.05% v/v FA) at 45°C: t [min]/B [%]: 0/2; 34/40; 34.5/95; 38.5/95; 39/2; 40/2 at a flow of 30 µl/min and a 5 min equilibration period under starting conditions.

Gradient 2: For analysis in the product ion scan (PIS) mode peptides were eluted with a linear gradient of solvent A and solvent B at 35°C: t [min]/B [%]: 0/2; 11/50; 11.5/95; 13.5/95; 14/2; 15/2 at a flow of 30 µl/min and an initial 5 min equilibration period under starting conditions.

2.3.2 | Mass spectrometry

The high-resolution hybrid mass spectrometer TripleTOF 5600$^+$ (TT5600$^+$, ABSciex, Darmstadt, Germany) was online coupled to the µLC system via an electrospray ionization (ESI) interface operating in positive ionization mode. In addition, a calibrant delivery system (CDS, ABSciex) was connected via an atmospheric pressure chemical ionization (APCI) interface which infused reserpine-containing APCI positive calibration solution (ABSciex) with a flow of 500 µl/min. Product ions in the range from *m/z* 174.091 to *m/z* 609.281 produced by collision-induced dissociation (CID) were used for automatic calibration of the TOF mass analyzer every fifth chromatographic run.

2.3.3 | IDA-based screening for alkylated peptides derived from alkylated transthyretin

For the identification of alkylated peptides derived from the proteolysis of alkylated transthyretin (TTR), IDA runs were carried out. After a survey MS scan (*m/z* 200 to *m/z* 1250 with a 250 ms accumulation time), MS/MS scans (*m/z* 100 to *m/z* 2500 with a 150 ms accumulation time) were monitored from precursor ions with a charge state of 1 to 4 (exclusion for 30 sec after two occurrences) using the following parameters for both scan types: curtain gas (CUR) $2.07{\cdot}10^5$ Pa (30 psi), heater gas (GS1) $2.76{\cdot}10^5$ Pa (40 psi), turbo ion spray gas (GS2) $3.45{\cdot}10^5$ Pa (50 psi), ion spray voltage floating (ISVF) 5500 V, temperature (TEM) 200°C and declustering potential (DP) 60 V. For the survey scan a collision energy (CE) of 10 V and for the MS/MS scan an ion release delay (IRD) of 67 ms and an ion release width (IRW) of 25 ms was applied with rolling collision energy. Additionally, a threshold of 100 counts per second (cps) signal intensity and a mass tolerance of 20 ppm was set.

MS/MS raw data files were interpreted with the ProteinPilot™ software (version 5.0.2, ABSciex) using the Paragon algorithm applied to the TTR FASTA file (UniProtKB - P02766 TTHY_HUMAN).

The alkylation by a HETE-moiety (C_4H_9OS) was considered as a possible modification at the following amino acids: arginine, asparagine, aspartic acid, cysteine, glutamic acid, glutamine, histidine, lysine, methionine, serine, threonine, tryptophan, and tyrosine.

Alkylated peptides suggested by the software were analyzed afterwards by µLC-ESI MS/HR MS working in PIS mode and spectra were confirmed manually by the PeakView 2.1 software (ABSciex).

2.3.4 | µLC-ESI MS/HR MS (PIS) of alkylated peptides

Product ions of C(-HETE)PLMVK ($[M + 2H]^{2+}$, *m/z* 397.702) and d_3-Atr ($[M + H]^+$, *m/z* 293.194, used as internal standard, IS) were monitored in a mass range from *m/z* 50 to *m/z* 850 with an accumulation time of 300 ms each. CE used for C(-HETE)PLMVK was 21 V and for d_3-Atr 42 V. DP was 60 V for C(-HETE)PLMVK and 100 V for d_3-Atr. The following parameters were the same for both precursors: collision energy spread (CES) 3 V, CUR $2.07{\cdot}10^5$ Pa (30 psi), GS1 $2.76{\cdot}10^5$ Pa (40 psi), GS2 $3.45{\cdot}10^5$ Pa (50 psi), IRD 67 ms, IRW 25 ms, ISVF 5500 V, and TEM 200°C.

Data was processed using the PeakView 2.1 and MultiQuant 2.1.1 software (ABSciex). Extracted ion chromatograms (XIC) were deduced from the total ion chromatograms (TIC) with a tolerance of ±0.005 Th.

2.3.5 | Incubation of plasma with SM

SM was diluted with EtOH to generate working solutions with concentrations ranging from 80 mM to 312.5 µM. Human plasma (975 µl) was spiked with EtOH (25 µl) for blanks or with working solutions (25 µl) for samples resulting in final SM concentrations of 2 mM, 1 mM, 500 µM, 250 µM, 125 µM, 62.50 µM, 31.25 µM, 15.63 µM, and 7.81 µM. A concentration of 1 mM SM in plasma was used as reference. Plasma was incubated at 37°C for 2 h under

gentle shaking. Samples were stored at −20°C until further processing.

2.3.6 | Labeling of magnetic beads with antibodies

The labeling of the magnetic beads with antibodies (Ab) was carried out according to a previous report.[28] In summary, magnetic beads labeled with Protein G (1 ml commercial suspension) were removed from the supernatant via a magnet. After washing the beads three times with Tween 20 containing PBS (PBST, 2 ml, pH 7.4), a commercial solution of anti-prealbumin antibody (ab185127, ab204997, clone: 9G6, clone: 10E1, 200 µl, 1 mg/ml) and PBST (4 ml) was added and incubated for 15 min on a roller mixer at RT. After removal of the supernatant, beads were washed twice with TEA buffer (2 ml, 200 mM TEA, 0.025% w/v NaN_3, pH 7.4). DMP solution (2 ml, 10.8 mg/ml in TEA buffer) was added and incubated for 30 min (roller mixer, RT). Afterwards, beads were washed with TRIS-buffered saline (2 ml, 20 mM TRIS, 0.9% w/v NaCl, pH 7.4). Finally, Ab-labeled beads were washed twice with PBST (1 ml) and resuspended in PBST (950 µl). Until further use, this bead suspension was stored at 4°C.

2.3.7 | Immunomagnetic separation of TTR and enzymatic cleavage by trypsin

TTR was extracted from plasma using immunomagnetic separation (IMS).[28] Plasma (200 µl) was mixed with beads (separated from 75 µl slurry in PBST, Section 2.3.6) followed by incubation at 20°C for 2 h under gentle shaking. Afterwards, beads were washed twice with PBST (500 µl) and resuspended in H_2O (75 µl). After addition of trypsin solution (10 µl, 250 µg/ml in 50 mM NH_4HCO_3), proteolysis was performed at 37°C for 4 h. Finally, the reaction solution was transferred into an UF device filled with 100 µl d_3-Atr solution (3 ng/ml in FA 0.5% v/v) for UF (15,000 RCF, 15 min, 20°C).

2.3.8 | Kinetics of alkylated TTR proteolysis with trypsin

TTR was extracted by IMS (Section 2.3.7) from 25 aliquots of reference plasma (200 µl, each). The beads of all 25 references were resuspended in 75 µl H_2O, each and combined afterwards. Trypsin solution (250 µl, 100 µg/ml in 50 mM NH_4HCO_3) was added and aliquots (50 µl) were taken after 0.25, 0.5, 1, 3, 5, 15, 30, 60, 90, 120, 240, 360, 480, 780, and 960 min of incubation at 37°C. Aliquots were immediately mixed with ACN (100 µl) to precipitate proteins and centrifuged afterwards (15,000 RCF, 10 min, 5°C). A portion of 120 µl supernatant was transferred into a glass vial. After evaporation to dryness under a gentle stream of nitrogen, the residue was dissolved in d_3-Atr solution (3 ng/ml in FA 0.5% v/v) and analyzed by µLC-ESI MS/HR MS (PIS) applying gradient 2 (Sections 2.3.4 and 2.3.1).

2.3.9 | Determination of the limit of identification of C(-HETE)PLMVK

For the determination of the limit of identification (LOI) of C(-HETE)PLMVK, plasma samples incubated with SM concentrations ranging from 7.81 µM to 2 mM were analyzed in triplicate, each. Plasma was prepared by IMS (Section 2.3.7) and tryptic cleavage (Section 2.3.7) and analyzed using µLC-ESI MS/HR MS (PIS) (Section 2.3.4) and gradient 2 (Section 2.3.1). This procedure was defined as the standard protocol for subsequent experiments. For determination of the LOI the OPCW, guidelines were applied.[29] The XICs of the two most intense product ions of C(-HETE)PLMVK, qualifier I ($[HETE]^+$, *m/z* 105.037) and qualifier II ($[M\text{-}HETE\text{-}NH_3 + H]^+$, *m/z* 673.341), were used to determine their corresponding peak areas. The ratio of the peak areas (qualifier II/qualifier I × 100 [%]) was calculated. According to the OPCW guidelines,[29] the presence of the biomarker is confirmed if the area ratio of a sample corresponded to the peak area ratio of a reference within a given tolerance interval. The LOI for C(-HETE)PLMVK was defined as the lowest concentration of SM at which all measurements of the triplicate met this criterion.

2.3.10 | Determination of selectivity

To determine the selectivity of C(-HETE)PLMVK detection, blank plasma from six individual donors (without prior incubation with SM) was analyzed in triplicate applying the standard protocol monitoring potential interferences.

2.3.11 | Individual differences in biomarker yield

References produced from the plasma of six individual donors were used to determine C(-HETE)PLMVK by the standard protocol in triplicate, each. Individual differences in the concentration of alkylated TTR were determined by the peak area obtained from the XICs of qualifier I.

2.3.12 | In vitro stability of alkylated TTR in plasma at 37°C

References were stored in triplicate at 37°C for 14 days. Aliquots (200 µl) were taken over a period of 14 days, processed by the standard protocol to monitor relative peak areas of qualifier I of C(-HETE)PLMVK as a measure of the stability of alkylated TTR.

2.3.13 | Stability of C(-HETE)PLMVK in the autosampler

The stability of C(-HETE)PLMVK, produced from reference by the standard protocol, was determined in the autosampler at 15°C. Over

a 24 h period, the reference was analyzed hourly for monitoring the time-dependent peak area obtained from the XIC of qualifier I.

2.3.14 | Freeze–thaw stability of alkylated TTR in plasma

References were subjected in triplicate to five freeze–thaw cycles. Each cycle included freezing of plasma at −20°C for at least 24 h and subsequent thawing for 1 h at RT. After each cycle, aliquots (200 µl) were prepared by the standard protocol, and peak areas obtained from XICs (qualifier I) were detected as a measure of the stability of alkylated TTR.

3 | RESULTS AND DISCUSSION

The identification of protein-adducts with SM is a relevant field of toxicological research focused on the identification of novel biomarkers and an improved understanding of SM-related pathophysiology.[9,30–32] Very recently, we introduced the 2D-thiol-DIGE method as a well-suited tool to identify proteins, alkylated by SM analogues at free cysteine residues.[27,33] CEES is a structural analogue of SM possessing only one reactive chlorinated carbon atom. Whereas the bifunctional SM, that possesses two reactive chlorinated carbon atoms, may induce crosslinks between two different proteins, CEES does not.[34,35] Therefore, plasma was initially incubated with CEES, to avoid crosslinks, thus making the protein mixture less complex and more suitable for electrophoretic separation.[36,37]

According to the principle of the 2D-thiol-DIGE method, proteins are labeled with IR maleimide dyes reacting with free thiol-groups of cysteines.[24] A reduced amount of free thiol-groups in a sample, caused by the previous alkylation, leads to a reduced amount of IR maleimide dye attached to the protein when compared to a non-alkylated blank. The use of one dye for the sample and another dye for the blank, differing in their spectroscopic properties, allows the combined detection in a subsequent 2D-DIGE. The combination of equal protein amounts of sample treated with DY-800 and blank treated with DY-680 enables the detection of different fluorescence intensities after 2D-DIGE. Fluorescence of DY-800 is displayed in green and of DY-680 in red color. Equal amounts of IR maleimide dye would lead to a color-overlay effect (orange color). Therefore, red coloration in the image overlay of sample and blank indicates a reduced amount of protein labeled with DY-800 in the sample and thus pointing to alkylated proteins.[27]

Accordingly, we used the 2D-thiol-DIGE technique to analyze human plasma for alkylated proteins. For this purpose, plasma samples incubated with CEES, as well as blanks were depleted from HSA and immunoglobulin G (IgG) for an improved electrophoretic resolution in the subsequent 2D-GE separation.[38]

Following this principle, an alkylated protein was identified by MALDI-TOF MS(/MS). Afterwards, appropriate procedures were developed to extract that protein from plasma and produce an alkylated peptide biomarker by proteolysis of the protein-adduct. Finally, this peptide was detected selectively by a µLC-ESI MS/HR MS (PIS) method. The applicability and suitability of this peptide as a biomarker were elaborated.

3.1 | 2D-thiol-DIGE and CBB-stained gel analysis of human plasma

2D-thiol-DIGE was performed with blanks (DY-680 labeled) and CEES-treated samples (DY-800 labeled). The individual fluorescence intensity was recorded and displayed in different colors (DY-680 in red, DY-800 in green). Beneath others, two intensely red colored spots were detected in blanks at a molecular weight of about 15 kDa and an isoelectric point (pI) of about 5 (Figure 1a). These spots were only faintly visible in the CEES-treated sample (Figure 1b). The overlay of DY-680 and DY-800 labeled spots (Figure 1c) documented the more prominent red color thus indicating the presence of two proteins that were effectively alkylated. The normalized spot volumes and the 3D visualization provided the significance of different IR dye staining. Results for Spot 1 are illustrated in Figure 1d,e (p-value = 0.000893, 4.7-fold change). Spot 2 showed a p-value of 0.00103 and a 2.3-fold change. To ensure that the difference in intensity was not the result of different protein concentrations, additional separately prepared CBB-stained gels from sample and blank were scanned for their staining intensity. As illustrated in Figure 1d,e the protein amounts were equal.

3.2 | Protein identification by MALDI-TOF MS(/MS)

The two proteins of interest, visualized by 2D-thiol-DIGE (Figure 1a–c), were identified as TTR (UniProtKB - P02766 TTHY_HUMAN) after tryptic in-gel digest of the corresponding CBB-stained gel spots by MALDI-TOF MS(/MS) with a sequence coverage of 98.8% for Spot 1 (Mascot probability score: 92) and 93.9% for Spot 2 (Mascot probability score: 118). The occurrence of TTR in two different spots was most presumable due to different posttranslational modifications such as phosphorylation that have been extensively described to be present in human plasma.[39–41]

TTR occurs as a β-sheet rich homotetrameric protein with a molecular weight of 55 kD. Each monomer subunit is composed of 127 amino acids.[42–45] It is synthesized in the liver and the choroid plexus as well as in smaller amounts in the retinal pigment epithelium and pancreas.[46] Predominantly present in plasma (100–400 µg/ml, corresponding to 0.5% of the total protein amount) and in cerebrospinal fluid (CSF, 10–20 µg/ml, corresponding to 25% of the total protein amount), TTR has a half-life of about 48 h.[46–51] TTR plays a major role in the transport of thyroxine and retinol and was thus denominated as (transporter of thyroxine and retinol) transthyretin.[52–54] Because of its migration anodally to albumin on GE, TTR was originally called prealbumin.[55] Aggregation of wild-type or mutant TTR leads to the

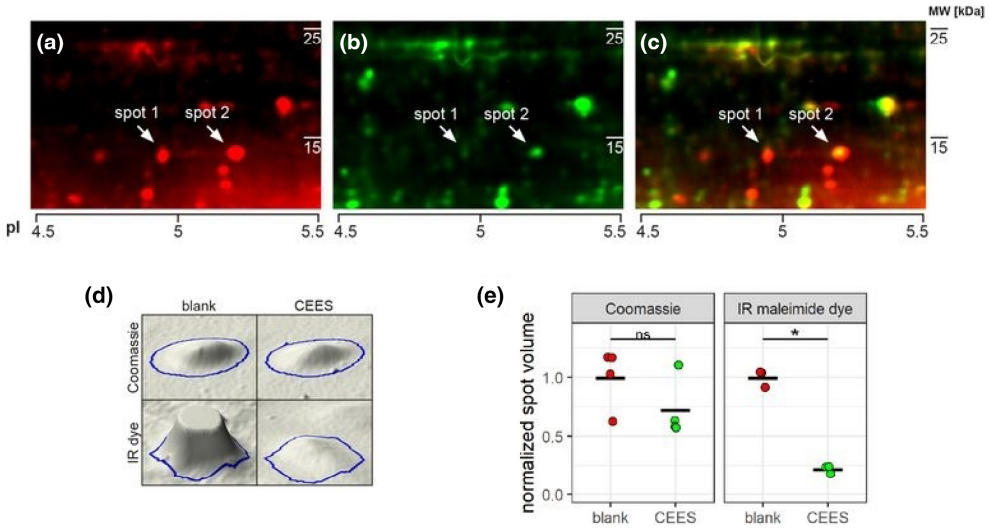

FIGURE 1 2D-thiol-DIGE analysis of plasma with and without CEES-treatment. Representative region (isoelectric point, pI, 4.5–5.5, 5–25 kDa) of a 2D-thiol-DIGE gel of (a) blank plasma (without 2-chloroethyl ethyl sulfide (CEES)-treatment) depleted from human serum albumin (HSA) and immunoglobulin G (IgG) stained with infrared (IR) 680 maleimide dye (red) and of (b) plasma incubated with CEES (5 mM) depleted from HSA and IgG stained with IR 800 maleimide dye (green). (c) the overlay of (a) and (b) indicates CEES-modified proteins by the red highlighted spots. Spot 1 and 2 label the two most intense spots, which proteins were identified by MALDI-TOF MS(/MS). (D, E) representative 3D montage and calculation of the associated normalized spot volumes for spot 1 revealed an almost equal amount of protein in blank and CEES-treated sample in Coomassie brilliant blue-stained gels ($n = 4$), whereas a significant difference was detected in the corresponding IR maleimide dye-stained gels ($n = 3$). MW: Molecular weight [Colour figure can be viewed at wileyonlinelibrary.com]

development of senile systemic amyloidosis (SSA) or familial amyloidotic polyneuropathies (FAP) and cardiomyopathies (FAC).[56–58] Furthermore, TTR is associated with diseases such as amyotrophic lateral sclerosis (ALS), frontotemporal dementia (FTD) and depression.[59–61] The cysteine residue at position 10 (Cys^{10}, the numbering used herein refers to the amino acid sequence without the propeptide) is the only one that is not disulfide-bridged and plays an important physiological role (Figure 2a,b).[62] Modifications such as S-sulfonation, S-cysteinylation or S-homocysteinylation affect the stability of TTR and thus its physiological function.[63–67] Cys^{10} is also essential in using TTR as a biomarker for, for example, oxidative stress and sarcopenia.[68–70] Therefore, Cys^{10} in TTR appears as the reasonable target for alkylation by SM.

3.3 | Detection of the alkylated biomarker peptide by μLC-ESI MS/HR MS

To identify the site of alkylation, the alkylated TTR was extracted from SM-treated plasma, proteolyzed with trypsin and analyzed by μLC-ESI MS/HR MS (IDA). Extraction of the well-known diagnostic ions at *m/z* 105.037 ($[HETE]^+$) and at *m/z* 137.009 ($[HETE{+}S]^+$) resulted in the detection and identification of the hexapeptide C(-HETE)PLMVK ($[M + 2H]^{2+}$, *m/z* 397.702) containing the alkylated Cys^{10} residue.[71] Following identification of this biomarker peptide, a μLC-ESI MS/HR MS (PIS) method was developed, selectively targeting the biomarker and its product ions. The XIC of the most intense product ion at *m/z* 105.037 ± 0.005 showed a narrow peak at a retention time (t_R) of 8.11 min (Figure 3a). This peak was not present in blanks and no interferences were detected (Figure 3b). The MS/MS spectrum of the peptide eluting at t_R 8.11 min showed the HETE-specific product ions at *m/z* 105.037 and at *m/z* 137.009 and signals of product ions representing the single charged peptide after the loss of the HETE-moiety alone ($[M\text{-}HETE{+}H]^+$, *m/z* 690.368) as well as after the loss of the HETE-moiety and an NH_3-group ($[M\text{-}HETE\text{-}NH_3 + H]^+$, *m/z* 673.341) (Figure 3d). In addition, product ions of the y-series were detected corresponding to peptides after the loss of the HETE-moiety (Figure 3d, marked with #). Accordingly, the alkylated peptide was identified and its alkylation site at Cys^{10} was confirmed. In the following, the procedure for biomarker detection was optimized and characterized.

3.3.1 | IMS of alkylated TTR

For extraction and purification of alkylated TTR from plasma, an IMS procedure was developed. Various monoclonal antibodies were tested and showed significant differences of the extraction yield monitored

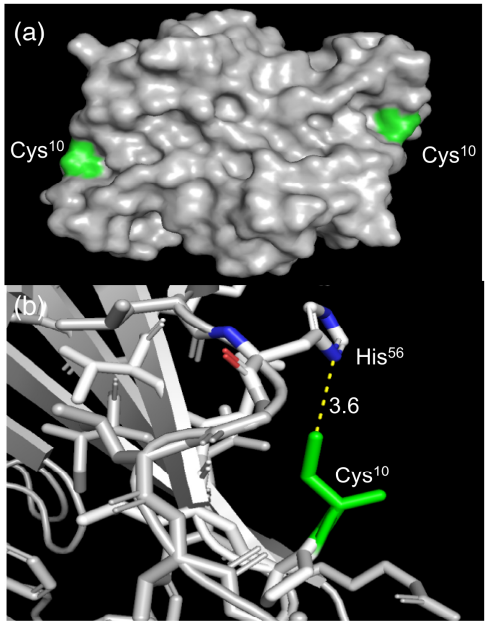

FIGURE 2 Crystal structure of transthyretin. (a) 3D model of transthyretin (PDB ID: 5CLZ) dimer with surface exposed Cys^{10} residues, highlighted in green. (b) Spatial proximity of Cys^{10} to His^{56} (Cys^{10}: Green, N: Blue, O: Red, distance in Å). The figure was created using Pymol v0.99 [Colour figure can be viewed at wileyonlinelibrary.com]

by the peak area of C(-HETE)PLMVK (data not shown). As the recombinant anti-prealbumin antibody ab185127 yielded the maximum amount of the marker peptide, this lot of antibody was used for the standard procedure.

3.3.2 | Kinetics of alkylated TTR proteolysis with trypsin

During proteolysis of alkylated TTR extracted from SM-treated plasma, the concentration of the alkylated hexapeptide C(-HETE) PLMVK increased for 2 h and then reached a plateau phase for at least 14 h (Figure 4). To ensure maximum yield of the peptide, a 4 h proteolysis period with trypsin was defined for the standard protocol.

3.3.3 | Determination of the LOI for C(-HETE) PLMVK

The determination of the LOI is essential for the characterization of a biomarker in order to assess its applicability and to enable the

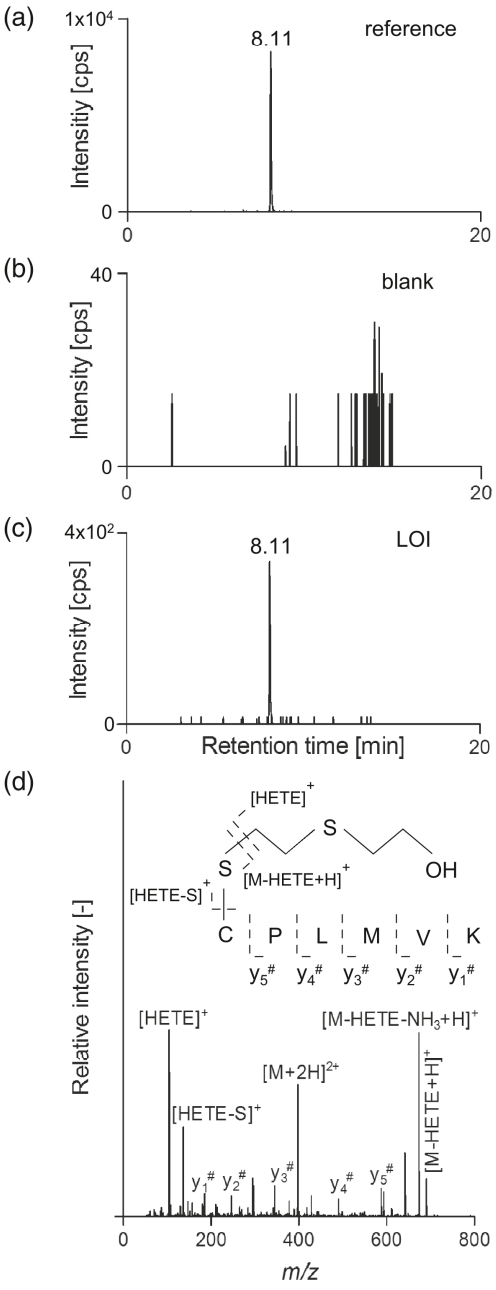

FIGURE 3 Mass spectrometric analysis of alkylated transthyretin. μLC-ESI MS/HR MS analysis of C(-HETE)PLMVK produced after immunomagnetic separation of sulfur mustard (SM)-treated plasma and trypsin-mediated proteolysis (HETE: Hydroxyethylthioethyl-moiety), (a) C(-HETE)PLMVK from reference (plasma incubated with SM, 1 mM), (b) plasma blank, (c) plasma sample spiked with SM (32.5 μM) corresponding to the limit of identification (LOI) of C(-HETE)PLMVK. For reasons of clarity, only the transition *m/z* 397.702 ($[M + 2H]^{2+}$) > *m/z* 105.037 ± 0.005 is displayed in (a), (b), and (c). (d) MS/HR MS of C(-HETE)PLMVK, $[M + 2H]^{2+}$: *m/z* 397.702, $[HETE]^{+}$: *m/z* 105.037 and $[HETE+S]^{+}$: *m/z* 137.009 represent product ions of the attached HETE-moiety. Besides $[HETE]^{+}$, the single protonated product ion resulting from the loss of HETE and NH_3 ($[M\text{-}HETE\text{-}NH_3 + H]^{+}$: *m/z* 673.341) was used for μLC-ESI MS/HR MS monitoring. Furthermore, the entire y-ion series ($y_{1-5}^{\#}$) of the single protonated CPLMVK ($[M\text{-}HETE+H]^{+}$: *m/z* 690.368) is assigned ($y_1^{\#}$: *m/z* 147.113, $y_2^{\#}$: *m/z* 246.181, $y_3^{\#}$: *m/z* 377.222, $y_4^{\#}$: *m/z* 490.306, $y_5^{\#}$: *m/z* 587.359, $^{\#}$ without HETE-moiety). All product ions showed a mass deviation ≤10 ppm, when compared to their theoretical mass

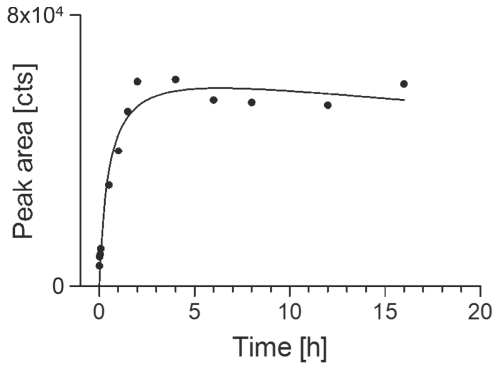

FIGURE 4 Formation of C(-HETE)PLMVK by tryptic cleavage of alkylated transthyretin. To determine the formation of C(-HETE)PLMVK (HETE: Hydroxyethylthioethyl-moiety), a reference (plasma incubated with sulfur mustard, 1 mM) was prepared by immunomagnetic separation to extract adducted transthyretin and subjected to proteolysis. Aliquots were taken after distinct periods to precipitate remaining proteins with acetonitrile. The alkylated peptide C(-HETE)PLMVK was detected in the supernatant by μLC-ESI MS/HR MS (product ion scan). Peak areas illustrated were deduced from the extracted ion chromatograms of the most prominent product ion at *m/z* 105.037 ± 0.005

comparison with other biomarkers of SM poisoning. Therefore, human plasma was incubated with SM concentrations in the range from 7.81 μM to 2 mM and samples were analyzed in triplicate following the standard protocol by μLC-ESI MS/HR MS (PIS) to monitor C(-HETE)PLMVK. The XICs of the two most intense product ions at *m/z* 105.037 and at *m/z* 673.341 were interpreted. Linearity was found in a concentration range from 15.63 μM to 2 mM SM (R^2 > 0.969) for both product ions. Thus, a broad range of dose-dependent adduct formation was shown indicating the reliability of the bioanalytical procedure. The measured peak area ratio of the two most abundant transitions (qualifier II/qualifier I) and their allowed tolerance interval according to OPCW guidelines[29] was found at 97 ± 19.4%. The LOI for C(-HETE)PLMVK was found corresponding to 31.25 μM SM in human plasma. This value is much higher than that reported for the HSA-derived biomarker C^{34}(-HETE)P (15.6 nM).[72] This is partly due to the distinctly lower plasma concentration of TTR (100–400 μg/ml) compared to HSA (40 mg/ml) giving rise to competing reactions.[49] Additionally, the Cys^{10} residue of TTR shows extensive binding to endogenous molecules such as cysteine, homocysteine, sulfate or reactive oxygen species.[63,65,67,68] Pereira et al. showed, that TTR is the major plasma protein susceptible to modification and oxidation, even when compared to HSA.[73] Therefore the amount of free Cys^{10}, that might be alkylated by SM, is reduced and minimizes the concentration of the biomarker. The different reactivity of TTR and HSA was attributed to the orientation of the cysteine side chains. The inwardly directed Cys^{34} residue of HSA seems to be less accessible for reaction partners than Cys^{10} of TTR,[74] which is located on the surface of the protein (Figure 2a). The position in TTR also enables the interaction of the thiol-group with a basic histidine residue (His^{56}) (Figure 2b). This confirmation stabilizes the thiolate ion, lowers the pKa value of the cysteine residue when compared to common cysteine residues and thus causes a high reactivity as a nucleophile.[75]

3.3.4 | Selectivity of the μLC-ESI MS/HR MS (PIS) method

Plasma blanks from six individuals were free of interferences for the product ions at *m/z* 105.037 and at *m/z* 673.341 as exemplarily shown in Figure 3b, thus allowing the unambiguous detection of C(-HETE)PLMVK.

3.3.5 | Individual differences in biomarker yield

The peak areas of the biomarker C(-HETE)PLMVK obtained from the XIC of *m/z* 105.037 resulting from SM-treated plasma of six individuals varied tremendously. The smallest and largest peak areas differed by a factor 2, whereas the relative standard deviation (RSD) for each individual was only 2.6% ($n = 3$), thus indicating high reproducibility and low variations of the procedure, in principle. In general, this broad interindividual variation might be attributed to different diseases, diet, age or the individual extent of endogenous modified Cys^{10} residues or simply to individual concentrations of TTR in plasma.[76–78] However, this phenomenon does not restrict the use of the SM-alkylated TTR-adduct for verification purposes in general.

3.3.6 | In vitro stability of alkylated TTR in plasma at 37°C

TTR alkylated at Cys^{10} was shown to be stable in plasma in vitro at 37°C for at least 14 days. Peak areas of C(-HETE)PLMVK did not

show any trend over the entire test period and only varied by 8.5% thus supporting the applicability of the alkylated peptide for verification purposes even if storage under cooling was not possible.

3.3.7 | Stability of C(-HETE)PLMVK in the autosampler

No area decrease of C(-HETE)PLMVK was detected within the 24 h test period. Areas varied by only 2.5%. The excellent stability is highly beneficial especially if a large number of samples have to be analyzed.

3.3.8 | Freeze–thaw stability of alkylated TTR in plasma

Peak areas of C(-HETE)PLMVK were constant over five freeze–thaw cycles only varying by 6.3%. Therefore, the TTR-adduct was shown to be stable under storage conditions typical for clinical samples thus favoring its use for analysis.

4 | CONCLUSION

Using 2D-thiol-DIGE and MALDI-TOF MS(/MS) analysis, TTR was identified as a novel target of SM-induced alkylation in plasma. The SM-modified peptide C(-HETE)PLMVK derived from TTR after tryptic cleavage was elaborated as a reliable biomarker. Due to the relatively short half-life of TTR in vivo (48 h), we account C(-HETE)PLMVK as a beneficial short time biomarker. In addition to plasma, CSF might be an interesting alternative source of TTR and the biomarker peptide due to the high relative concentration of TTR there in. The possible influence of SM-alkylation on the in vivo stability of TTR and related pathophysiological effects, as already known from structurally similar modifications at TTR, might be subject of future investigations.

ACKNOWLEDGEMENTS

The authors thank Marina Dentzel and Stefanie Oswald for their excellent technical support. Part of the work was supported by the German Research Foundation (Deutsche Forschungsgemeinschaft, DFG, Grant/Award Number Research Training Group GRK 2338).

ORCID

Robin Lüling https://orcid.org/0000-0002-6392-2542
Dirk Steinritz https://orcid.org/0000-0002-2073-5683
Horst Thiermann https://orcid.org/0000-0001-6539-0263
Theo Rein https://orcid.org/0000-0003-2850-4289
Harald John https://orcid.org/0000-0002-7126-6709

REFERENCES

1. Kroening KK, Easter RN, Richardson DD, Willison SA, Caruso JA. *Analysis of Chemical Warfare Degradation Products*. Chichester, West Sussex, United Kingdom: Wiley; 2011.
2. John H, Balszuweit F, Steinritz D, Kehe K, Worek F, Thiermann H. Toxicokinetic aspects of nerve agents and vesicants. In: *Handbook of Toxicology of Chemical Warfare Agents*. Elsevier; 2020:875-919.
3. Darchini-Maragheh E, Blain PG, Balali-Mood M. Delayed complications and long-term effects of SM poisonings: experience of Iran-Iraq war. In: Balali-Mood M, Abdollahi M, eds. *Basic and Clinical Toxicology of Mustard Compounds*. Cham: Springer International Publishing; 2015:101-134.
4. Ghabili K, Agutter PS, Ghanei M, Ansarin K, Shoja MM. Mustard gas toxicity: the acute and chronic pathological effects. *J Appl Toxicol*. 2010;30(7):627-643. https://doi.org/10.1002/jat.1581
5. United Nations Treaty Collection. Convention on the prohibition of the development, production, stockpiling and use of chemical weapons and on their destruction. https://www.opcw.org/sites/default/files/documents/CWC/CWC_en.pdf
6. Patočka J. Syria conflict and chemical weapons: what is the reality? *MMSL*. 2016;85(1):39-43. https://doi.org/10.31482/mmsl.2016.006
7. Sezigen S, Kenar L. Recent sulfur mustard attacks in Middle East and experience of health professionals. *Toxicol Lett*. 2020;320:52-57. https://doi.org/10.1016/j.toxlet.2019.12.001
8. Noort D, Benschop HP, Black RM. Biomonitoring of exposure to chemical warfare agents: a review. *Toxicol Appl Pharmacol*. 2002;184(2):116-126. https://doi.org/10.1006/taap.2002.9449
9. John H, Thiermann H. Poisoning by organophosphorus nerve agents and pesticides: an overview of the principle strategies and current progress of mass spectrometry-based procedures for verification. *J Mass Spectr Adv Clin Lab*. 2021;19:20-31. https://doi.org/10.1016/j.jmsacl.2021.01.002
10. Yue L, Wei Y, Chen J, et al. Abundance of four sulfur mustard-DNA adducts ex vivo and in vivo revealed by simultaneous quantification in stable isotope dilution-ultrahigh performance liquid chromatography-tandem mass spectrometry. *Chem Res Toxicol*. 2014;27(4):490-500. https://doi.org/10.1021/tx4003403
11. Carol-Visser J, van der Schans M, Fidder A, et al. Development of an automated on-line pepsin digestion-liquid chromatography-tandem mass spectrometry configuration for the rapid analysis of protein adducts of chemical warfare agents. *J Chromatogr B Analyt Technol Biomed Life Sci*. 2008;870(1):91-97. https://doi.org/10.1016/j.jchromb.2008.06.008
12. Black RM, Clarke RJ, Harrison JM, Read RW. Biological fate of sulphur mustard: identification of valine and histidine adducts in haemoglobin from casualties of sulphur mustard poisoning. *Xenobiotica*. 1997;27(5):499-512. https://doi.org/10.1080/004982597240460
13. Siegert M, Kranawetvogl A, Thiermann H, John H. Glutathione as an antidote for sulfur mustard poisoning: mass spectrometric investigations of its potency as a chemical scavenger. *Toxicol Lett*. 2018;293:31-37. https://doi.org/10.1016/j.toxlet.2017.12.013
14. Lüling R, Singer H, Popp T, et al. Sulfur mustard alkylates steroid hormones and impacts hormone function in vitro. *Arch Toxicol*. 2019;93(11):3141-3152. https://doi.org/10.1007/s00204-019-02571-x
15. John H, Siegert M, Gandor F, et al. Optimized verification method for detection of an albumin-sulfur mustard adduct at Cys(34) using a hybrid quadrupole time-of-flight tandem mass spectrometer after direct plasma proteolysis. *Toxicol Lett*. 2016;244:103-111. https://doi.org/10.1016/j.toxlet.2015.09.027
16. Gandor F, Gawlik M, Thiermann H, John H. Evidence of sulfur mustard exposure in human plasma by LC-ESI-MS-MS detection of the albumin-derived alkylated HETE-CP dipeptide and chromatographic investigation of its cis/trans isomerism. *J Anal Toxicol*. 2015;39(4):270-279. https://doi.org/10.1093/jat/bkv010
17. Smith JR, Capacio BR, Korte WD, Woolfitt AR, Barr JR. Analysis for plasma protein biomarkers following an accidental human exposure to sulfur mustard. *J Anal Toxicol*. 2008;32(1):17-24. https://doi.org/10.1093/jat/32.1.17

18. Noort D, Fidder A, Degenhardt-Langelaan CEAM, Hulst AG. Retrospective detection of sulfur mustard exposure by mass spectrometric analysis of adducts to albumin and hemoglobin: an in vivo study. *J Anal Toxicol*. 2008;32(1):25-30. https://doi.org/10.1093/jat/32.1.25
19. Ünlü M, Morgan ME, Minden JS. Difference gel electrophoresis: a single gel method for detecting changes in protein extracts. *Electrophoresis*. 1997;18(11):2071-2077. https://doi.org/10.1002/elps.1150181133
20. Arentz G, Weiland F, Oehler MK, Hoffmann P. State of the art of 2D DIGE. *Proteomics Clin Appl*. 2015;9(3–4):277-288. https://doi.org/10.1002/prca.201400119
21. Kirana C, Peng L, Miller R, et al. Combination of laser microdissection, 2D-DIGE and MALDI-TOF MS to identify protein biomarkers to predict colorectal cancer spread. *Clin Proteomics*. 2019;16(1):1-13. https://doi.org/10.1186/s12014-019-9223-7
22. Liu H, Zhang J, Zhou P, Sun H, Katsarou M, Drakoulis N. Exploration of vascular adhesion protein-1 expression in patients with conjunctivitis associated systemic lupus erythematosus using 2D-DIGE. *Exp Ther Med*. 2019;18(6):5072-5077. https://doi.org/10.3892/etm.2019.8009
23. Shaw J, Rowlinson R, Nickson J, et al. Evaluation of saturation labelling two-dimensional difference gel electrophoresis fluorescent dyes. *Proteomics*. 2003;3(7):1181-1195. https://doi.org/10.1002/pmic.200300439
24. Riederer IM, Riederer BM. Differential protein labeling with thiol-reactive infrared DY-680 and DY-780 maleimides and analysis by two-dimensional gel electrophoresis. *Proteomics*. 2007;7(11):1753-1756. https://doi.org/10.1002/pmic.200601007
25. Lilley KS, Razzaq A, Dupree P. Two-dimensional gel electrophoresis: recent advances in sample preparation, detection and quantitation. *Curr Opin Chem Biol*. 2002;6(1):46-50. https://doi.org/10.1016/S1367-5931(01)00275-7
26. Stephens AN, Hannan NJ, Rainczuk A, et al. Post-translational modifications and protein-specific isoforms in endometriosis revealed by 2D DIGE. *J Proteome Res*. 2010;9(5):2438-2449. https://doi.org/10.1021/pr901131p
27. Lüling R, Schmeißer W, Siegert M, et al. Identification of creatine kinase and alpha-1 antitrypsin as protein targets of alkylation by sulfur mustard. *Drug Test Anal*. 2020;13(2):268-282. https://doi.org/10.1002/dta.2916
28. Sporty JLS, Lemire SW, Jakubowski EM, et al. Immunomagnetic separation and quantification of butyrylcholinesterase nerve agent adducts in human serum. *Anal Chem*. 2010;82(15):6593-6600. https://doi.org/10.1021/ac101024z
29. Organisation for the Prohibition of Chemical Weapons, Technical Secretariat. Work instruction for the reporting of the results of the OPCW biomedical proficiency tests: Quality management system document No.: QDOC/LAB/WI/BioPT04. 2018.
30. Steinritz D, Striepling E, Rudolf K-D, et al. Medical documentation, bioanalytical evidence of an accidental human exposure to sulfur mustard and general therapy recommendations. *Toxicol Lett*. 2016;244:112-120. https://doi.org/10.1016/j.toxlet.2015.08.1105
31. van der Schans GP, Noort D, Mars-Groenendijk RH, et al. Immunochemical detection of sulfur mustard adducts with keratins in the stratum corneum of human skin. *Chem Res Toxicol*. 2002;15(1):21-25. https://doi.org/10.1021/tx0100136
32. Lüling R, John H, Gudermann T, et al. Transient receptor potential channel A1 (TRPA1) regulates sulfur mustard-induced expression of heat shock 70 kDa protein 6 (HSPA6) in vitro. *Cell*. 2018;7(9):126. https://doi.org/10.3390/cells7090126
33. Steinritz D, Lüling R, Siegert M, et al. Alkylated epidermal creatine kinase as a biomarker for sulfur mustard exposure: comparison to adducts of albumin and DNA in an in vivo rat study. *Arch Toxicol*. 2021;95(4):1323-1333. https://doi.org/10.1007/s00204-021-03005-3
34. Dillman JF, McGary KL, Schlager JJ. Sulfur mustard induces the formation of keratin aggregates in human epidermal keratinocytes. *Toxicol Appl Pharmacol*. 2003;193(2):228-236. https://doi.org/10.1016/j.taap.2003.08.003
35. Mol MAE, van der Schans GP, Lohman PHM. Quantification of sulfur mustard-induced DNA interstrand cross-links and single-strand breaks in cultured human epidermal keratinocytes. *Mut Res/DNA Repair*. 1993;294(3):235-245. https://doi.org/10.1016/0921-8777(93)90006-3
36. Sack GH, Fenselau C, Kan M-NN, Kan LS, Wood GW, Lau P-Y. Characterization of the products of alkylation of 2′-deoxyadenosine and 2′-deoxyguanosine by chloroethyl ethyl sulfide. *J Org Chem*. 1978;43(20):3932-3936. https://doi.org/10.1021/jo00414a028
37. Gould NS, White CW, Day BJ. A role for mitochondrial oxidative stress in sulfur mustard analog 2-chloroethyl ethyl sulfide-induced lung cell injury and antioxidant protection. *J Pharmacol Exp Ther*. 2009;328(3):732-739. https://doi.org/10.1124/jpet.108.145037
38. Björhall K, Miliotis T, Davidsson P. Comparison of different depletion strategies for improved resolution in proteomic analysis of human serum samples. *Proteomics*. 2005;5(1):307-317. https://doi.org/10.1002/pmic.200400900
39. Eckerskorn C, Strupat K, Schleuder D, et al. Analysis of proteins by direct-scanning infrared-MALDI mass spectrometry after 2D-PAGE separation and electroblotting. *Anal Chem*. 1997;69(15):2888-2892. https://doi.org/10.1021/ac970077e
40. Herosimczyk A, Dejeans N, Sayd T, Ozgo M, Skrzypczak WF, Mazur AM. Plasma proteome analysis: 2D gels and chips. *J Physiol Pharmacol: Off J Polish Physiol Soc*. 57(7):81-93.
41. Zhu K, Zhao J, Lubman DM, Miller FR, Barder TJ. Protein pI shifts due to posttranslational modifications in the separation and characterization of proteins. *Anal Chem*. 2005;77(9):2745-2755. https://doi.org/10.1021/ac048494w
42. Gonzalez G, Offord RE. The subunit structure of prealbumin. *Biochem J*. 1971;125(1):309-317. https://doi.org/10.1042/BJ1250309
43. Kanda Y, Goodman D, Canfield RE, Morgan FJ. The amino acid sequence of human plasma prealbumin. *J Biol Chem*. 1974;249(21):6796-6805.
44. Monaco HL, Rizzi M, Coda A. Structure of a complex of two plasma proteins: transthyretin and retinol-binding protein. *Science*. 1995;268(5213):1039-1041. https://doi.org/10.1126/science.7754382
45. Blake C, Geisow MJ, Oatley SJ, Rérat B, Rérat C. Structure of prealbumin: secondary, tertiary and quaternary interactions determined by fourier refinement at 1.8 Å. *J Mol Biol*. 1978;121(3):339-356. https://doi.org/10.1016/0022-2836(78)90368-6
46. Jacobsson B, Collins VP, Grimelius L, Pettersson T, Sandstedt B, Carlström A. Transthyretin immunoreactivity in human and porcine liver, choroid plexus, and pancreatic islets. *J Histochem Cytochem*. 1989;37(1):31-37. https://doi.org/10.1177/37.1.2642294
47. Buxbaum JN, Reixach N. Transthyretin: the servant of many masters. *Cell Mol Life Sci*. 2009;66(19):3095-3101. https://doi.org/10.1007/s00018-009-0109-0
48. Aleshire SL, Bradley CA, Richardson LD, Parl FF. Localization of human prealbumin in choroid plexus epithelium. *J Histochem Cytochem*. 1983;31(5):608-612. https://doi.org/10.1177/31.5.6341455
49. Berninger RW, Booker SV, Talamo RC. Serum prealbumin levels in alpha1-antitrypsin deficiency (PiZ). *Metabolism*. 1982;31(3):299-302. https://doi.org/10.1016/0026-0495(82)90069-5
50. Serot JM, Christmann D, Dubost T, Couturier M. Cerebrospinal fluid transthyretin: aging and late onset Alzheimer's disease. *J Neurol Neurosurg Psychiatry*. 1997;63(4):506-508. https://doi.org/10.1136/jnnp.63.4.506
51. Stabilini R, Vergani C, Agostoni A, Agostoni RV. Influence of age and sex on prealbumin levels. *Clin Chim Acta*. 1968;20(2):358-359. https://doi.org/10.1016/0009-8981(68)90173-3

52. Robbins J. Transthyretin from discovery to now. *Clin Chem Lab Med*. 2002;40(12):1183-1190. https://doi.org/10.1515/CCLM.2002.208
53. Robbins J, Rall JE. The interaction of thyroid hormones and protein in biological fluids. *Recent Prog Horm Res*. 1957;13:161-202.
54. Raz A, Goodman DS. The interaction of thyroxine with human plasma praealbumin and with the praealbumin-retinol-binding protein complex. *J Biol Chem*. 1969;244(12):3230-3237.
55. Seibert FB, Nelson JW. Electrophoretic study of the blood protein response in tuberculosis. *J Biol Chem*. 1942;143(1):29-38. https://doi.org/10.1016/S0021-9258(18)72655-0
56. Murakami T, Maeda S, Yi S, et al. A novel transthyretin mutation associated with familial amyloidotic polyneuropathy. *Biochem Biophys Res Commun*. 1992;182(2):520-526. https://doi.org/10.1016/0006-291X(92)91763-G
57. Ruberg FL, Berk JL. Transthyretin (TTR) cardiac amyloidosis. *Circulation*. 2012;126(10):1286-1300. https://doi.org/10.1161/CIRCULATIONAHA.111.078915
58. Pitkänen P, Westermark P, Cornwell GG. Senile systemic amyloidosis. *Am J Pathol*. 1984;117(3):391-399.
59. Fleming CE, Nunes AF, Sousa MM. Transthyretin: more than meets the eye. *Prog Neurobiol*. 2009;89(3):266-276. https://doi.org/10.1016/j.pneurobio.2009.07.007
60. Iridoy MO, Zubiri I, Zelaya MV, et al. Neuroanatomical quantitative proteomics reveals common pathogenic biological routes between amyotrophic lateral sclerosis (ALS) and frontotemporal dementia (FTD). *Int J Mol Sci*. 2018;20(1):4. https://doi.org/10.3390/ijms20010004
61. Sullivan GM, Mann JJ, Oquendo MA, Lo ES, Cooper TB, Gorman JM. Low cerebrospinal fluid transthyretin levels in depression: correlations with suicidal ideation and low serotonin function. *Biol Psychiatry*. 2006;60(5):500-506. https://doi.org/10.1016/j.biopsych.2005.11.022
62. Takaoka Y, Ohta M, Miyakawa K, et al. Cysteine 10 is a key residue in amyloidogenesis of human transthyretin Val30Met. *Am J Pathol*. 2004;164(1):337-345. https://doi.org/10.1016/S0002-9440(10)63123-9
63. Kingsbury JS, Laue TM, Klimtchuk ES, Théberge R, Costello CE, Connors LH. The modulation of transthyretin tetramer stability by cysteine 10 adducts and the drug diflunisal. Direct analysis by fluorescence-detected analytical ultracentrifugation. *J Biol Chem*. 2008;283(18):11887-11896. https://doi.org/10.1074/jbc.M709638200
64. Leri M, Rebuzzini P, Caselli A, et al. S-Homocysteinylation effects on transthyretin: worsening of cardiomyopathy onset. *Biochim Biophys Acta Gen Subj*. 2020;1864(1):129453. https://doi.org/10.1016/j.bbagen.2019.129453
65. Lim A, Sengupta S, McComb ME, et al. In vitro and in vivo interactions of homocysteine with human plasma transthyretin. *J Biol Chem*. 2003;278(50):49707-49713. https://doi.org/10.1074/jbc.M306748200
66. Gales L, Saraiva MJ, Damas AM. Structural basis for the protective role of sulfite against transthyretin amyloid formation. *Biochim Biophys Acta*. 2007;1774(1):59-64. https://doi.org/10.1016/j.bbapap.2006.10.015
67. Zhang Q, Kelly JW. Cys10 mixed disulfides make transthyretin more amyloidogenic under mildly acidic conditions. *Biochemistry*. 2003;42(29):8756-8761. https://doi.org/10.1021/bi030077a
68. Sharma M, Khan S, Rahman S, Singh LR. The extracellular protein, transthyretin is an oxidative stress biomarker. *Front Physiol*. 2019;10:5. https://doi.org/10.3389/fphys.2019.00005
69. Summers FA, Morgan PE, Davies MJ, Hawkins CL. Identification of plasma proteins that are susceptible to thiol oxidation by hypochlorous acid and N-chloramines. *Chem Res Toxicol*. 2008;21(9):1832-1840. https://doi.org/10.1021/tx8001719
70. Ingenbleek Y. Plasma transthyretin as a biomarker of sarcopenia in elderly subjects. *Nutrients*. 2019;11(4):895. https://doi.org/10.3390/nu11040895
71. Noort D, Hulst AG, de Jong LP, Benschop HP. Alkylation of human serum albumin by sulfur mustard in vitro and in vivo: mass spectrometric analysis of a cysteine adduct as a sensitive biomarker of exposure. *Chem Res Toxicol*. 1999;12(8):715-721. https://doi.org/10.1021/tx9900369
72. Siegert M, Gandor F, Kranawetvogl A, Börner H, Thiermann H, John H. Methionine329 in human serum albumin: a novel target for alkylation by sulfur mustard. *Drug Test Anal*. 2019;11(5):659-668. https://doi.org/10.1002/dta.2548
73. Pereira CD, Minamino N, Takao T. Free thiol of transthyretin in human plasma most accessible to modification/oxidation. *Anal Chem*. 2015;87(21):10785-10791. https://doi.org/10.1021/acs.analchem.5b03431
74. Blum M-M, Richter A, Siegert M, Thiermann H, John H. Adduct of the blistering warfare agent sesquimustard with human serum albumin and its mass spectrometric identification for biomedical verification of exposure. *Anal Bioanal Chem*. 2020;412(28):7723-7737. https://doi.org/10.1007/s00216-020-02917-w
75. Griffiths SW, King J, Cooney CL. The reactivity and oxidation pathway of cysteine 232 in recombinant human alpha 1-antitrypsin. *J Biol Chem*. 2002;277(28):25486-25492. https://doi.org/10.1074/jbc.M203089200
76. Chiang H-L, Lyu R-K, Tseng M-Y, et al. Analyses of transthyretin concentration in the cerebrospinal fluid of patients with Guillain-Barré syndrome and other neurological disorders. *Clin Chim Acta*. 2009;405(1–2):143-147. https://doi.org/10.1016/j.cca.2009.04.022
77. Rocha JC, Almeida MF, Carmona C, et al. The use of prealbumin concentration as a biomarker of nutritional status in treated phenylketonuric patients. *Ann Nutr Metab*. 2010;56(3):207-211. https://doi.org/10.1159/000276641
78. Ingenbleek Y, Young VR. Significance of transthyretin in protein metabolism. *Clin Chem Lab Med*. 2002;40(12):1281-1291. https://doi.org/10.1515/CCLM.2002.222

How to cite this article: Schmeißer W, Lüling R, Steinritz D, Thiermann H, Rein T, John H. Transthyretin as a target of alkylation and a potential biomarker for sulfur mustard poisoning: Electrophoretic and mass spectrometric identification and characterization. *Drug Test Anal*. 2022;14(1):80-91. doi:10.1002/dta.3146

3.2 Zweite Veröffentlichung

3.2.1 Artikel

Highly stable peptide adducts from hard keratins as biomarkers to verify local sulfur mustard exposure of hair by high-resolution mass spectrometry

W. Schmeißer, M. Siegert, H. Thiermann, T. Rein, H. John.
Archives of Toxicology, 96(8):2287-2298, 2022.
DOI: 10.1007/s00204-022-03307-0

Zu Beginn sollte untersucht werden, ob Haarkeratine Zielstrukturen einer S-Lost-Exposition sind und daraus resultierende Alkylierungen nachgewiesen werden können. Dafür wurden S-Lost-exponierte Haare einem Lyseverfahren unterzogen, welches die Haarproteine in Lösung brachte, um diese anschließend mit Pepsin zu proteolysieren. Die generierten Peptide wurden mittels LC aufgetrennt und mit einem gekoppelten QExactivTM Plus Orbitrap Massenspektrometer in einem Daten abhängigen Messmodus (englisch „data dependent MS2“) vermessen. Unter Berücksichtigung der für S-Lost charakteristischen kovalenten HETE-Modifikation konnten die drei Heptapeptide AlaGlu(-HETE)IleArgSerAspLeu (AE(-HETE)IRSDL), PheLysThrIleGlu(-HETE)GluLeu (FKTIE(-HETE)EL) und LeuGlu(-HETE)ThrLysLeuGlnPhe (LE(-HETE)TKLQF) identifiziert werden, welche alle an einer Glutaminsäure (Glu) alkyliert waren.

Für die genauere Charakterisierung der drei potentiellen Biomarkerpeptide wurden gezielte Analysen (englisch „targeted analysis“) mittels LC-TOF-MS/HR-MS durchgeführt. Über spezifische Produktionen der b- und y-Reihe konnten die Glutaminsäuren als Alkylierungsstellen bestätigt werden. Nur die erste der beiden Glutaminsäuren in FKTIE(-HETE)EL wies die HETE-Modifikation auf.

Danach wurden die Haarkeratine als Ursprung der gemessenen drei alkylierten Heptapeptide geprüft. Nach der Lyse von mit S-Lost (Probe) und ohne S-Lost (Blank) inkubierten Haaren, wurden die gelösten Proteine mittels SDS-PAGE aufgetrennt und mit CBB angefärbt. Die in Probe und Blank sichtbaren zwei Hauptbanden bei 45 kDa und 60 kDa Molekulargewicht konnten eindeutig den beiden Haarkeratintypen I und II zugeordnet werden (*101*). Nach In-Gel Proteolyse mit Pepsin konnten AE(-HETE)IRSDL, FKTIE(-HETE)EL und LE(-HETE)TKLQF in den Banden der Probe nachgewiesen werden. Im Blank war keines der adduktierten Peptide detektierbar. Dies bewies, dass Haarkeratine von S-Lost alkyliert wurden.

Um eine möglichst hohe Ausbeute an zu detektierenden Biomarkerpeptiden zu gewährleisten, wurden die Lyse von S-Lost-inkubierten Haaren und die anschließende Proteolyse in einem zeitlichen Verlauf betrachtet. Für die Standardaufarbeitung wurde für die optimale simultane Detektion von AE(-HETE)IRSDL, FKTIE(-HETE)EL und LE(-HETE)TKLQF die Zeit von 4 h für die Lyse und 2 h für die Proteolyse ermittelt.

Bei der Untersuchung der Inkubationszeit von Haaren mit S-Lost wurde ein maximaler Alkylierungsgrad der Haarkeratine nach 20 min ermittelt. Eine wichtige Beobachtung dabei war, dass ein wässriges Milieu ein entscheidender Faktor für die Bildung von S-Lost-Addukten

an Haarkeratinen ist. Sowohl eine von S-Lost im wässrigen Milieu bevorzugte Bildung des hochreaktive Episulfonium Ions als auch eine durch Wasser verbesserte Aufnahme von S-Lost in das Haar könnte dieses Beobachtung erklären. Mit diesem Wissen wurde der Einfluss von Schweiß auf die Bildung der S-Lost-induzierten Addukten im Haar untersucht. Dabei zeigte sich eine deutlich erhöhte Konzentration an AE(-HETE)IRSDL, FKTIE(-HETE)EL und LE(-HETE)TKLQF im Vergleich zur Standardinkubation mit Wasser. Dies ist wahrscheinlich auf die durch Salze im Schweiß verlangsamte Hydrolyse von S-Lost und die damit erhöhte zur Adduktbildung zur Verfügung stehende Menge an S-Lost zurückzuführen (*25*). Diese Ergebnisse zeigten die Eignung der Methode in einem Expositionsszenario mit schweißnassen Haaren und einer durchgeführten Dekontamination mit Wasser.

Die Ermittlung des LOD für die drei Biomarkerpetide wurde anhand der OVCW-Kriterien durchgeführt. Für 10 mg Haare ergaben sich dabei für AE(-HETE)IRSDL und FKTIE(-HETE)EL jeweils 190 µM S-Lost, sowie 47.5 µM S-Lost für LE(-HETE)TKLQF. Da im Falle realer Expositionsszenarien davon auszugehen ist, dass Haare mit reinem S-Lost (8 M) in flüssigem oder gasförmigen Zustand benetzt werden, ist die Methode hervorragend für die Verifikation geeignet. Diese Eignung bestätigte auch die Prüfung der Selektivität der Methode, bei der in Messungen von Blankhaaren (ohne S-Lost) 7 verschiedener Personen keinerlei störende Interferenzen detektierbar waren.

Die analoge Prüfung von S-Lost-inkubierten Haarproben von 7 verschiedenen Personen sollte zeigen, ob es interindividuelle Unterschiede in der Ausbeute an Biomarkerpeptiden gibt. Hier konnte gezeigt werden, dass alle drei Biomarkerpeptide mit geringer Standardabweichung in allen Proben eindeutig nachweisbar waren. Die dabei auftretenden Abweichungen zwischen den Personen sind auf die sehr individuelle Menge und Zusammensetzung an Keratin im Haar zurückzuführen (*85*).

Ob über die Haarkeratinaddukte auch Aussagen einer regiospezifischen Exposition möglich sind, wurde anhand von Achsel,- Bart-, Bauch-, Intim- und Kopfhaaren getestet. Unabhängig vom Ursprung der Haare konnten die drei Biomarkerpeptide eindeutig nachgewiesen werden. Diese Erweiterung des Methodenspektrums auf alle Körperhaare ist überaus vorteilhaft, da besonders warme und feuchte Körperregionen, wie Achseln oder der Intimbereich, anfällig für S-Lost sind (*4, 58*).

Abschließend sollte die Stabilität von vorhandenen S-Lost-Addukten in Haaren beim Waschen der Haare mit Shampoo, sowie der Lagerung von Haaren untersucht werden. Sowohl 5 Waschzyklen mit Shampoo, als auch die Lagerung über 14 Wochen bei Raumtemperatur und unter Einfluss von Licht und Sauerstoff, verringerten die detektierbaren Konzentrationen der drei Biomarkerpeptide nicht.
Damit ermöglicht die entwickelte Methode zur Haaranalytik, über die drei Biomarkerpeptide AE(-HETE)IRSDL, FKTIE(-HETE)EL und LE(-HETE)TKLQF, die eindeutige Verifikation einer S-Lost-Exposition und dies über den bisher längsten bekannten Postexpositions-Zeitraum.

Archives of Toxicology
https://doi.org/10.1007/s00204-022-03307-0

ANALYTICAL TOXICOLOGY

Highly stable peptide adducts from hard keratins as biomarkers to verify local sulfur mustard exposure of hair by high-resolution mass spectrometry

Wolfgang Schmeißer[1] · Markus Siegert[1,2,4] · Horst Thiermann[1] · Theo Rein[3] · Harald John[1]

Received: 26 January 2022 / Accepted: 27 April 2022

Abstract
In the recent past, the blister agent sulfur mustard (SM) deployed by the terroristic group Islamic State has caused a huge number of civilian and military casualties in armed conflicts in the Middle East. The vaporized or aerolized agent might be inhaled and have direct contact to skin and hair. Reaction products of SM with plasma proteins (adducts) represent well-established systemic targets for the bioanalytical verification of exposure. The SM-derived hydroxyethylthioethyl (HETE)-moiety is attached to nucleophilic amino acid side chains and allows unambiguous adduct detection. For shipping of common blood and plasma samples, extensive packaging rules are to be followed as these matrices are considered as potentially infectious material. In contrast, hair is considered as non-infectious thus making its handling and transportation much less complicated. Therefore, we addressed this matrix to develop a procedure for bioanalytical verification. Following optimized lysis of SM-treated human scalp hair and pepsin-catalyzed proteolysis of adducts of keratin type I and II, microbore liquid chromatography–electrospray ionization high-resolution tandem-mass spectrometry (µLC–ESI MS/HR MS) was used to detect three alkylated keratin-derived biomarker peptides: AE(-HETE)IRSDL, FKTIE(-HETE)EL, and LE(-HETE)TKLQF simultaneously. All bear the HETE-moiety bound to a glutamic acid residue. Protein adducts were stable for at least 14 weeks at ambient temperature and contact to air, and were not affected by washing the hair with shampoo. The biomarker peptides were also obtained from beard, armpit, abdominal, and pubic hair. This is the first report introducing stable local peptide adduct biomarkers from hair, that is easily accessible by a non-invasive sampling process.

Keywords Hydroxyethylthioethyl-moiety · Organisation for the Prohibition of Chemical Weapons · Peptide biomarker · Protein adducts · Vesicant

Abbreviations

CBB	Coomassie Brilliant Blue
CE	Collision energy
CID	Collision-induced dissociation
CWA	Chemical warfare agent
CWC	Chemical weapons convention
d_3-Atr	Triple deuterated atropine
ddMS2	Data-dependent tandem-mass spectrometry
ESI	Electrospray ionization
FA	Formic acid
Fwhm	Full width at half maximum
HETE	Hydroxyethylthioethyl-moiety
HEK	Human epidermal keratinocytes
HR MS	High-resolution mass spectrometry

✉ Harald John
HaraldJohn@bundeswehr.org

Wolfgang Schmeißer
wolfgang1schmeisser@bundeswehr.org

Markus Siegert
markus.siegert@student.hu-berlin.de

Horst Thiermann
HorstThiermann@bundeswehr.org

Theo Rein
theorein@mpipsykl.mpg.de

[1] Bundeswehr Institute of Pharmacology and Toxicology, Neuherbergstrasse 11, 80937 Munich, Germany

[2] Department of Chemistry, Humboldt-Universität Zu Berlin, Brook-Taylor-Strasse 2, 12489 Berlin, Germany

[3] Max Planck Institute of Psychiatry, Kraepelinstrasse 2-10, 80804 Munich, Germany

[4] Proteros Biostructures GmbH, Bunsenstrasse 7a, 82152 Planegg, Germany

Published online: 16 May 2022

IATA	International Air Transport Association
iPrOH	Iso-propanol
ISVF	Ion spray voltage floating
µLC	Micro-liquid chromatography
LOI	Limit of identification
MS	Mass spectrometry
MS/MS	Tandem-mass spectrometry
MW	Molecular weight
MWCO	Molecular weight cut-off
NMR	Nuclear magnetic resonance
OPCW	Organisation for the Prohibition of Chemical Weapons
pI	Isoelectric point
PIS	Product ion scan
Qual	Qualifier ion
RCF	Relative centrifugal force
RSD	Relative standard deviation
RT	Room temperature
SDS-PAGE	Sodium dodecylsulfate polyacrylamide gel electrophoresis
SM	Sulfur mustard, (bis(2-chloroethyl) sulfide)
t_R	Retention time
TOF	Time-of-flight
UF	Ultrafiltration
XIC	Extracted ion chromatogram

Introduction

Vesicants—a subgroup of chemical warfare agents (CWA)—cause a variety of local and systemic clinical symptoms depending on the dose and time of exposure including blisters and erythema (Ghabili et al. 2010). Sulfur mustard (SM, bis(2-chloroethyl)sulfide, CAS No. 505-60-2) is the most prominent representative of these blister agents. It has been used repeatedly in armed conflicts in the recent past, e.g., in the Syrian Arab Republic and Northern Iraq deployed by the terroristic group Islamic State as well as in the Iran–Iraq war in large scale (John et al. 2019; Sezigen and Kenar 2020). SM is banned by the Chemical Weapons Convention (CWC) which adherence is supervised by the Organisation for the Prohibition of Chemical Weapons (OPCW) (https://www.opcw.org/sites/default/files/documents/CWC/ CWC_en.pdf). To investigate the alleged use of CWA, laboratories designated by the OPCW for the analysis of biomedical samples target specific systemic biomarkers and biotransformation products (Blum et al. 2014; John et al. 2020).

Especially, reaction products (adducts) of SM formed with human proteins such as serum albumin after incorporation are highly useful for biomedical verification due to their long-term traceability for up to several weeks post-exposure (John et al. 2019, 2020; Steinritz et al. 2016; Xu et al. 2014). Such adducts possess the SM-characteristic hydroxyethylthioethyl (HETE)-moiety that is attached to nucleophilic side chains of certain amino acids including, e.g., cysteine, methionine, and glutamic acid (John et al. 2016, 2019; Siegert et al. 2019; Steinritz et al. 2016, 2021). Proteolysis of these protein adducts generates biomarker peptides that can be detected by liquid chromatography–mass spectrometry.

In real case exposure scenarios with vaporized or aerosolized SM, the agent will have direct contact to skin and hair (John et al. 2019; Sezigen and Kenar 2020; Steinritz et al. 2016). Accordingly, the formation of adducts with local proteins is expected (Steinritz et al. 2021). Typical forensic methods make use of hair to detect, e.g., drugs, that either stick to the surface of the hair or have been incorporated into the hair during its growth (Ferreira et al. 2019). However, these methods do not target agent-induced covalent protein modifications and do not detect adducted peptide biomarkers.

Hair predominantly consists of the structural proteins hard keratins (65–95% w/w) (Robbins 2012), that are subdivided into two types. Type I keratins possess a molecular weight (MW) of 40–50 kDa and an isoelectric point (pI) at acidic pH values. Eleven type I keratins are known, which are numbered as K 31–K 40 including K 33A and K 33B (Langbein et al. 2001; Schweizer et al. 2006). Type II keratins possess an MW of 55–65 kDa, a pI at neutral to slightly basic pH values and comprise 6 proteins (K 81–K 86) (Langbein et al. 2001; Schweizer et al. 2006). Keratins are particularly rich in cysteines that form a large number of intra- and intermolecular disulfide bridges (Lubec et al. 1987; Robbins 2012; Robbins and Kelly 1970). This high level of crosslinking is responsible for the structural rigidity and insolubility of hair (Lubec et al. 1987). Accordingly, analysis of human hair proteins requires their initial lysis to reduce and thus cleave disulfide bridges and make the proteins soluble (Adav et al. 2018).

The analysis of covalent hair protein modifications is addressed by only a very limited number of reports so far (Adav et al. 2018; Barthélemy et al. 2012; Grosvenor et al. 2016; Lee et al. 2006; Watson et al. 1998). Desamination (Adav et al. 2018), oxidation (Barthélemy et al. 2012; Grosvenor et al. 2016), mono-, di-, and trimethylation (Lee et al. 2006; Watson et al. 1998), and phosphorylation and ubiquitination (Lee et al. 2006) were reported as posttranslational modifications. In addition, keratin-acetaldehyde adducts were found in murine hair after feeding ethanol (Watson et al. 1998). The formation of SM adducts with soft keratins from skin (van der Schans et al. 2002) and from cultured human epidermal keratinocytes (HEK) (Dillman et al. 2003; Mol et al. 2008) has already been shown but adducts of hard hair keratins with SM or any other CWA have never been described before.

In principle, hair specimens are beneficial for forensic analysis as it is easily accessible in a non-invasive process and not subject to the regulations of the International Air Transport Association (IATA) for potentially infectious material thus not requiring the adherence to complex rules for packaging and shipping (International Air Transport Association 2021; U.S. Department of Labor 2021). Therefore, the aim of this study was to investigate potential keratin adducts in human hair and develop the first micro-liquid chromatography–electrospray ionization high-resolution tandem-mass spectrometry (μLC–ESI MS/HR MS) method for the detection of related local peptide biomarkers for the verification of SM exposure.

Materials and methods

Chemicals

Chemicals were purchased from common commercial sources. Pepsin from porcine gastric mucosa was from Sigma-Aldrich (Steinheim, Germany, lot no. SLBQ1670V), 2D-Quant Kit from GE Healthcare (Freiburg, Germany), NaOCl solution for decontamination from Carl Roth (Karlsruhe, Germany), deuterated atropine (d_3-Atr) from CDN Isotopes (Pointe-Claire, Quebec, Canada), and hair shampoo from a common commercial provider. SM was provided by the German Ministry of Defense and checked in-house for integrity and purity by NMR. Working solutions of SM were prepared in acetonitrile yielding concentrations ranging from 15 μM to 50 mM. Scalp hair was a donation from 7 human non-exposed male and female individuals. Additional beard, abdominal, armpit, and pubic hair was obtained from one male individual. Pooled scalp hair was produced by mixing equal amounts of minced hair from all donors. Sweat was collected from the skin of several volunteers after intense physical activity and purified from particles by ultrafiltration (UF) prior to use (Amicon Ultra-0.5 centrifugal filter unit, 0.5 mL, molecular weight cut-off, MWCO, 10 kDa, Merck Millipore, Billerica, Massachusetts, USA).

Initial rinsing of hair

Hair was rinsed three times with methanol (70% v/v) and three times with H_2O prior to air drying (16 h, room temperature, RT). Afterwards, the hair was cut into pieces (2–3 mm length) and stored at RT until use.

Incubation of hair with SM

Pieces of hair (10 mg in total) were covered with SM working solutions (150 μL) for references (25 mM SM) and standards (diverse SM concentrations) and with neat acetonitrile (150 μL) for blanks and mixed with H_2O (450 μL, each). After 30 min, the mixture was centrifuged (15,000 RCF, 10 min, 25 °C), the liquid phase was discarded, and hair was washed three times with acetonitrile (200 μL). Subsequently, the hair was dried at RT for 1 h and stored at −20 °C prior to use. Scalp hair from seven individuals and pooled hair as well as scalp, beard, abdominal, armpit, and pubic hair from one individual was incubated ($n = 3$, each).

Lysis of hair

Lysis of hair was performed based on the Shindai method (Fujii et al. 2013). In brief, following the standard protocol, lysis buffer (700 μL, 20 mM Tris–HCL, 2.6 M thiourea, 5 M urea, 20 mM dithiothreitol, pH 9.0) was added to hair (10 mg) and shaken constantly for 4 h (50 °C). After centrifugation (15,000 RCF, 10 min, 25 °C), 500 μL was transferred into a reaction vial followed by carbamidomethylation with iodoacetamide (26 μL, 1 mM) under gentle shaking in the dark (1 h, 50 °C). During method optimization, different periods of lysis were tested (0.25 h, 0.5 h, 1 h, 2 h, 4 h, 8 h, 12 h, 16 h, 20 h, and 24 h).

Proteolysis of keratins

Following the standard protocol, the reaction mixture obtained after lysis and carbamidomethylation (500 μL) was subjected to UF (15,000 RCF, 10 min, 35 °C). The retentate was washed 2-times by UF after the addition of H_2O (300 μL) and subsequently two times after the addition of formic acid (FA, 300 μL, 10% v/v). Proteolysis of proteins in the retentate was performed by adding pepsin solution (100 μL, 2.5 mg/mL in FA 10% v/v) and FA (300 μL, 10% v/v) under constant shaking (2 h, 42 °C). During method optimization, diverse periods for proteolysis were tested (1.5 min, 3 min, 5 min, 10 min, 15 min, 30 min, 45 min, 60 min, 90 min, 120 min, 150 min, 180 min, 210 min, 240 min, 270 min, and 300 min). After UF (15,000 RCF, 15 min, 20 °C), 30 μL of the filtrate was mixed with 60 μL d_3-Atr solution (3 ng/mL in FA 0.5% v/v) prior to μLC–ESI MS/HR MS analysis. Measurements were performed using either an Orbitrap system working in data-dependent tandem-MS mode (ddMS2) or a quadrupole time-of-flight (TOF) system operating in product ion scan (PIS) mode.

μLC-ESI MS/HR MS (ddMS2) analysis

For identification of alkylated peptides by μLC–ESI MS/HR MS, the ddMS2 mode was carried out using a QExactive plus Orbitrap mass spectrometer (Thermo Scientific, Bremen, Germany) working with positive ESI. The common

instrumental equipment and software used were the same as described recently (Blum et al. 2020; John et al. 2021). An Acquity HSS T3 column (50 × 1.0 mm I.D., 1.8 µm, 100 Å, Waters, Eschborn, Germany) protected by a precolumn (Security Guard™ Ultra Cartiges UHPLC C18 peptide 2.1 mm I.D., Phenomenex, Aschaffenburg, Germany) was used for chromatographic separation of 20 µL sample volume at 30 °C with a linear gradient of solvent A (0.05% v/v FA) and solvent B (acetonitrile/H_2O 80:20 v/v, 0.05% v/v FA) at a flow of 30 µL/min: t [min]/B [%]: 0/0; 3/0; 35/40; 35.5/95; 39.5/95; 40/0.

The ddMS2 approach was comprised of an initial full MS scan followed by MS/MS of the ten most intense ions (top 10) (John et al. 2021). The following parameters were applied for full MS: spray voltage 3.5 kV, capillary temperature 250 °C, sheath gas flow rate 23 arbitrary units (a.u.), mass spectrometric resolution at full width at half maximum (fwhm) 70,000; automatic gain control (AGC) target 3.0×10^6, maximum injection time (MIT) 100 ms, and scan range *m/z* 200—*m/z* 1500. For ddMS2, the following settings were used: fwhm 17,500, AGC target 1.0×10^5, MIT 150 ms, isolation window 1.6 m/z, normalized collision energy (NCE) 30; minimum AGC target 3.0×10^3, intensity threshold 2.0×10^4, charge inclusion 2–7, and dynamic exclusion 30 s.

Data interpretation

MS/MS spectra of peptides fragmented by ddMS2 were analyzed by the Proteome Discoverer 2.1 software (Thermo Scientific) and measurements were matched to a database containing amino acid sequences of all hair keratins (K 31–K 40, K 81–K 86) taken from the UniProt database considering the SM-derived HETE-attachment (+ 104.030 Da at Cys, Asp, Glu, His, Met) and carbamidomethylation (+ 57.021 Da at Cys) using the Sequest HT algorithm. Peptides proposed to bear SM alkylation were manually checked for the presence of a signal at *m/z* 105.037 representing the cleaved $[HETE]^+$-moiety. The identity of proposed alkylated peptides was subsequently confirmed by µLC–ESI MS/HR MS analysis in PIS mode.

µLC–ESI MS/HR MS (PIS) analysis

For µLC–ESI MS/HR MS (PIS) analysis, a microLC 200 pump (Eksigent Technologies LLC, Dublin, CA, USA) on-line coupled to a TripleTOF 5600^+ mass spectrometer ($TT5600^+$, ABSciex, Darmstadt, Germany) was used as described recently (Schmeißer et al. 2021). Chromatographic separation (30 °C, 30 µL/min) of 20 µL sample was performed on an Acquity HSS T3 (100 × 1.0 mm I.D., 1.8 µm, 100 Å, Waters), protected by a precolumn as described above. After 5 min of equilibration under starting conditions, a gradient of solvent A and solvent B was applied: t [min]/B [%]: 0/5; 4/29; 12.5/32; 16/50; 16.5/95; 18.5/95; 19/5; 20/5.

Product ions of the double-protonated alkylated peptides AE(-HETE)IRSDL, FKTIE(-HETE)EL, and LE(-HETE)TKLQF were obtained after collision-induced dissociation (CID) and monitored in the mass range from *m/z* 50 to *m/z* 950 with an accumulation time of 100 ms, each. Individual masses of precursor ions and of the two most intense product ions (qualifier I and qualifier II) are listed in Table 1. The following MS parameters were the same for the three alkylated peptides: collision energy spread (CES) 3 V, curtain gas (CUR) 2.07×10^5 Pa (30 psi), heater gas (GS1) 2.76×10^5 Pa (40 psi), turbo ion spray gas (GS2) 3.45×10^5 Pa (50 psi), ion release delay (IRD) 67 ms, ion release width (IRW) 25 ms, ion spray voltage floating (ISVF) 5000 V, and temperature (TEM) 200 °C.

Selectivity of the µLC–ESI MS/HR MS (PIS) method and interindividual differences in biomarker yield

Blank and reference hair from 7 donors (scalp, 10 mg, $n = 3$, each) as well as blank and reference scalp, beard, abdominal, armpit, and pubic hair (10 mg, $n = 3$, each) from one individual were prepared according to the standard protocol and analyzed by µLC–ESI MS/HR MS (PIS) to monitor any

Table 1 MS parameters for the detection of hair keratin-derived biomarkers and internal standard

Compound	Precursor ion	*m/z*	DP [V]	CE [V]	Qual I *m/z*	Qual II *m/z*	Peak area ratio Qual II/Qual I [%]
AE(-HETE)IRSDL	$[M+2H]^{2+}$	454.2	50	24	803.4258	105.0369	60.2
FKTIE(-HETE)EL	$[M+2H]^{2+}$	492.3	40	22	879.4822	105.0369	68.7
LE(-HETE)TKLQF	$[M+2H]^{2+}$	491.8	50	22	878.4982	105.0369	86.7
d_3-Atr	$[M+H]^+$	293.2	100	42	127.1309	93.0699	51.0

Settings were used for µLC–ESI MS/HR MS (PIS) analysis on a $TT5600^+$ system. d3-Atr (triple deuterated atropine) was used as internal standard. For each peptide, the qualifier I (Qual I) represents the [M + H] lost $HETE^+$ ion (single protonated peptide backbone after the loss of the $[HETE]^+$-moiety), whereas Qual II is the cleaved $[HETE]^+$-ion. CE: collision energy, DP: declustering potential, HETE: hydroxyethylthioethyl-moiety

interference in blanks and to compare individual biomarker peak areas in references.

Limit of identification of biomarker peptides

Pooled scalp hair (10 mg) was incubated with SM working solutions ($n = 3$) to generate standards corresponding to SM concentrations of 12 µM, 24 µM, 48 µM, 96 µM, 190 µM, 390 µM, 780 µM, 1.56 mM, 3.125 mM, 6.25 mM, 12.5 mM, 25 mM, and 50 mM. Following the standard protocol, relative peak area ratios of the respective qualifier II to qualifier I of the three biomarker peptides (Table 1, given in percent) were calculated. The limit of identification (LOI) was defined as the lowest concentration of SM at which all measurements of the triplicate met the area ratios obtained from pooled hair reference.

Stability of biomarker peptides in the autosampler

To evaluate the stability of the three biomarker peptides stored in the autosampler at 15 °C, pooled hair reference (scalp, 10 mg) was prepared according to the standard protocol and analyzed by µLC–ESI MS/HR MS (PIS) hourly within a period of 24 h. Biomarker peak areas were determined to monitor relative concentration–time profiles.

Time-dependent adduct formation in the presence of water

Pooled scalp hair (10 mg) was mixed with SM working solution (150 µL, 25 mM) and additionally with either H_2O or acetonitrile (450 µL, each). The liquid phase was discarded after 1 min, 2 min, 5 min, 10 min, 15 min, 20 min, 25 min, 30 min, 60 min, 90 min, and 120 min (tested as separate incubation mixtures, n = 3, each). Immediately afterwards, acetonitrile (200 µL) was added to the hair for vortex-mixing. Removal of the liquid phase and addition of another acetonitrile portion (200 µL) was repeated five times. Following standard lysis and proteolysis, the samples were analyzed by µLC–ESI MS/HR MS (PIS) to monitor the relative time-dependent concentrations of all three biomarker peptides.

Influence of sweat on adduct formation

Pooled hair (scalp, 10 mg) was incubated with SM either in the presence of H_2O (450 µL, $n = 3$) or in the presence of sweat (450 µL, $n = 3$). Subsequent sample preparation and analysis were done according to the standard protocol to determine the peak areas of the three biomarker peptides.

SDS-PAGE of lysed hair and in-gel proteolysis with pepsin

After lysis of blank and pooled hair reference (scalp, 10 mg, $n = 3$, each), the supernatant containing 30 µg protein (quantified by 2D-Quant Kit) was separated by SDS-PAGE (NuPAGE™ 4–12% bis Tris Gel, Thermo Fisher Scientific, Waltham, MA, USA). Subsequent staining with Coomassie Brilliant Blue (CBB) and in-gel proteolysis (2 h) were carried out according to common protocols (Thermo Fisher Scientific 2021) but using pepsin (2.5 mg/mL FA 10% v/v) instead of trypsin. The three biomarker peptides were detected by µLC–ESI MS/HR MS (PIS).

Stability of alkylated keratins in hair during storage

To characterize the stability of alkylated keratins in hair, pooled hair reference (scalp, 10 mg, $n = 63$) was stored under the following conditions: − 20 °C in the dark and exclusion of air (condition I, $n = 21$); 25 °C in the dark and exclusion of air (condition II, $n = 21$) and 25 °C with daylight and contact to air (condition III, $n = 21$). Hair was analyzed weekly ($n = 3$ per condition) according to the standard protocol over a period of 7 weeks monitoring the relative concentration–time profiles of all three biomarker peptides. In addition, the period of analysis for condition III was prolonged for another 7 week period (14 weeks in total).

Stability of alkylated keratins in hair during wash cycles with shampoo

Pooled hair reference (scalp, 10 mg) was mixed with 500 µL of a water–shampoo mixture (H_2O/shampoo 4:1 v/v) and shaken for 5 min (40 °C). After centrifugation (15,000 RCF, 10 min, 25 °C), the supernatant was removed and the procedure was repeated five times with 500 µL H_2O instead of the water–shampoo mixture. Finally, the hair was dried at RT for 24 h. This entire wash cycle with shampoo and water was repeated on 4 consecutive days. After each cycle, samples ($n = 3$) were processed according to the standard protocol and analyzed by µLC–ESI MS/HR MS (PIS). Peak areas of all biomarker peptides were compared to those of references not subjected to any wash cycle.

Safety considerations

SM is a highly toxic blister agent. Only trained personnel wearing laboratory protective clothes should handle it under the fume hood. Decontamination of all materials that have come into contact with SM is mandatory. Decontamination should be done by submerging the material into alkaline NaOCl solution and leaving it in the solution for several hours.

Results and discussion

Blood and plasma, that are the most common specimens used for verification analysis, are often considered as potentially infectious material if no further information about the health of the donor or the status of the sample itself is available (International Air Transport Association 2021). Accordingly, strict rules for shipment have to be followed with respect to triple packaging. The use of a leak-proof primary receptacle, a leak-proof secondary receptacle containing absorbent material and a clearly labelled rigid outer package shall prevent from the discharge of the sample and allow immediate identification by its UN specification number e.g., UN 3373 (biological substance, category B). If there is a minimal likelihood that pathogens are present, such blood and plasma samples might be categorized and labelled as "exempt human specimens", but they still require triple packaging. In contrast, hair is in principle considered as non-infectious material (U.S. Department of Labor 2021) and can easily be transported even in cabin luggage and presented at security checkpoints in clear containers (such as zip-lock bags) making passage of samples much easier. In addition, it is easily accessible by a non-invasive process. Therefore, hair represents a highly valuable alternative specimen for the verification of SM exposure and was thus addressed in the present study. Initially, the formation of SM adducts had to be proven after lysis and proteolysis.

Identification of alkylated peptides by µLC–ESI MS/HR MS

Alkylation of proteins by SM in aqueous media typically yields an attached HETE-moiety still present in biomarker peptides after proteolysis (John et al. 2016, 2019, 2020; Siegert et al. 2019; Steinritz et al. 2021). MS fragmentation of these adducted peptides typically produces the $[HETE]^+$-product ion at *m/z* 105.037 (John et al. 2016, 2019; Siegert et al. 2019; Steinritz et al. 2016, 2021) that thus represents a diagnostic ion indicating alkylation. To identify so far unknown alkylated peptides, hair incubated with SM was lysed, proteolyzed with pepsin, and analyzed by µLC–ESI MS/HR MS (ddMS2) using an Orbitrap mass spectrometer for optimum mass resolution (Blum et al. 2020; John et al. 2021). Even though the use of trypsin would have simplified the prediction of cleaved peptides, pepsin was used, because the acidic proteolysis conditions prevent the hydrolysis of alkylated amino acids, therefore optimizing adduct yield.

Precursor ions, that yielded the $[HETE]^+$-ion, were correlated to keratin amino acid sequences known from UniProt database entries. For mass spectrometric structural confirmation of proposed peptide adducts selective µLC–ESI MS/HR MS (PIS) analyses were performed considering different charge states of the proposed precursor ions. Optimum properties in terms of signal intensity and chromatographic behavior were found for the three double-protonated alkylated heptapeptides AE(-HETE)IRSDL ($[M+2H]^{2+}$, *m/z* 454.2), FKTIE(-HETE)EL ($[M+2H]^{2+}$, *m/z* 492.3) and LE(-HETE)TKLQF ($[M+2H]^{2+}$, *m/z* 491.8) all bearing an alkylated glutamic acid residue (Table 1). The peptide AEIRSDL derived either from K 31 (UniProtKB Q15323) or K 33A/B (UniProtKB O76009/Q14525). FKTIEEL was produced from either K 31, K 33A/B or K 34 (UniProtKB O76011) and LETKLQF originated either from K 81 (UniProtKB Q14533) or K 83 (UniProtKB P78385) or K 86 (UniProtKB O43790). These assignments were also supported by SDS-PAGE analysis as described below (section: SDS-PAGE of lysed hair and in-gel proteolysis with pepsin).

Monitoring of biomarker peptides by µLC–ESI MS/HR MS (PIS)

A triple TOF mass spectrometer was used to establish a µLC–ESI MS/HR MS (PIS) method for biomarker analysis (Fig. 1). Mass spectrometric parameters of the method (collision energy, declustering potential, ISVF) were optimized for the detection of the individual product ions (qualifier I and qualifier II, Fig. 1; Table 1) with maximum intensity. For all three peptides, the respective most prominent product ion was the single charged peptide backbone $[M+H]^+$ after loss of HETE ($[M+H]^+_{\text{lost HETE}}$, qualifier I) resulting from the loss of the $[HETE]^+$-moiety (qualifier II, Table 1) as illustrated in Fig. 2.

AE(-HETE)IRSDL: The extracted ion chromatogram (XIC) of qualifier I (*m/z* 803.426, Fig. 1A) showed a major narrow peak at the retention time (t_R) of 7.0 min and a much smaller well separated peak at t_R 7.4 min. In addition to qualifier I and II, the MS/MS spectrum of the first eluting compound showed a large number of product ions with minor intensity representing the b- and y-series with and without the attached HETE-moiety (Fig. 2A, Table SI 1). The presence of the alkylated a_2- (*m/z* 277.122) and alkylated b_2-ion (*m/z* 305.117) unambiguously proved the site of alkylation at the glutamic acid residue (Table SI 1). The latter ions were not present in the MS/MS spectrum of the second eluting compound (t_R 7.4 min, data not shown). Nevertheless, the peptide was also identified as alkylated AEIRSDL. Its fragmentation yielded an alkylated y_5-ion (*m/z* 707.375) documenting alkylation at one of the five C-terminal amino acid residues. No additional product ions containing the HETE-moiety were found, thus preventing the identification of the exact alkylation site. It

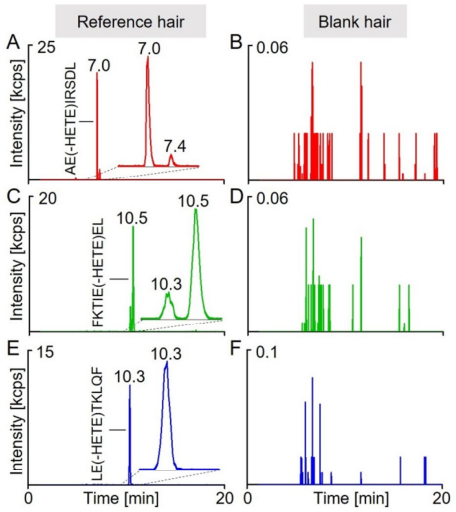

Fig. 1 µLC–ESI MS/HR MS (PIS) detection of biomarker peptides of sulfur mustard exposure of hair. µLC–ESI MS/HR MS (PIS) analysis of pooled hair reference exposed to sulfur mustard (25 mM, left column) and blank hair (right column) after lysis and proteolysis with pepsin. For reasons of clarity, only the individual mass traces of the most intense product ions (qualifier I) are depicted. **A**, **B** AE(-HETE)IRSDL at t_R 7.0 min, *m/z* 454.2 > *m/z* 803.426. **C**, **D** FKTIE(-HETE)EL at t_R 10.5 min, *m/z* 492.3 > *m/z* 879.482, and **E**, **F** LE(-HETE)TKLQF at t_R 10.3 min, *m/z* 491.8 > *m/z* 878.498. Product ion traces were extracted with ± 0.005 Da. **A** The additional peak at t_R 7.4 min corresponded to a positional isomer of AE(-HETE)IRSDL bearing the HETE-moiety most presumably attached to the aspartic acid residue. **C** The peak at t_R 10.3 min corresponded to a $^{13}C_1$-variant of LE(-HETE)TKLQF exhibiting nearly identical precursor and product ion masses as FKTIE(-HETE)EL. HETE: hydroxyethylthioethyl-moiety

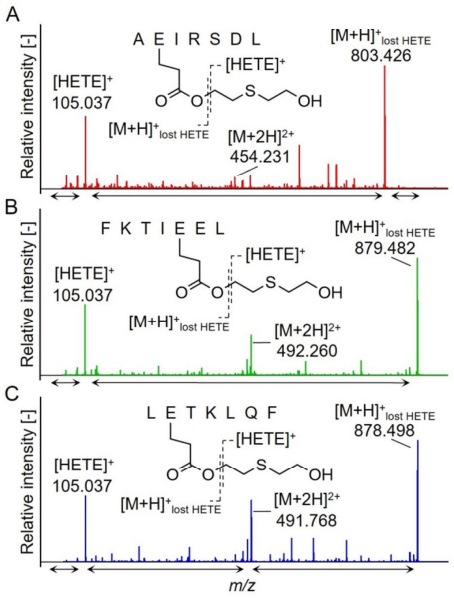

Fig. 2 Product ion spectra of biomarker peptides. Pooled hair reference exposed to sulfur mustard (25 mM) was lysed, proteolyzed with pepsin, and analyzed by µLC–ESI MS/HR MS (PIS). Spectra were extracted from chromatographic peaks (Fig. 1) and the most prominent product ions obtained from the double-protonated precursor ions $[M+2H]^{2+}$ are labelled. **A** AE(-HETE)IRSDL. **B** FKTIE(-HETE)EL. **C** LE(-HETE)TKLQF. $[M+H]^+_{lost\ HETE}$ represents the single protonated peptide backbone after the loss of the hydroxyethylthioethyl $[HETE]^+$-moiety. All product ions showed a mass deviation ≤ 10 ppm, when compared to their theoretical mass (Table SI 1-SI 3). For better visualization of less abundant product ions not labelled in this figure, their signal intensities were multiplied by a factor of 3 in the marked ranges (↔)

appears most likely that the side chain of aspartic acid was alkylated. Accordingly, we herein introduce only the first eluting unambiguously identified adduct AE(-HETE)IRSDL as a biomarker peptide. No interference was detected in blank hair (Fig. 1B), thus documenting highest selectivity of the method.

FKTIE(-HETE)EL: The XIC of qualifier I (*m/z* 879.482) showed one peak at t_R 10.3 min and a second one at t_R 10.5 min (Fig. 1C). Based on the respective MS/MS data (Fig. 2B, Table SI 2), the larger second peak (t_R 10.5 min) correlated to FKTIE(-HETE)EL. The presence of the alkylated y_3-ion (*m/z* 494.217) indicated the alkylation of the glutamic acid residue at position 5 in the heptapeptide (Table SI 2). This identification was also supported by the absence of an ion at *m/z* 365.174 that might have been indicative for the alkylation at the alternative glutamic acid residue at position 6 (alkylated y_2-ion).

The peptide of the smaller peak (t_R 10.3 min) was identified by MS/MS as LE(-HETE)TKLQF. The simultaneous detection of both alkylated peptides was due to the fact that the exact so-called ^{12}C-monoisotopic mass of both peptides differs by only 0.984 Da. Therefore, the masses of the double charged precursor (*m/z* 492.259) and single charged qualifier I (*m/z* 879.482) of FKTIE(-HETE)EL were nearly identical to the corresponding masses of the $^{13}C_1$-variant of LE(-HETE)TKLQF (m/z 492.269 and m/z 879.501). Accordingly, the latter adduct was also subjected to fragmentation and its product ions were detected. However, the $^{13}C_1$-variant did not interfere with FKTIE(-HETE)EL due to robust chromatographic baseline separation of both peaks, the excellent reproducibility of retention times (± 0.03 min), as well as their stable chromatographic resolution ($R = 1.8$, $\Delta t_R = 0.2$ min) observed during the entire period of method

development and validation. Furthermore, no interference was found in blank hair (Fig. 1D) thus making FKTIE(-HETE)EL a useful biomarker.

LE(-HETE)TKLQF: The XIC of qualifier I (*m/z* 878.498) showed a single peak at t_R 10.3 min (Fig. 1E). No interference was found in blank hair (Fig. 1F), thus proving excellent selectivity of this biomarker also (Table SI 3).

SDS-PAGE of lysed hair and in-gel proteolysis with pepsin

The CBB-stained SDS-PAGE of lysed hair showed one prominent band at 45 kDa (Fig. 3A, I) and another one at 60 kDa (Fig. 3A, II) for both reference (Fig. 3A, 2nd lane) and blank hair (Fig. 3A, 3rd lane). In-gel proteolysis with pepsin revealed the presence of AE(-HETE)IRSDL and FKTIE(-HETE)EL (45 kDa band) and of LE(-HETE)TKLQF (60 kDa band) in the reference documenting their origin from type I (40–50 kDa) and type II (55–65 kDa) hair keratins (Deb-Choudhury et al. 2016). No bands indicating crosslinked keratins were found in contrast to linkage between soft keratin 5 and 14 described earlier in HEK-cells (Dillman et al. 2003). No alkylated peptides were detected in the corresponding bands of blank hair indicating the absence of interferences and documenting the selectivity of biomarker analysis.

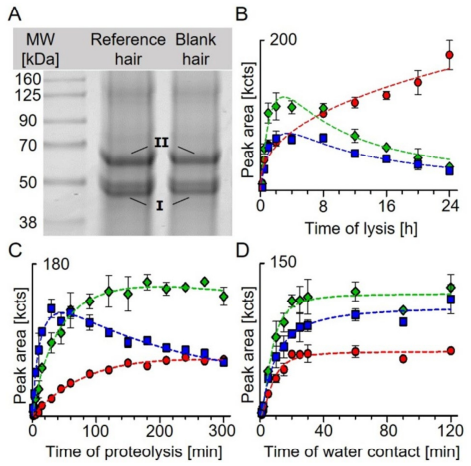

Fig. 3 Formation of biomarker peptides while sample preparation. **A** SDS-PAGE of proteins from lysed reference (2nd lane) and blank hair (3rd lane) stained with Comassie Brilliant Blue. I and II mark bands of type I and type II keratins. The peptides AE(-HETE)IRSDL and FKTIE(-HETE)EL derived from the 45 kDa band (I), whereas LE(-HETE)TKLQF was obtained from the 60 kDa band (II). **B** Formation of biomarker peptides during lysis of reference hair exposed to 25 mM sulfur mustard. After indicated periods, samples ($n=3$) were proteolyzed for 2 h with pepsin and analyzed. **C** Formation of biomarker peptides during proteolysis of reference hair. At indicated time points, aliquots ($n=3$) were analyzed. **D** Formation of biomarker peptides depending on the contact time of SM-incubated hair with water. At distinct time points ($n=3$), the supernatant was discarded and hair was washed with acetonitrile. After lysis and proteolysis, analysis was performed. Depicted peak areas of the qualifier I (Table 1) of AE(-HETE)IRSDL (red filled circles), FKTIE(-HETE)EL (green filled diamonds), and LE(-HETE)TKLQF (blue filled squares) were determined by µLC–ESI MS/HR MS (PIS) analysis. Data points represent the mean and SD of triplicate analysis, each

Lysis of hair

During lysis, disulfide bridges were reduced and the complex structure of linked and folded hair proteins destroyed. Therefore, a large amount of hair proteins was dissolved as required for peptide biomarker generation. The time for lysis was varied between 0.25 h and 24 h to define a reasonable period considering both high biomarker yield and best suitability for the laboratory workflow. The peak areas of the three biomarker peptides increased rapidly within the first 2 h (Fig. 3B). Whereas the concentration of AE(-HETE)IRSDL (red filled circles, Fig. 3B) continued to increase afterwards, those of FKTIE(-HETE)EL (green filled diamonds, Fig. 3B) and LE(-HETE)TKLQF (blue filled squares, Fig. 3B) decreased continuously. Accordingly, for the standard protocol, 4 h were selected for lysis providing high concentrations of each biomarker best suited for simultaneous analysis.

Proteolysis of alkylated keratins

During proteolysis of alkylated keratins derived from reference hair, the concentrations of AE(-HETE)IRSDL (red filled circles, Fig. 3C) and FKTIE(-HETE)EL (green filled diamonds, Fig. 3C) reached a plateau after approx. 130 min. In contrast, LE(-HETE)TKLQF (blue filled squares, Fig. 3C) reached its maximum after about 35 min and continuously decreased afterwards. This was most presumable due to the progressing proteolysis of the peptide rather than to hydrolysis of the HETE-moiety as under acidic conditions applied esters of glutamic acid are known to be stable (John et al. 2019). This assumption was also supported by the stability of AE(-HETE)IRSDL and FKTIE(-HETE)EL (Fig. 3C) which both also contain an alkylated glutamic acid residue. For the standard protocol, a 120 min incubation period was set, providing high concentrations for all three biomarker peptides.

Selectivity of the µLC–ESI MS/HR MS (PIS) method and interindividual differences in biomarker yield

No interferences were recorded for qualifier I and qualifier II of all biomarker peptides in blank hair taken from 7

individuals as exemplarily shown in Fig. 1 (right panel), thus documenting highest selectivity of the method. The yield of the three biomarker peptides resulting from SM-incubated hair from 7 individuals ($n = 3$) varied noticeably (Fig. 4A). These differences were most presumable due to the variable composition of human hair consisting of 65–95% w/w keratin (Robbins 2012) as well as to the keratin-dependent extent of intermolecular disulfide crosslinks affecting the efficacy of lysis. However, alkylated peptides were found in high concentrations in the hair of each individual thus documenting the suitability of these biomarkers.

In addition to scalp hair, all three biomarker peptides were also detected in SM-exposed hair taken from other parts of the body (beard, armpit, abdominal and pubic area) (Fig. 4B). The respective yields varied tremendously (Fig. 4B). This phenomenon might have been due to different amounts of keratin or a hair structure-dependent protein yield after lysis. However, the method was shown to be applicable to these hair samples as well and provided reproducible biomarker yields for each origin (RSD ≤ 19%).

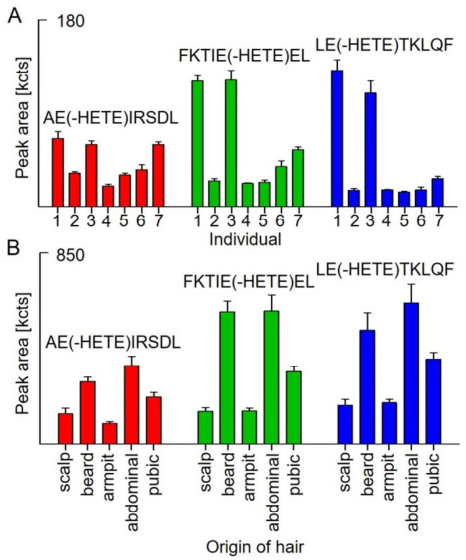

Fig. 4 Individual yield of biomarker peptides derived from human hair keratins. Biomarker peptides were analyzed by µLC–ESI MS/HR MS (PIS) after lysis and proteolysis with pepsin of reference hair exposed to 25 mM sulfur mustard. **A** Scalp hair taken from seven human individuals (1–7). **B** Hair from indicated parts of the body of one male individual. Peak areas resulted from extracted ion chromatograms of the qualifier I (±0.005 Da) of AE(-HETE)IRSDL (red bars), FKTIE(-HETE)EL (green bars) and LE(-HETE)TKLQF (blue bars). Bars represent mean and SD from triplicate analysis, each. HETE: hydroxyethylthioethyl-moiety

In principle, this adaptability is highly important when considering that warm and moist areas of the body are typically heavily affected by SM as shown especially for armpit and pubic area (John et al. 2019; Sezigen and Kenar 2020; Steinritz et al. 2016).

Stability of biomarker peptides in the autosampler

All three biomarker peptides did not show any degradation (RSD ≤ 9.1%) within the 24 h test period, thus documenting excellent stability best suited for analysis of large sample sets (data not shown).

LOI of biomarker peptides

Hair was incubated with SM in the presence of water yielding concentrations ranging from 3 µM to 12.5 mM. Peak areas of the individual qualifier I showed linear correlations ($R^2 \geq 0.994$) between 6 µM and 12.5 mM SM for all biomarkers, thus documenting dose-dependent and reproducible alkylation of hair keratins (data not shown). LOI values obtained from 10 mg hair were as follows: AE(-HETE)IRSDL and FKTIE(-HETE)EL both 190 µM and LE(-HETE)TKLQF 47.5 µM. The low dimension of the LOI documents that only minimum amounts of SM are required for adduct formation and detection. Accordingly, the method is highly suited for real case exposure scenarios where vapor or aerosols of undiluted SM (8 M as liquid) will cover the hair of victims.

Time-dependent adduct formation in the presence of water

After incubation of hair with SM in the absence of water, no biomarker peptides were detected, independent of the incubation time. In contrast, in the presence of water, the yields of all biomarker peptides increased rapidly within the first 20 min before reaching a plateau, thus indicating an essential role of water for adduct formation (Fig. 3D). The presence of water might be a prerequisite for both the formation of the episulfonium ion representing the highly reactive electrophilic intermediate of SM (John et al. 2020) as well as the transportation of SM into the hair. Hair may absorb up to 32% w/w water depending on the relative humidity of ambient air (Robbins 2012) supporting alkylation. In real cases of SM exposure, water will be present in, e.g., sweaty hair and during decontamination and hair washing, thus inducing adduct formation with SM that still sticks to the hair making our method highly suited for verification.

Influence of sweat on adduct formation

In the presence of sweat during incubation of hair with SM, resulting biomarker concentrations were reproducible (RSD ≤ 9%, $n = 3$) and about twice as high as obtained with pure water. The higher yield was most presumably due to the salty sweat matrix (1 g minerals/L) (Montain et al. 2007) minimizing the rate of hydrolysis of SM that occurs as a concurrent reaction to alkylation. The period of half-change of SM in H_2O at 25 °C is about 6 min, whereas the time for hydrolysis in salt water is prolonged by a factor of 3.5 (Bizzigotti et al. 2009). These results support the suitability of our procedure for real cases of sweat-wetted hair exposure.

Stability of alkylated keratins in hair during storage and wash cycles with shampoo

The concentration of all three biomarker peptides was constant (RSD ≤ 19%) over the entire storage period of hair of 7 weeks under different conditions, thus documenting no degradation of keratin adducts (data not shown). Even a prolonged storage time of another 7 weeks (14 weeks in total) under condition III (25 °C, daylight, contact to air) did not provoke any degradation. Furthermore, 5 wash cycles with the use of shampoo did not affect the biomarker yield (RSD ≤ 6%). This stability is highly important for sample shipment and storage as well as delayed sample taking. As the hair shaft is not subject to biotransformation processes, trimmed as well as untrimmed hair will be valuable specimens for post-exposure analysis targeting long-lasting biomarkers.

Conclusion

We herein present for the first time a method very well suited for the long-term biomedical verification of SM exposure in hair by µLC–ESI MS/HR MS (PIS) targeting adducts with hard keratins of hair. Three alkylated peptides obtained after proteolysis are presented as valuable biomarkers. As hair is not considered as potentially infectious material, its handling and shipping are possible without the need to adhere to the strict IATA packaging regulations (International Air Transport Association 2021). Accordingly, hair samples are highly valuable specimens as they can easily be taken by any non-specialized person thus not requiring authorized and qualified health personnel with access to appropriate equipment for blood drawing and subsequent centrifugation. This is an important advantage especially in crisis regions with non-optimum medical infrastructure (John et al. 2016).

As SM-induced alkylation of keratins requires the presence of water, collected contaminated hair should be covered with water for at least 20 min prior to sample preparation, thus allowing optimum adduct formation with SM that still might stick to the surface of the hair. The high stability and insensitivity to washing with shampoo makes hair an ideal specimen for biomarker analysis and allowed a longer period of traceability than that already known from HETE-hemoglobin adducts (12 weeks) (Xu et al. 2014). Evidence of exposure might presumably be possible, even though hair might be cut several weeks up to months after exposure. Future studies might transfer the method to hair and wool from animals to expand and improve the toolbox of verification methods of SM exposure.

Acknowledgements The authors gratefully acknowledge the excellent technical support provided by Marina Dentzel and Stefanie Oswald.

Funding Open Access funding enabled and organized by Projekt DEAL. The work was supported by the German Research Foundation (Deutsche Forschungsgemeinschaft, DFG, Grant/Award Number Research Training Group GRK 2338).

Declarations

Conflict of interest The authors declare no conflict of interest.

References

Adav SS, Subbaiaih RS, Kerk SK, Lee AY, Lai HY, Ng KW, Sze SK, Schmidtchen A (2018) Studies on the proteome of human hair - identification of histones and deamidated keratins. Sci Rep 8(1):1599. https://doi.org/10.1038/s41598-018-20041-9

Barthélemy NR, Bednarczyk A, Schaeffer-Reiss C, Jullien D, van Dorsselaer A, Cavusoglu N (2012) Proteomic tools for the investigation of human hair structural proteins and evidence of weakness sites on hair keratin coil segments. Anal Biochem 421(1):43–55. https://doi.org/10.1016/j.ab.2011.10.011

Bizzigotti GO, Castelly H, Hafez AM, Smith WHB, Whitmire MT (2009) Parameters for evaluation of the fate, transport, and environmental impacts of chemical agents in marine environments. Chem Rev 109(1):236–256. https://doi.org/10.1021/cr0780098

Blum MM, Mamidanna RVSM (2014) Analytical chemistry and the Chemical Weapons Convention. Anal Bioanal Chem 406(21):5067–5069. https://doi.org/10.1007/s00216-014-7931-4

Blum MM, Richter A, Siegert M, Thiermann H, John H (2020) Adduct of the blistering warfare agent sesquimustard with human serum albumin and its mass spectrometric identification for biomedical verification of exposure. Anal Bioanal Chem 412(28):7723–7737. https://doi.org/10.1007/s00216-020-02917-w

Deb-Choudhury S, Plowman JE, Harland DP (2016) Isolation and analysis of keratins and keratin-associated proteins from hair and wool. Methods Enzymol 568:279–301. https://doi.org/10.1016/bs.mie.2015.07.018

Dillman JF, McGary KL, Schlager JJ (2003) Sulfur mustard induces the formation of keratin aggregates in human epidermal keratinocytes. Toxicol Appl Pharmacol 193(2):228–236. https://doi.org/10.1016/j.taap.2003.08.003

Ferreira C, Paulino C, Quintas A (2019) Extraction procedures for hair forensic toxicological analysis: a mini-review. Chem Res Toxicol 32(12):2367–2381. https://doi.org/10.1021/acs.chemrestox.9b00301

Fujii T, Takayama S, Ito Y (2013) A novel purification procedure for keratin-associated proteins and keratin from human hair. J Biol Macromol 13(3):92–106. https://doi.org/10.14533/jbm.13.92

Ghabili K, Agutter PS, Ghanei M, Ansarin K, Shoja MM (2010) Mustard gas toxicity: the acute and chronic pathological effects. J Appl Toxicol 30(7):627–643. https://doi.org/10.1002/jat.1581

Grosvenor AJ, Marsh J, Thomas A, Vernon JA, Harland DP, Clerens S, Dyer JM (2016) Oxidative modification in human hair: the effect of the levels of Cu (II) ions, UV exposure and hair pigmentation. Photochem Photobiol 92(1):144–149. https://doi.org/10.1111/php.12537

International Air Transport Association (2021) Dangerous Goods Regulation. 62nd ed. Montreal, Canada

John H, Willoh S, Hörmann P, Siegert M, Vondran A, Thiermann H (2016) Procedures for analysis of dried plasma using microsampling devices to detect sulfur mustard-albumin adducts for verification of poisoning. Anal Chem 88(17):8787–8794. https://doi.org/10.1021/acs.analchem.6b02199

John H, Koller M, Worek F, Thiermann H, Siegert M (2019) Forensic evidence of sulfur mustard exposure in real cases of human poisoning by detection of diverse albumin-derived protein adducts. Arch Toxicol 93(7):1881–1891. https://doi.org/10.1007/s00204-019-02461-2

John H, Dentzel M, Siegert M, Thiermann H (2021) accepted) A non-targeted high-resolution mass spectrometric workflow for the detection of butyrylcholinesterase-derived adducts with organophosphorus toxicants and structural characterization of their phosphyl-moiety after in-source fragmentation. Anal Chem. https://doi.org/10.1021/acs.analchem.1c04116

John H, Balszuweit F, Steinritz D, Kehe K, Worek F, Thiermann H (2020) Toxicokinetic aspects of nerve agents and vesicants. In: "Handbook of Toxicology of Chemical Warfare Agents" 3 Ed (R. Gupta, ed.), Elsevier Inc./Academic Press, San Diego pp. 875–929; ISBN: 978–0–12–819090–6.

Langbein L, Rogers MA, Winter H, Praetzel S, Schweizer J (2001) The catalog of human hair keratins. II. Expression of the six type II members in the hair follicle and the combined catalog of human type I and II keratins. J Biol Chem 276(37):35123–35132. https://doi.org/10.1074/jbc.M103305200

Lee YJ, Rice RH, Lee YM (2006) Proteome analysis of human hair shaft: from protein identification to posttranslational modification. Mol Cell Proteomics 5(5):789–800. https://doi.org/10.1074/mcp.M500278-MCP200

Lubec G, Nauer G, Seifert K, Strouhal E, Porteder H, Szilvassy J, Teschler M (1987) Structural stability of hair over three thousand years. J Archaeol Sci 14(2):113–120. https://doi.org/10.1016/0305-4403(87)90001-X

Mol MAE, van den Berg RM, Benschop HP (2008) Proteomic assessment of sulfur mustard-induced protein adducts and other protein modifications in human epidermal keratinocytes. Toxicol Appl Pharmacol 230(1):97–108. https://doi.org/10.1016/j.taap.2008.02.006

Montain SJ, Cheuvront SN, Lukaski HC (2007) Sweat mineral-element responses during 7 h of exercise-heat stress. Int J Sport Nutr Exerc Metab 17(6):574–582. https://doi.org/10.1123/ijsnem.17.6.574

Robbins CR (2012) Chemical and Physical Behavior of Human Hair, 5th edn. Springer, Berlin Heidelberg. https://doi.org/10.1007/978-3-642-25611-0

Robbins CR, Kelly CH (1970) Amino acid composition of human hair. Text Res J 40(10):891–896. https://doi.org/10.1177/004051757004001005

Schmeißer W, Lüling R, Steinritz D, Thiermann H, Rein T, John H (2021) Transthyretin as a target of alkylation and a potential biomarker for sulfur mustard poisoning: electrophoretic and mass spectrometric identification and characterization. Drug Test Anal 14:80–91. https://doi.org/10.1002/dta.3146

Schweizer J, Bowden PE, Coulombe PA, Langbein L, Lane EB, Magin TM, Maltais L, Omary MB, Parry DAD, Rogers MA, Wright MW (2006) New consensus nomenclature for mammalian keratins. J Cell Biol 174(2):169–174. https://doi.org/10.1083/jcb.200603161

Thermo Fisher Scientific (2021, accessed October 13) Instructions: In-Gel Tryptic Digestion Kit. https://www.thermofisher.com/document-connect/document-connect.html?url=https%3A%2F%2Fassets.thermofisher.com%2FTFS-Assets%2FLSG%2Fmanuals%2FMAN0011497_InGel_Tryptic_Digest_UG.pdf.

Sezigen S, Kenar L (2020) Recent sulfur mustard attacks in Middle East and experience of health professionals. Toxicol Lett 320:52–57. https://doi.org/10.1016/j.toxlet.2019.12.001

Siegert M, Gandor F, Kranawetvogl A, Börner H, Thiermann H, John H (2019) Methionine329 in human serum albumin: a novel target for alkylation by sulfur mustard. Drug Test Anal 11(5):659–668. https://doi.org/10.1002/dta.2548

Steinritz D, Striepling E, Rudolf KD, Schröder-Kraft C, Püschel K, Hullard-Pulstinger A, Koller M, Thiermann H, Gandor F, Gawlik M, John H (2016) Medical documentation, bioanalytical evidence of an accidental human exposure to sulfur mustard and general therapy recommendations. Toxicol Lett 244:112–120. https://doi.org/10.1016/j.toxlet.2015.08.1105

Steinritz D, Lüling R, Siegert M, Herbert J, Mückter H, Taeger CD, Gudermann T, Dietrich A, Thiermann H, John H (2021) Alkylated epidermal creatine kinase as a biomarker for sulfur mustard exposure: comparison to adducts of albumin and DNA in an in vivo rat study. Arch Toxicol 95(4):1323–1333. https://doi.org/10.1007/s00204-021-03005-3

U.S. Department of Labor (2021, accessed August 24) Definition of Terms: OSHA - Occupational Safety & Health Administration. Definition of Terms. https://www.jems.com/wp-content/uploads/content/dam/jems/migrated/images/files-30/OSHA-Definition-of-Terms-0.pdf.

van der Schans GP, Noort D, Mars-Groenendijk RH, Fidder A, Chau LF, de Jong LPA, Benschop HP (2002) Immunochemical detection of sulfur mustard adducts with keratins in the stratum corneum of human skin. Chem Res Toxicol 15(1):21–25. https://doi.org/10.1021/tx0100136

Watson RR, Solkoff D, Wang JY, Seeto K (1998) Detection of ethanol consumption by ELISA assay measurement of acetaldehyde

adducts in murine hair. Alcohol 16(4):279–284. https://doi.org/10.1016/S0741-8329(98)00014-7

Xu H, Nie Z, Zhang Y, Li C, Yue L, Yang W, Chen J, Dong Y, Liu Q, Lin Y, Wu B, Feng J, Li H, Guo L, Xie J (2014) Four sulfur mustard exposure cases: overall analysis of four types of biomarkers in clinical samples provides positive implication for early diagnosis and treatment monitoring. Toxicol Rep 1:533–543. https://doi.org/10.1016/j.toxrep.2014.07.017

3.2.2 Supplement

Supporting Information

Adducts of hard keratins from hair for verification of exposure to sulfur mustard by high-resolution mass spectrometry

Wolfgang Schmeißer[1], Markus Siegert[1,2,a], Horst Thiermann[1], Theo Rein[3], Harald John*[,1]

[1] Bundeswehr Institute of Pharmacology and Toxicology, Neuherbergstrasse 11, 80937 Munich, Germany

[2] Department of Chemistry, Humboldt-Universität zu Berlin, Brook-Taylor-Strasse 2, 12489 Berlin, Germany

[3] Max Planck Institute of Psychiatry, Kraepelinstrasse 2-10, 80804 Munich, Germany

[a] present address: Proteros Biostructures GmbH, Bunsenstrasse 7a, 82152 Planegg, Germany

* Address correspondence to this author.

Bundeswehr Institute of Pharmacology and Toxicology

Neuherbergstrasse 11, 80937 Munich, Germany

Phone: +49-89-992692-2311. Fax: +49-89-992692-2333.

E-mail: HaraldJohn@bundeswehr.org

Table of Content

Table S1

MS/HR MS data of the double protonated AE(-HETE)IRSDL biomarker peptide

ion	elemental composition	m/z theoretical	m/z measured	Δ m/z [mmu]	Δ m/z [ppm]
AE(-HETE)IRSDL $^{2H+}$	$C_{37}H_{68}N_{10}O_{14}S$	454.2313	454.232	+1.1	+2.4
y_6	$C_{34}H_{62}N_9O_{13}S$	836.4182	836.420	+1.5	+1.8
AEIRSDL	$C_{33}H_{59}N_{10}O_{13}$	803.4258	803.428	+2.5	+3.1
y_7-HETE-17	$C_{33}H_{56}N_9O_{13}$	786.3992	786.403	+3.6	+4.6
y_7-HETE-18	$C_{33}H_{57}N_{10}O_{12}$	785.4152	785.419	+4.2	+5.4
b_6	$C_{31}H_{54}N_9O_{12}S$	776.3607	776.359	-1.5	-1.9
y_6-HETE-18	$C_{30}H_{52}N_9O_{11}$	714.3781	714.381	+2.5	+3.5
b_6-HETE	$C_{27}H_{46}N_9O_{11}$	672.3311	672.334	+2.4	+3.6
b_5-HETE	$C_{23}H_{41}N_8O_8$	557.3042	557.303	-0.8	-1.5
y_6-HETE	$C_{30}H_{54}N_9O_{12}$	732.3887	732.391	+2.1	+2.9
b_5	$C_{27}H_{49}N_8O_9S$	661.3338	661.337	+2.9	+4.3
y_5	$C_{25}H_{47}N_8O_9$	603.3461	603.348	+1.5	+2.5
y_3-18	$C_{25}H_{45}N_8O_8$	585.3355	585.339	+3.1	+5.3
y_4	$C_{19}H_{36}N_7O_8$	490.2620	490.264	+1.7	+3.5
y_4-17	$C_{19}H_{33}N_6O_8$	473.2354	473.237	+1.5	+3.2
y_4-18	$C_{19}H_{34}N_7O_7$	472.2514	472.249	-2.4	-5.1
b_4-HETE	$C_{20}H_{36}N_7O_6$	470.2722	470.274	+2.2	+4.7
a_4-HETE	$C_{19}H_{36}N_7O_5$	442.2772	442.276	-0.9	-2.1
y_3	$C_{13}H_{24}N_3O_7$	334.1609	334.162	+0.7	+2.0
b_3-HETE	$C_{14}H_{24}N_3O_5$	314.1711	314.170	-0.7	-2.2
b_2	$C_{12}H_{21}N_2O_5S$	305.1166	305.119	+2.0	+6.6
b_2-18	$C_{12}H_{19}N_2O_4S$	287.1060	287.104	-1.6	-5.6
a_2	$C_{11}H_{21}N_2O_4S$	277.1217	277.124	+2.2	+7.9
y_2	$C_{10}H_{19}N_2O_5$	247.1289	247.130	+1.0	+4.0
b_2-HETE	$C_8H_{13}N_2O_4$	201.0870	201.088	+0.7	+3.7
y_1	$C_6H_{14}NO_2$	132.1019	132.101	-0.5	-3.6
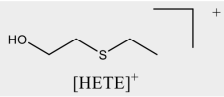 [HETE]$^+$	C_4H_9OS	105.0369	105.037	+0.1	+1.0
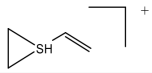	C_4H_7S	87.0261	87.026	-0.2	-2.3
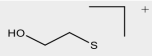	C_2H_5OS	77.0056	77.006	0.0	0.0

Data were extracted from the biomarker peak (t_R 7.0 min, Fig. 1A) obtained from µLC-ESI MS/HR MS (PIS) analysis of hair incubated with sulfur mustard (25 mM) followed by pepsin-catalyzed proteolysis. A triple TOF mass spectrometer was used. The corresponding MS/HR MS spectrum is shown in Figure 2A. The exact mass of the single protonated biomarker is *m/z* 907.4554.

Table S2

MS/HR MS data of the double protonated FKTIE(-HETE)EL biomarker peptide

ion	elemental composition	m/z theoretical	m/z measured	Δ m/z [mmu]	Δ m/z [ppm]
FKTIE(-HETE)EL $^{2H+}$	$C_{45}H_{76}N_8O_{14}S$	492.2595	492.262	+2.2	+4.5
FKTIEEL	$C_{41}H_{67}N_8O_{13}$	879.4822	879.485	+2.4	+2.7
y_7-HETE-18	$C_{41}H_{65}N_8O_1$	861.4717	861.474	+2.3	+2.6
b_6	$C_{39}H_{62}N_7O_{12}S$	852.4172	852.417	-0.4	-0.5
y_6	$C_{36}H_{66}N_7O_{13}S$	836.4434	836.442	-1.2	-1.5
b_6-18	$C_{39}H_{60}N_7O_{12}S$	834.4066	834.407	0.0	+0.1
a_7-HETE	$C_{40}H_{65}N_8O_{11}$	833.4767	833.475	-1.3	-1.5
b_6-HETE	$C_{35}H_{54}N_7O_{11}$	748.3876	748.390	+2.7	-3.7
y_6-HETE	$C_{32}H_{58}N_7O_{12}$	732.4138	732.419	+4.7	+6.5
y_5	$C_{30}H_{54}N_5O_{12}S$	708.3484	708.348	0.0	0.0
y_5-18	$C_{30}H_{52}N_5O_{11}S$	690.3379	690.341	+3.5	+5.0
y_5-HETE	$C_{26}H_{45}N_5O_{11}$	604.3188	604.316	-2.4	-4.0
y_5-HETE-18	$C_{26}H_{44}N_5O_{10}$	586.3083	586.310	+1.6	+2.7
y_4-HETE	$C_{22}H_{39}N_4O_9$	503.2712	503.271	+0.1	+0.1
y_3	$C_{20}H_{36}N_3O_9S$	494.2167	494.219	+1.9	+3.8
b_4	$C_{25}H_{40}N_5O_5$	490.3024	490.304	+1.5	+3.1
y_3-18	$C_{20}H_{34}N_3O_8S$	476.2061	476.204	-2.6	-5.5
a_4	$C_{24}H_{40}N_5O_4$	462.3075	462.305	-2.3	-4.9
y_3-HETE	$C_{16}H_{28}N_3O_8$	390.1871	390.188	+0.9	+2.4
b_3	$C_{19}H_{29}N_4O_4$	377.2183	377.219	+1.1	+2.9
b_2	$C_{15}H_{22}N_3O_2$	276.1707	276.172	+1.1	+3.8
y_2	$C_{11}H_{21}N_2O_5$	261.1445	261.145	+0.4	+1.5
y_2-18	$C_{11}H_{19}N_2O_4$	243.1339	243.135	+0.9	+3.8
y_1	$C_6H_{14}NO_2$	132.1019	132.102	-0.3	-2.1
a_1	C_8H_9N	120.0808	120.081	+0.6	+4.8
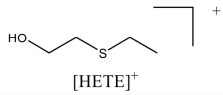 [HETE]$^+$	C_4H_9OS	105.0369	105.037	+0.1	+0.6
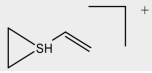	C_4H_7S	87.0261	87.026	0.0	-0.3
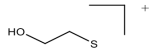	C_2H_5OS	77.0056	77.005	-0.8	-10.4
	C_2H_5S	61.0107	61.011	-0.2	-3.0

Data were extracted from the biomarker peak (t_R 10.5 min, Fig. 1C) obtained from µLC-ESI MS/HR MS (PIS) analysis of hair incubated with sulfur mustard (25 mM) followed by pepsin-catalyzed proteolysis. A triple TOF mass spectrometer was used. The corresponding MS/HR MS spectrum is shown in Figure 2B. The exact mass of the single protonated biomarker is *m/z* 983.5118.

Table S3

MS/HR MS data of the double protonated LE(-HETE)TKLQF biomarker peptide

ion	elemental composition	m/z theoretical	m/z measured	Δ m/z [mmu]	Δ m/z [ppm]
LE(-HETE)TKLQF $^{2H+}$	$C_{45}H_{77}N_9O_{13}S$	491.7675	491.770	+2.3	+4.6
LETKLQF	$C_{41}H_{68}N_9O_{12}$	878.4982	878.501	+2.9	+3.3
y_6	$C_{39}H_{65}N_8O_{12}S$	869.4437	869.445	+1.5	+1.8
y_7-HETE-17	$C_{41}H_{65}N_8O_{12}$	861.4717	861.479	+6.9	+8.0
y_7-HETE-18	$C_{41}H_{66}N_9O_{11}$	860.4876	860.491	+3.3	+3.9
y_6-18	$C_{39}H_{63}N_8O_{11}S$	851.4332	851.433	-0.3	-0.4
b_7-HETE-18	$C_{41}H_{64}N_9O_{10}$	842.4771	842.480	+2.8	+3.4
a_7-HETE	$C_{40}H_{66}N_9O_{10}$	832.4927	832.495	+2.6	+3.1
b_6	$C_{36}H_{65}N_8O_{11}S$	817.4488	817.447	-1.5	-1.9
b_6-17	$C_{36}H_{62}N_7O_{11}S$	800.4223	800.426	+3.5	+4.4
b_6-18	$C_{36}H_{62}N_8O_{10}S$	799.4382	799.444	+6.1	+7.6
y_6-HETE	$C_{35}H_{57}N_8O_{11}$	765.4141	765.417	+2.7	+3.5
y_6-HETE-18	$C_{35}H_{55}N_8O_{10}$	747.4036	747.405	+1.0	+1.4
b_6-HETE	$C_{32}H_{57}N_8O_{19}$	713.4192	713.421	+1.8	+2.6
b_6-HETE-18	$C_{32}H_{55}N_8O_9$	695.4087	695.406	-2.5	-3.7
b_5	$C_{31}H_{57}N_6O_9S$	689.3902	689.390	-0.1	-0.2
a_5-HETE	$C_{31}H_{57}N_8O_9$	685.4243	685.426	+1.4	+2.1
b_5-18	$C_{31}H_{55}N_6O_8S$	671.3797	671.382	+2.8	+4.2
y_5	$C_{30}H_{50}N_7O_8$	636.3715	636.373	+1.9	+2.9
z_5-17	$C_{30}H_{47}N_6O_8$	619.3450	619.349	+4.4	+7.1
y^5-18	$C_{30}H_{47}N_7O_7$	618.3610	618.361	+3.8	+6.1
b_5-HETE	$C_{27}H_{49}N_6O_8$	585.3606	585.362	+1.4	+2.4
b_4	$C_{25}H_{46}N_5O_8S$	576.3062	576.305	-1.6	-2.7
b_5-HETE-18	$C_{27}H_{47}N_6O_7$	567.3501	567.351	+0.6	+1.0
a_5-HETE	$C_{26}H_{49}N_6O_7$	557.3657	557.366	+0.1	+0.2
y_4	$C_{26}H_{43}N_6O_6$	535.3239	535.325	+1.1	+2.1
y_4-17	$C_{26}H_{40}N_5O_6$	518.2973	518.301	+3.9	+7.4
y_4-18	$C_{26}H_{41}N_6O_5$	517.3133	517.316	+2.6	+5.0
b_4-HETE	$C_{21}H_{38}N_5O_7$	472.2766	472.278	+1.8	+3.8
b_4-HETE-18	$C_{21}H_{36}N_5O_6$	454.2660	454.267	+1.1	+2.5
b_3	$C_{19}H_{34}N_3O_7S$	448.2112	448.215	+4.2	+9.5
y_3	$C_{20}H_{31}N_4O_5$	407.2289	407.230	+1.6	+3.9
b_2	$C_{15}H_{27}N_2O_5S$	347.1635	347.165	+1.6	+4.6
b_3-HETE	$C_{15}H_{26}N_3O_6$	344.1816	344.182	+0.5	+1.5
b_3-HETE-18	$C_{15}H_{24}N_3O_5$	326.1711	326.172	+0.5	+1.7
b_2-18	$C_{15}H_{25}N_2O_4S$	329.1530	329.155	+1.7	+5.0
a_2	$C_{14}H_{27}N_2O_4S$	319.1686	319.168	-0.5	-1.5
y_2	$C_{14}H_{20}N_3O_4$	294.1448	294.146	+1.4	+4.7
y_2-17	$C_{14}H_{17}N_2O_4$	277.1194	277.119	+1.1	+4.1
b_2-HETE	$C_{11}H_{19}N_2O_4$	243.1339	243.135	+1.4	+5.8
b_2-HETE-18	$C_{11}H_{17}N_2O_3$	225.1234	225.123	-0.6	-2.6
a_2-HETE	$C_{10}H_{19}N_2O_3$	215.1390	215.139	+0.1	+0.4
y_1	$C_9H_{12}NO_2$	166.0863	166.087	+0.6	+3.6
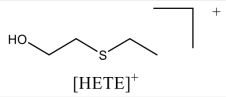 [HETE]$^+$	C_4H_9OS	105.0369	105.037	+0.1	+1.1

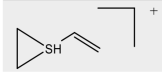	C_4H_7S	87.0261	87.026	-0.1	-0.9
a_1	$C_5H_{11}N$	86.0964	86.096	-0.3	-3.1
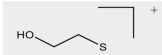	C_2H_5OS	77.0056	77.005	-0.1	-1.3
	C_2H_5S	61.0107	61.011	+0.0	-0.5

Data were extracted from the biomarker peak (t_R 10.3 min, Fig. 1E) obtained from µLC-ESI MS/HR MS (PIS) analysis of hair incubated with sulfur mustard (25 mM) followed by pepsin-catalyzed proteolysis. A triple TOF mass spectrometer was used. The corresponding MS/HR MS spectrum is shown in Figure 2C. The exact mass of the single protonated biomarker is *m/z* 982.5278.

4 Zusammenfassung

Der eindeutige Nachweis des völkerrechtswidrigen Einsatzes von Bis(2-chlorethyl)sulfid (S-Lost) in Syrien und im Nordirak in jüngster Vergangenheit, stellt die notwendige Grundlage für Sanktionen durch den Sicherheitsrat der Vereinten Nationen dar und zeigt die Bedeutung der Verifikationsanalytik. Dabei spielt die Detektion von S-Lost-induzierten Addukten endogener Proteine, aufgrund der langen Nachweisbarkeit entsprechender Biomarkerpeptide, eine zentrale Rolle. Deshalb sollten in der vorliegenden Dissertation neue Proteine identifiziert werden, welche von S-Lost alkyliert werden, um daraus spezifische Peptide zu generieren und deren Einsatz als potentielle Biomarker zu charakterisieren.

Mit der zweidimensionalen Differenz-Gelelektrophorese und anschließender matrixunterstützter Laser-Desorption/Ionisation Flugzeitmassenspektrometrie konnte das Plasmaprotein Transthyretin (TTR) als Zielstruktur von Alkylanzien identifiziert werden. Nach proteolytischer Spaltung von S-Lost-inkubiertem Plasma mit Trypsin und Flüssigchromatographie gekoppelt mit hochauflösender Massenspektrometrie (LC-MS/HR-MS) wurde das Hexapeptid Cys(-HETE)ProLeuMetValLys (C(-HETE)PLMVK) identifiziert, das die charakteristische S-Lost-induzierte Hydroxyethylthioethyl (HETE)-Einheit am Cystein in Position 10 in TTR aufweist. Nach einer optimierten Aufarbeitung mittels immunomagnetischer Separation von adduktiertem TTR aus Plasma, konnte C(-HETE)PLMVK selektiv und auch nach 14 Tagen bei 37°C *in vitro* detektiert werden. C(-HETE)PLMVK wurde in S-Lost-inkubiertem Plasma von 7 verschiedenen Individuen detektiert und wies unter Berücksichtigung der OVCW-Kriterien zur Bestimmung der Nachweisgrenze eine Konzentration von 31.25 µM S-Lost auf. Damit stellt adduktiertes TTR ein neuartiges Biomarkermolekül für den Nachweis einer S-Lost-Exposition dar.

Die Probenmatrices Blut, Plasma oder Urin, aus denen etablierte Biomarker gewonnen werden, gelten als potentiell infektiöses Material und bedingen damit eine aufwendige Handhabung bezüglich Beprobung und Versand. Hingegen gelten Haare, die überwiegend aus den strukturgebenden Proteinen Hartkeratinen bestehen, als nicht infektiös und stellen damit eine wesentlich einfacher zu handhabende Probenmatrix dar. Nach der Lyse von S-Lost-inkubierten Kopfhaaren, um die Haarproteine zu solubilisieren, und anschließender Pepsin katalysierter Proteolyse wurden mittels LC-MS/HR-MS drei an Glutaminsäuren alkylierte Heptapeptide identifiziert. AlaGlu(-HETE)IleArgSerAspLeu, PheLysThrIleGlu(-HETE)GluLeu und LeuGlu(-HETE)ThrLysLeuGlnPhe ließen sich eindeutig Hartkeratinen als Ursprung zuordnen und waren in S-Lost-behandelten Haaren von 7 verschiedenen Spendern nachweisbar. Neben Kopfhaaren konnten die Biomarkerpeptide auch in Achsel,- Bart-, Bauch- und Intimhaaren selektiv detektiert werden. Die Bildung der Addukte im Haar benötigen ein wässriges Milieu, wie es bei einer einfachen Dekontamination mit Wasser oder bei schweißnassen Haaren der Fall ist. Gebildete Addukte sind bei intensiver Waschung der Haare mit Shampoo und der Lagerung bei Raumtemperatur unter Einfluss von Licht und Luft über mindestens 14 Wochen stabil. Damit konnten zum ersten Mal aus Haaren gewonnene adduktierte Peptide als Biomarker etabliert werden, die regioselektiv und über den bisher längsten bekannten Zeitraum die Verifikation einer S-Lost-Exposition ermöglichen.

5 Summary

The unambiguous evidence of the recent use of bis(2-chloroethyl)sulfide (S-Lost) in Syria and Northern Iraq, which is contrary to international law, provides the necessary framework for sanctions by the United Nations Security Council and demonstrates the relevance of verification analysis. The detection of S-Lost-induced adducts of endogenous proteins is a key issue in this context due to the long detectability of corresponding biomarker peptides. Therefore, the aim of this thesis was to identify new proteins that are alkylated by S-Lost in order to generate specific peptides and to characterise their application as potential biomarkers.

Two-dimensional difference gel electrophoresis followed by matrix-assisted laser desorption/ionization time-of-flight mass spectrometry identified the plasma protein transthyretin (TTR) as a target structure of alkylating agents. After trypsin-catalyzed proteolysis of S-Lost incubated plasma and liquid chromatography coupled with high-resolution mass spectrometry (LC-MS/HR-MS), the hexapeptide Cys(-HETE)ProLeuMetValLys (C(-HETE)PLMVK) was identified, bearing the characteristic S-Lost-induced hydroxyethylthioethyl (HETE) group at the cysteine in position 10 in TTR. After optimised preparation by immunomagnetic separation of adducted TTR from plasma, C(-HETE)PLMVK was detected selectively and also after 14 days at 37°C *in vitro*. C(-HETE)PLMVK was detected in S-Lost-incubated plasma from 7 different individuals and showed a concentration of 31.25 µM S-Lost, taking into account the OVCW criteria for determining the limit of detection. Therefore, alkylated TTR represents a novel biomarker molecule for the verification of an S-Lost exposure.

The sample matrices blood, plasma or urine which are used to obtain established biomarkers are considered as potentially infectious material and therefore require complex handling with regard to sampling and shipping. Hair consisting predominantly of the structure-providing proteins hard keratins are considered as non-infectious and thus represents an easy-to-handle sample matrix. After lysis of S-Lost-incubated scalp hair to solubilise the hair proteins and subsequent pepsin-catalyzed proteolysis, three heptapeptides each alkylated at a glutamic acid residue were identified by LC-MS/HR-MS. AlaGlu(-HETE)IleArgSerAspLeu, PheLysThrIleGlu(-HETE)GluLeu and LeuGlu(-HETE)ThrLysLeuGlnPhe were clearly attributable to hard keratins as the origin and were detected in S-Lost-treated hair from 7 different donors. In addition to scalp hair, the biomarker peptides were also selectively detected in armpit, beard, abdominal, and pubic hair. The formation of the adducts in hair requires an aqueous milieu, which is the case when decontamination is simply done with water or when the hair is sweaty. Protein adducts were not affected by washing the hair with shampoo, and were stable for at least 14 weeks at ambient temperature and contact to air. This is the first time local peptide adduct biomarkers from hair were established allowing the verification of S-Lost exposure over the longest period known so far.

6 Literaturverzeichnis

1. United Nations Treaty Collection. Convention on the prohibition of Convention on the prohibition of the development, production, stockpiling and use of chemical weapons and on their destruction. https://www.opcw.org/sites/default/files/documents/CWC/CWC_en.pdf (abgerufen am 01.02.2024).

2. Organisation for the Prohibition of Chemical Weapons. Article XII - Measures to Redress a Situation and to Ensure Compliance, including Sanctions. https://www.opcw.org/chemical-weapons-convention/articles/article-xii-measures-redress-situation-and-ensure-compliance (abgerufen am 01.02.2024).

3. Blum, M.-M.; Richter, A.; Siegert, M.; Thiermann, H.; John, H. Adduct of the blistering warfare agent sesquimustard with human serum albumin and its mass spectrometric identification for biomedical verification of exposure. *Analytical and bioanalytical chemistry* **2020**, 412 (28), 7723–7737. DOI: 10.1007/s00216-020-02917-w.

4. John, H.; Koller, M.; Worek, F.; Thiermann, H.; Siegert, M. Forensic evidence of sulfur mustard exposure in real cases of human poisoning by detection of diverse albumin-derived protein adducts. *Archives of toxicology* **2019**, 93 (7), 1881–1891. DOI: 10.1007/s00204-019-02461-2.

5. Blum, M.-M.; Mamidanna, R. V. S. M. Analytical chemistry and the Chemical Weapons Convention. *Analytical and bioanalytical chemistry* **2014**, 406 (21), 5067–5069. DOI: 10.1007/s00216-014-7931-4.

6. Thiermann, H.; Gonder, S.; John, H.; Kehe, K.; Koller, M.; Steinritz, D.; Worek, F. Chemische Kampfstoffe. *Toxikologie*, Vohr, H.-W., Ed., **2010**, pp 201–233. DOI: 10.1002/9783527635542.ch9.

7. Rosenblatt, D. H.; Small, M. J.; Kimmell, T. A.; Anderson, A. W. Background chemistry for chemical warfare agents and decontamination processes in support of delisting waste streams at the U.S. Army Dugway Proving Ground, Utah **1996,** DOI: 10.2172/258187.

8. Young, Robert A. & Bast, Cheryl B. Mustards and Vesicants. *Handbook of toxicology of chemical*, Elsevier, **2009**, pp 93–108.

9. Despretz, C.-M. Des composes triples du chlore. *Annales de chimie et de physique* **1822** (21), 438.

10. Niemann, A. Ueber die Einwirkung des braunen Chlorschwefels auf Elaylgas. *Annalen der Chemie und Pharmacie* **1860**, 113 (3), 288–292. DOI: 10.1002/jlac.18601130304.

11. Guthrie, F. Ueber einige Derivate der Kohlenwasserstoffe CnHn. *Annalen der Chemie und Pharmacie* **1860**, 116 (2), 234–249. DOI: 10.1002/jlac.18601160211.

12. Meyer, V. Ueber Thiodiglykolverbindungen. *Berichte der Deutschen Chemischen Gesellschaft* **1886**, 19 (2), 3259–3266. DOI: 10.1002/cber.188601902358.

13. Duchovic, R. J.; Vilensky, J. A. Mustard Gas: Its Pre-World War I History. *Journal of Chemical Education* **2007**, 84 (6), 944. DOI: 10.1021/ED084P944.

14. Gilchrist, H. L.; United States. A Comparative Study of World War Casualties from Gas and Other Weapons. Washington, DC: *U.S. Government Printing Office* **1928**, 1–5.

15. Wattana, M.; Bey, T. Mustard gas or sulfur mustard: an old chemical agent as a new terrorist threat. *Prehospital and disaster medicine* **2009**, 24 (1), 19-29; discussion 30-1. DOI: 10.1017/s1049023x0000649x.

16. Darchini-Maragheh, E.; Balali-Mood, M. Delayed Complications and Long-term Management of Sulfur Mustard Poisoning: Recent Advances by Iranian Researchers (Part I of II). *Iranian Journal of Medical Sciences* **2018**, 43 (2), 103–124. DOI: 10.30476/ijms.2018.40516

17. Pechura, C. M., Rall, D. P., Eds. Veterans at Risk: The health effects of mustard gas and Lewisite; *National Academy Press* **1993**.

18. Balali-Mood, M.; Hefazi, M. The pharmacology, toxicology, and medical treatment of sulphur mustard poisoning. *Fundamental & clinical pharmacology* **2005**, 19 (3), 297-315. DOI: 10.1111/j.1472-8206.2005.00325.x.

19. Kehe, K.; Szinicz, L. Medical aspects of sulphur mustard poisoning. *Toxicology* **2005**, 214 (3), 198–209. DOI: 10.1016/j.tox.2005.06.014.

20. Khateri, S.; Ghanei, M.; Keshavarz, S.; Soroush, M.; Haines, D. Incidence of lung, eye, and skin lesions as late complications in 34,000 Iranians with wartime exposure to mustard agent. *Journal of occupational and environmental* medicine **2003**, 45 (11), 1136–1143. DOI: 10.1097/01.jom.0000094993.20914.d1.

21. Balali-Mood, M.; Hefazi, M. Comparison of early and late toxic effects of sulfur mustard in Iranian veterans. *Basic & clinical pharmacology & toxicology* **2006**, 99 (4), 273–282. DOI: 10.1111/j.1742-7843.2006.pto_429.x.

22. NobelPrize.org. Organisation for the Prohibition of Chemical Weapons (OPCW) – Facts. https://www.nobelprize.org/prizes/peace/2013/opcw/facts/ (abgerufen am 01.02.2024).

23. Sezigen, S.; Kenar, L. Recent sulfur mustard attacks in Middle East and experience of health professionals. *Toxicology letters* **2020**, 320, 52–57. DOI: 10.1016/j.toxlet.2019.12.001.

24. Masterson, J.; Quinn, L. Timeline of Syrian Chemical Weapons Activity, 2012-2022. Julia Masterson and Leanne Quinn. https://www.armscontrol.org/factsheets/Timeline-of-Syrian-Chemical-Weapons-Activity (abgerufen am 01.02.2024).

25. Bizzigotti, G. O.; Castelly, H.; Hafez, A. M.; Smith, W. H. B.; Whitmire, M. T. Parameters for Evaluation of the Fate, Transport, and Environmental Impacts of Chemical Agents in Marine Environments. *Chemical Reviews* **2009**, 109 (1), 236–256. DOI: 10.1021/cr0780098.

26. Malhotra, R. C.; Ganesan, K.; Sugendran, K.; Swamy, R. V. Chemistry and Toxicology of Sulphur Mustard- A Review. *Defence Science Journal* **1999**, 49 (2), 97–116. DOI: 10.14429/DSJ.49.3793.

27. Organisation for the Prohibition of Chemical Weapons. Practical Guide for Medical Management of Chemical Warfare Casualties. https://www.opcw.org/sites/default/files/documents/2019/05/Full%20version%202019_Medical%20Guide_WEB.pdf (accessed 2024-01-02).

28. Agency for Toxic Substances and Disease Registry (ATSDR). Toxicological profile for Sulfur Mustard: chemical and physical information **2003**, 119–123 (abgerufen am 01.02.2024).

29. Papirmeister, B.; Gross, C. L.; Petrali, J. P.; Meier, H. L. Pathology Produced by Sulfur Mustard in Human Skin Grafts on Athymic Nude Mice. II. Ultrastructural Changes. *Journal of Toxicology: Cutaneous and Ocular Toxicology* **1984**, 3 (4), 393–408. DOI: 10.3109/15569528409036290.

30. Kehe, K.; Balszuweit, F.; Steinritz, D.; Thiermann, H. Molecular toxicology of sulfur mustard-induced cutaneous inflammation and blistering. *Toxicology* **2009**, 263 (1), 12-19. DOI: 10.1016/j.tox.2009.01.019.

31. Steinritz, D.; Emmler, J.; Hintz, M.; Worek, F.; Kreppel, H.; Szinicz, L.; Kehe, K. Apoptosis in sulfur mustard treated A549 cell cultures. *Life sciences* **2007**, 80 (24-25), 2199–2201. DOI: 10.1016/j.lfs.2006.11.052.

32. Schmidt, A.; Steinritz, D.; Rudolf, K.-D.; Thiermann, H.; Striepling, E. Accidental sulfur mustard exposure: A case report. *Toxicology letters* **2018**, 293, 62–66. DOI: 10.1016/j.toxlet.2017.11.023.

33. Dachir, S.; Cohen, M.; Kamus-Elimeleh, D.; Fishbine, E.; Sahar, R.; Gez, R.; Brandeis, R.; Horwitz, V.; Kadar, T. Characterization of acute and long-term pathologies of superficial and deep dermal sulfur mustard skin lesions in the hairless guinea pig model. Wound repair and regeneration : official publication of the Wound Healing Society [and] the European Tissue Repair Society **2012**, 20 (6), 852–861. DOI: 10.1111/j.1524-475X.2012.00830.x.

34. Renshaw, B. Observations on the role of water in the susceptibility of human skin to injury by vesicant vapors. *The Journal of investigative dermatology* **1947**, 9 (2), 75–85. DOI: 10.1038/jid.1947.71.

35. Ghabili, K.; Agutter, P. S.; Ghanei, M.; Ansarin, K.; Shoja, M. M. Mustard gas toxicity: the acute and chronic pathological effects. *Journal of Applied Toxicology* **2010**, 30 (7), 627–643. DOI: 10.1002/jat.1581.

36. Sahebkar, A.; Antonelli-Incalzi, R.; Panahi, Y.; Ghanei, M.; Pedone, C. Mustard lung and COPD: common features and treatment? The Lancet. *Respiratory medicine* **2015**, 3 (10), 747–748. DOI: 10.1016/S2213-2600(15)00363-X.

37. John, H.; Balszuweit, F.; Steinritz, D.; Kehe, K.; Worek, F.; Thiermann, H. Toxicokinetic aspects of nerve agents and vesicants. *Handbook of Toxicology of Chemical Warfare Agents*; Elsevier, **2020**, pp 875–919. DOI: 10.1016/B978-0-12-819090-6.00052-0.

38. Chilcott, R. P.; Jenner, J.; Carrick, W.; Hotchkiss, S. A. M.; Rice, P. Human skin absorption of bis-2-(chloroethyl)sulphide (sulphur mustard)in vitro. *Journal of Applied Toxicology* **2000**, 20 (5), 349–355. DOI: 10.1002/1099-1263(200009/10)20:5<349:AID-JAT713>3.0.CO;2-O.

39. Maisonneuve, A.; Callebat, I.; Debordes, L.; Coppet, L. Biological fate of sulphur mustard in rat: toxicokinetics and disposition. *Xenobiotica; the fate of foreign compounds in biological systems* **1993**, 23 (7), 771–780. DOI: 10.3109/00498259309166783.

40. Drasch, G.; Kretschmer, E.; Kauert, G.; Meyer, L. von. Concentrations of mustard gas bis(2-chloroethyl)sulfide in the tissues of a victim of a vesicant exposure. Journal of forensic sciences **1987**, 32 (6), 1788–1793, PMID: 3430139.

41. Xu, H.; Nie, Z.; Zhang, Y.; Li, C.; Yue, L.; Yang, W.; Chen, J.; Dong, Y.; Liu, Q.; Lin, Y.; Wu, B.; Feng, J.; Li, H.; Guo, L.; Xie, J. Four sulfur mustard exposure cases: Overall analysis of four types of biomarkers in clinical samples provides positive implication for early diagnosis and treatment monitoring. *Toxicology reports* **2014**, 1, 533–543. DOI: 10.1016/j.toxrep.2014.07.017.

42. Noort, D.; Benschop, H. P.; Black, R. M. Biomonitoring of Exposure to Chemical Warfare Agents: A Review. *Toxicology and applied pharmacology* **2002**, 184 (2), 116-126. DOI: 10.1006/taap.2002.9449.

43. Valdez, C. A.; Leif, R. N.; Hok, S.; Hart, B. R. Analysis of chemical warfare agents by gas chromatography-mass spectrometry: methods for their direct detection and derivatization approaches for the analysis of their degradation products. *Reviews in Analytical Chemistry* **2018**, 37 (1). DOI: 10.1515/revac-2017-0007.

44. Black, R. M.; Clarke, R. J.; Harrison, J. M.; Read, R. W. Biological fate of sulphur mustard: identification of valine and histidine adducts in haemoglobin from casualties of sulphur mustard poisoning. *Xenobiotica; the fate of foreign compounds in biological systems* **1997**, 27 (5), 499–512. DOI: 10.1080/004982597240460.

45. Black, R. M.; Read, R. W. Detection of trace levels of thiodiglycol in blood, plasma and urine using gas chromatography-electron-capture negative-ion chemical ionisation mass spectrometry. *Journal of chromatography* **1988**, 449 (1), 261–270. DOI: 10.1016/S0021-9673(00)94385-1.

46. Black, R. M.; Read, R. W. Methods for the analysis of thiodiglycol sulphoxide, a metabolite of sulphur mustard, in urine using gas chromatography-mass spectrometry. *Journal of chromatography* **1991**, 558 (2), 393–404. DOI: 10.1016/0021-9673(91)80006-3.

47. Barr, J. R.; Pierce, C. L.; Smith, J. R.; Capacio, B. R.; Woolfitt, A. R.; Solano, M. I.; Wooten, J. V.; Lemire, S. W.; Thomas, J. D.; Ash, D. H.; Ashley, D. L. Analysis of urinary metabolites of sulfur mustard in two individuals after accidental exposure. *Journal of analytical toxicology* **2008**, 32 (1), 10–16.

48. Black, R. M.; Read, R. W. Biological fate of sulphur mustard, 1,1'-thiobis(2-chloroethane): identification of beta-lyase metabolites and hydrolysis products in human urine. *Xenobiotica; the fate of foreign compounds in biological systems* **1995**, 25 (2), 167–173. DOI: 10.3109/00498259509061842.

49. Siegert, M.; Kranawetvogl, A.; Thiermann, H.; John, H. N-Acetylcysteine as a chemical scavenger for sulfur mustard: New insights by mass spectrometry. *Drug testing and analysis* **2018**, 10 (2), 243–253. DOI: 10.1002/dta.2299.

50. Lüling, R.; Singer, H.; Popp, T.; John, H.; Boekhoff, I.; Thiermann, H.; Daumann, L. J.; Karaghiosoff, K.; Gudermann, T.; Steinritz, D. Sulfur mustard alkylates steroid hormones and impacts hormone function in vitro. *Archives of toxicology* **2019**, 93 (11), 3141–3152. DOI: 10.1007/s00204-019-02571-x.

51. Cheng, X.; Liu, C.; Yang, Y.; Liang, L.; Chen, B.; Yu, H.; Xia, J.; Liu, S.; Li, Y. Advances in sulfur mustard-induced DNA adducts: Characterization and detection. *Toxicology letters* **2021**, 344, 46–57. DOI: 10.1016/j.toxlet.2021.03.004.

52. Fidder, A.; Noort, D.; Jong, A. L. de; Trap, H. C.; Jong, L. P. de; Benschop, H. P. Monitoring of in vitro and in vivo exposure to sulfur mustard by GC/MS determination of the N-terminal valine adduct in hemoglobin after a modified Edman degradation. *Chemical research in toxicology* **1996**, 9 (4), 788–792. DOI: 10.1021/tx9502150.

53. Fox, M.; Scott, D. The genetic toxicology of nitrogen and sulphur mustard. *Mutation research* **1980**, 75 (2), 131–168. DOI: 10.1016/0165-1110(80)90012-3.

54. Fidder, A.; Noort, D.; Jong, L. P. A. de; Benschop, H. P.; Hulst, A. G. N7-(2-hydroxyethylthioethyl)-guanine: a novel urinary metabolite following exposure to sulphur mustard. *Archives of toxicology* **1996**, 70 (12), 854–855. DOI: 10.1007/s002040050350.

55. Davison, C.; Rozman, R. S.; Smith, P. K. Metabolism of bis-beta-chloroethyl sulfide (sulfur mustard gas). *Biochemical pharmacology* **1961**, 7, 65–74. DOI: 10.1016/0006-2952(61)90127-7.

56. Organisation for the Prohibition of Chemical Weapons. Praktischer Leitfaden zur Medizinischen Versorgung von Chemiekampfstoffopfern. https://www.opcw.org/sites/default/files/documents/2019/07/Praktische%20Anleitung%20zur%20medizinischen%20Versorgung%20von%20Chemiekampfstoff%20Opfern-Juni-2019.pdf (abgerufen am 01.02.2024).

57. Spiandore, M.; Piram, A.; Lacoste, A.; Prevost, P.; Maloni, P.; Torre, F.; Asia, L.; Josse, D.; Doumenq, P. Efficacy of scalp hair decontamination following exposure to vapours of sulphur mustard simulants 2-chloroethyl ethyl sulphide and methyl salicylate. *Chemico-biological interactions* **2017**, 267, 74–79. DOI: 10.1016/j.cbi.2016.07.018.

58. Steinritz, D.; Striepling, E.; Rudolf, K.-D.; Schröder-Kraft, C.; Püschel, K.; Hullard-Pulstinger, A.; Koller, M.; Thiermann, H.; Gandor, F.; Gawlik, M.; John, H. Medical documentation, bioanalytical evidence of an accidental human exposure to sulfur mustard and general therapy recommendations. *Toxicology letters* **2016**, 244, 112–120. DOI: 10.1016/j.toxlet.2015.08.1105.

59. Lüling, R.; John, H.; Gudermann, T.; Thiermann, H.; Mückter, H.; Popp, T.; Steinritz, D. Transient Receptor Potential Channel A1 (TRPA1) Regulates Sulfur Mustard-Induced Expression of Heat Shock 70 kDa Protein 6 (HSPA6) In Vitro. *Cells* **2018**, 7 (9). DOI: 10.3390/cells7090126.

60. Mol, M. A. E.; van den Berg, R. M.; Benschop, H. P. Proteomic assessment of sulfur mustard-induced protein adducts and other protein modifications in human epidermal keratinocytes. *Toxicology and applied pharmacology* **2008**, 230 (1), 97–108. DOI: 10.1016/j.taap.2008.02.006.

61. van der Schans, G. P.; Noort, D.; Mars-Groenendijk, R. H.; Fidder, A.; Chau, L. F.; Jong, L. P. A. de; Benschop, H. P. Immunochemical detection of sulfur mustard adducts with keratins in the stratum corneum of human skin. *Chemical research in toxicology* **2002**, 15 (1), 21–25. DOI: 10.1021/tx0100136.

62. Arentz, G.; Weiland, F.; Oehler, M. K.; Hoffmann, P. State of the art of 2D DIGE. *Proteomics Clinical applications* **2015**, 9 (3-4), 277–288. DOI: 10.1002/prca.201400119.

63. Unlü, M.; Morgan, M. E.; Minden, J. S. Difference gel electrophoresis: a single gel method for detecting changes in protein extracts. *Electrophoresis* **1997**, 18 (11), 2071-2077. DOI: 10.1002/elps.1150181133.

64. Lüling, R.; Schmeißer, W.; Siegert, M.; Mückter, H.; Dietrich, A.; Thiermann, H.; Gudermann, T.; John, H.; Steinritz, D. Identification of creatine kinase and alpha-1 antitrypsin as protein targets of alkylation by sulfur mustard. *Drug testing and analysis* **2021**, 13 (2), 268–282. DOI: 10.1002/dta.2916.

65. Sack, G. H.; Fenselau, C.; Kan, M.-N. N.; Kan, L. S.; Wood, G. W.; Lau, P.-Y. Characterization of the products of alkylation of 2'-deoxyadenosine and 2'-deoxyguanosine by chloroethyl ethyl sulfide. *Journal of Organic Chemistry* **1978**, 43 (20), 3932–3936. DOI: 10.1021/jo00414a028.

66. Gould, N. S.; White, C. W.; Day, B. J. A role for mitochondrial oxidative stress in sulfur mustard analog 2-chloroethyl ethyl sulfide-induced lung cell injury and antioxidant protection. The *Journal of pharmacology and experimental therapeutics* **2009**, 328 (3), 732–739. DOI: 10.1124/jpet.108.145037.

67. Björhall, K.; Miliotis, T.; Davidsson, P. Comparison of different depletion strategies for improved resolution in proteomic analysis of human serum samples. *Proteomics* **2005**, 5 (1), 307–317. DOI: 10.1002/pmic.200400900.

68. Shaw, J.; Rowlinson, R.; Nickson, J.; Stone, T.; Sweet, A.; Williams, K.; Tonge, R. Evaluation of saturation labelling two-dimensional difference gel electrophoresis fluorescent dyes. *Proteomics* **2003**, 3 (7), 1181–1195. DOI: 10.1002/pmic.200300439.

69. Riederer, I. M.; Riederer, B. M. Differential protein labeling with thiol-reactive infrared DY-680 and DY-780 maleimides and analysis by two-dimensional gel electrophoresis. *Proteomics* **2007**, 7 (11), 1753–1756. DOI: 10.1002/pmic.200601007.

70. Kirana, C.; Peng, L.; Miller, R.; Keating, J. P.; Glenn, C.; Shi, H.; Jordan, T. W.; Maddern, G. J.; Stubbs, R. S. Combination of laser microdissection, 2D-DIGE and MALDI-TOF MS to identify protein biomarkers to predict colorectal cancer spread. *Clinical proteomics* **2019**, 16, 3. DOI: 10.1186/s12014-019-9223-7.

71. John, H.; Siegert, M.; Gandor, F.; Gawlik, M.; Kranawetvogl, A.; Karaghiosoff, K.; Thiermann, H. Optimized verification method for detection of an albumin-sulfur mustard adduct at Cys(34) using a hybrid quadrupole time-of-flight tandem mass spectrometer after direct plasma proteolysis. *Toxicology letters* **2016**, 244, 103–111. DOI: 10.1016/j.toxlet.2015.09.027.

72. Organisation for the Prohibition of Chemical Weapons. https://www.opcw.org/ (accessed 2024-01-02).

73. Noort, D.; Hulst, A. G.; Jong, L. P. de; Benschop, H. P. Alkylation of human serum albumin by sulfur mustard in vitro and in vivo: mass spectrometric analysis of a cysteine adduct as a sensitive biomarker of exposure. *Chemical research in toxicology* **1999**, 12 (8), 715–721. DOI: 10.1021/tx9900369.

74. Gandor, F.; Gawlik, M.; Thiermann, H.; John, H. Evidence of Sulfur Mustard Exposure in Human Plasma by LC-ESI-MS-MS Detection of the Albumin-Derived Alkylated HETE-CP Dipeptide and Chromatographic Investigation of Its Cis/Trans Isomerism. *Journal of analytical toxicology* **2015**, 39 (4), 270–279. DOI: 10.1093/jat/bkv010.

75. Chen, B.; Zhang, Q.; Ren, Z.; Zhang, T.; Yu, H.; Liu, C.; Yang, Y.; Xu, P.; Liu, S. A proteomics strategy for the identification of multiple sites in sulfur mustard-modified HSA and screening potential biomarkers for retrospective analysis of exposed human plasma. *Analytical and bioanalytical chemistry* **2022**, 414 (14), 4179–4188. DOI: 10.1007/s00216-022-04070-y.

76. Siegert, M.; Gandor, F.; Kranawetvogl, A.; Börner, H.; Thiermann, H.; John, H. Methionine329 in human serum albumin: A novel target for alkylation by sulfur mustard. *Drug testing and analysis* **2019**, 11 (5), 659–668. DOI: 10.1002/dta.2548.

77. Andacht, T. M.; Pantazides, B. G.; Crow, B. S.; Fidder, A.; Noort, D.; Thomas, J. D.; Blake, T. A.; Johnson, R. C. An enhanced throughput method for quantification of sulfur mustard adducts to human serum albumin via isotope dilution tandem mass spectrometry. *Journal of analytical toxicology* **2014**, 38 (1), 8–15. DOI: 10.1093/jat/bkt088.

78. Hallez, F.; Combès, A.; Desoubries, C.; Bossée, A.; Pichon, V. Development of a liquid chromatography-tandem mass spectrometry (LC-MS/MS) method for the analysis of tryptic digest of human hemoglobin exposed to sulfur mustard. Journal of chromatography. B, *Analytical technologies in the biomedical and life* sciences **2021**, 1163, 122518. DOI: 10.1016/j.jchromb.2020.122518.

79. Occupational Safety & Health Administration. Bloodborne Pathogens and Needlestick Prevention: Hazard Recognition. https://www.osha.gov/bloodborne-pathogens/hazards (abgerufen am 01.02.2024).

80. International Air Transport Association. Dangerous Goods Regulation. https://www.iata.org/en/publications/dgr/ (abgerufen am 01.02.2024).

81. International Maritime Organization. The International Maritime Dangerous Goods (IMDG) Code. https://www.imo.org/en/OurWork/Safety/Pages/DangerousGoods-default.aspx (abgerufen am 01.02.2024).

82. United Nations Economic Commission for Europe. Agreement concerning the International Carriage of Dangerous Goods by Road. https://unece.org/adr-2021-files (abgerufen am 01.02.2024).

83. John, H.; Willoh, S.; Hörmann, P.; Siegert, M.; Vondran, A.; Thiermann, H. Procedures for Analysis of Dried Plasma Using Microsampling Devices to Detect Sulfur Mustard-Albumin Adducts for Verification of Poisoning. *Analytical chemistry* **2016**, 88 (17), 8787–8794. DOI: 10.1021/acs.analchem.6b02199.

84. Ferreira, C.; Paulino, C.; Quintas, A. Extraction Procedures for Hair Forensic Toxicological Analysis: A Mini-Review. *Chemical research in toxicology* **2019**, 32 (12), 2367–2381. DOI: 10.1021/acs.chemrestox.9b00301.

85. Scheufler, F. Haare im Fokus der forensischen Analytik. Chemie in unserer Zeit **2018**, 52 (1), 26-33. DOI: 10.1002/ciuz.201700760.

86. Spiandore, M.; Piram, A.; Lacoste, A.; Josse, D.; Doumenq, P. Hair analysis as a useful procedure for detection of vapour exposure to chemical warfare agents: simulation of sulphur mustard with methyl salicylate. *Drug testing and analysis* **2014**, 6 Suppl 1, 67-73. DOI: 10.1002/dta.1659.

87. Capacio, B. R.; Smit, J. R.; Gordon, R. K.; Haigh, J. R.; Barr, J. R.; Lukey, B. J. Clinical Detection of Exposure to Chemical Warfare Agents: Vesicants. In Chemical warfare agents: Chemistry, pharmacology, toxicology, and therapeutics, 2nd ed.; Romano Jr., J. A., Lukey, B. J., Salem, H., Eds.; *CRC Press*, **2008**, pp 515–530.

88. Robbins, C. R.; Kelly, C. H. Amino Acid Composition of Human Hair. *Textile Research Journal* **1970**, 40 (10), 891–896. DOI: 10.1177/004051757004001005.

89. Robbins, C. R. Chemical and Physical Behavior of Human Hair; *Springer Berlin Heidelberg*, **2012**. DOI: 10.1007/978-3-642-25611-0.

90. Adav, S. S.; Subbaiaih, R. S.; Kerk, S. K.; Lee, A. Y.; Lai, H. Y.; Ng, K. W.; Sze, S. K.; Schmidtchen, A. Studies on the Proteome of Human Hair - Identification of Histones and Deamidated Keratins. *Scientific reports* **2018**, 8 (1), 1599. DOI: 10.1038/s41598-018-20041-9.

91. Fujii, T.; Takayama, S.; Ito, Y. A novel purification procedure for keratin-associated proteins and keratin from human hair. *International Journal of Biological Macromolecules* **2013**, 13 (3), 92-106. DOI: 10.14533/jbm.13.92.

92. Lubec, G.; Nauer, G.; Seifert, K.; Strouhal, E.; Porteder, H.; Szilvassy, J.; Teschler, M. Structural stability of hair over three thousand years. *Journal of Archaeological Science* **1987**, 14 (2), 113-120. DOI: 10.1016/0305-4403(87)90001-X.

93. Barthélemy, N. R.; Bednarczyk, A.; Schaeffer-Reiss, C.; Jullien, D.; van Dorsselaer, A.; Cavusoglu, N. Proteomic tools for the investigation of human hair structural proteins and evidence of weakness sites on hair keratin coil segments. *Analytical biochemistry* **2012**, 421 (1), 43–55. DOI: 10.1016/j.ab.2011.10.011.

94. Lee, Y. J.; Rice, R. H.; Lee, Y. M. Proteome analysis of human hair shaft: from protein identification to posttranslational modification. *Molecular & cellular proteomics : MCP* **2006**, 5 (5), 789–800. DOI: 10.1074/mcp.M500278-MCP200.

95. Dillman, J. F.; McGary, K. L.; Schlager, J. J. Sulfur mustard induces the formation of keratin aggregates in human epidermal keratinocytes. *Toxicology and applied pharmacology* **2003**, 193 (2), 228–236. DOI: 10.1016/j.taap.2003.08.003.

96. Zhu, K.; Zhao, J.; Lubman, D. M.; Miller, F. R.; Barder, T. J. Protein pI shifts due to posttranslational modifications in the separation and characterization of proteins. *Analytical chemistry* **2005**, 77 (9), 2745–2755. DOI: 10.1021/ac048494w.

97. Sporty, J. L. S.; Lemire, S. W.; Jakubowski, E. M.; Renner, J. A.; Evans, R. A.; Williams, R. F.; Schmidt, J. G.; van der Schans, M. J.; Noort, D.; Johnson, R. C. Immunomagnetic separation and quantification of butyrylcholinesterase nerve agent adducts in human serum. *Analytical chemistry* **2010**, 82 (15), 6593–6600. DOI: 10.1021/ac101024z.

98. Leri, M.; Rebuzzini, P.; Caselli, A.; Luti, S.; Natalello, A.; Giorgetti, S.; Marchese, L.; Garagna, S.; Stefani, M.; Paoli, P.; Bucciantini, M. S-Homocysteinylation effects on transthyretin: worsening of cardiomyopathy onset. *Biochimica et biophysica acta. General subjects* **2020**, 1864 (1), 129453. DOI: 10.1016/j.bbagen.2019.129453.

99. Kingsbury, J. S.; Klimtchuk, E. S.; Théberge, R.; Costello, C. E.; Connors, L. H. Expression, purification, and in vitro cysteine-10 modification of native sequence recombinant human transthyretin. *Protein expression and purification* **2007**, 53 (2), 370–377. DOI: 10.1016/j.pep.2007.01.004.

100. Berninger, R. W.; Booker, S. V.; Talamo, R. C. Serum prealbumin levels in alpha 1-antitrypsin deficiency (PiZ). *Metabolism: clinical and experimental* **1982**, 31 (3), 299-302. DOI: 10.1016/0026-0495(82)90069-5.

101. Deb-Choudhury, S.; Plowman, J. E.; Harland, D. P. Isolation and Analysis of Keratins and Keratin-Associated Proteins from Hair and Wool. *Methods in enzymology* **2016**, 568, 279–301. DOI: 10.1016/bs.mie.2015.07.018.

7 Abbildungs- und Tabellenverzeichnis

Abbildungen

Tabelle

Danksagung

An erster Stelle gilt mein Dank meinem wissenschaftlichen Betreuer Prof. Dr. Harald John für die Möglichkeit, Wissenschaft in einem hochprofessionellen Umfeld kennenlernen zu dürfen. Die vertrauensvolle Zusammenarbeit, die fachlichen Gespräche und die Vermittlung von Liebe zum Detail haben mich beeindruckt und geprägt.

Bei meinem Doktorvater Prof. Dr. Theo Rein möchte ich mich herzlich für die gute Betreuung und die gewährten Freiheiten bei der Ausgestaltung der Promotion bedanken.

Den Leitern des Instituts für Pharmakologie und Toxikologie der Bundeswehr Prof. Dr. Horst Thiermann und Prof. Dr. Franz Worek gebührt mein Dank für die umfassende Unterstützung als wissenschaftlicher Mitarbeiter und die Schaffung der hervorragenden Arbeitsbedingungen.

Großes Dankschön geht an Dr. Karin Viktoria Niessen, die mich in das Instituts eingeführt und als Weiterbildungsbeauftragte bis zum Abschluss des Fachapothekers für Toxikologie und Ökologie begleitet hat.

Robin Lüling und Prof. Dr. Dirk Steinritz danke ich für die hervorragende, arbeitsgruppenübergreifende Zusammenarbeit sowie die fachliche und methodische Unterstützung beim Anfertigen der Publikationen.

Weiterer Dank gilt der gesamten Arbeitsgruppe John: insbesondere Dr. Markus Siegert für die Einarbeitung, Hilfestellung und unerschöpfliche Geduld, Tamara Kranawetvogl für die exzellente Laborgemeinschaft und die freundschaftliche Zusammenarbeit, Marina Dentzel und Stefanie Oswald für die optimalen Laborbedingungen und die technische Unterstützung.

Ein herzliches Dankeschön allen Mitstreitern und Freunden am Institut für das Miteinander innerhalb und außerhalb der Arbeit, die gegenseitige Motivation und die vielen geteilten Erlebnisse.

Spezieller Dank geht an Amelie, Simone und Corbinian für ihr offenes Ohr, die Geduld bei oft fremden Problematiken und die vielen inspirierenden Gespräche.

Ganz besonderer Dank geht an meine wunderbare Familie für ihre uneingeschränkte Fürsorge und Anteilnahme in und an allen Lebenslagen. Der familiäre Zusammenhalt ist ein unermesslicher Rückhalt für mich.

Meine uneingeschränkte Dankbarkeit und Liebe gilt Cathy für unsere gemeinsame Zeit, ihre Geduld, ihr immerwährender Beistand und die Gabe Leichtigkeit in mein Leben zu bringen.